การวิเคราะห์โครงสร้างและหน้าที่ของ crustin*Pm*1 และ crustin*Pm*7 จากกุ้งกุลาดำ

Penaeus monodon

นางสาวโศภชา อารยเมธากร

วิทยานิพนธ์นี้เป็นส่วนหนึ่งของการศึกษาตามหลักสูตรปริญญาวิทยาศาสตรมหาบัณฑิต
สาขาวิชาเทคโนโลยีชีวภาพ
คณะวิทยาศาสตร์ จุฬาลงกรณ์มหาวิทยาลัย
ปีการศึกษา 2556
ลิขสิทธิ์ของจุฬาลงกรณ์มหาวิทยาลัย

STRUCTURE AND FUNCTION ANALYSIS OF crustin*Pm*1 AND crustin*Pm*7 FROM
BLACK TIGER SHRIMP *Penaeus monodon*

Miss Sopacha Arayamethakorn

A Thesis Submitted in Partial Fulfillment of the Requirements

for the Degree of Master of Science Program in Biotechnology

Faculty of Science

Chulalongkorn University

Academic Year 2013

Thesis Title	STRUCTURE AND FUNCTION ANALYSIS OF crustin*Pm*1 AND crustin*Pm*7 FROM BLACK TIGER SHRIMP *Penaeus monodon*
By	Miss Sopacha Arayamethakorn
Field of Study	Biotechnology
Thesis Advisor	Professor Anchalee Tassanakajon, Ph.D.
Thesis Co-Advisor	Assistant Professor Kuakarun Krosong, Ph.D.

Accepted by the Faculty of Science, Chulalongkorn University in Partial Fulfillment of the Requirements for the Master's Degree

⋯⋯⋯⋯⋯⋯⋯⋯⋯⋯⋯⋯⋯⋯Dean of the Faculty of Science

(Professor Supot Hannongbua, Ph.D.)

THESIS COMMITTEE

⋯⋯⋯⋯⋯⋯⋯⋯⋯⋯⋯⋯⋯⋯Chairman

(Assistant Professor Kanoktip Pachdibumrung, Ph.D.)

⋯⋯⋯⋯⋯⋯⋯⋯⋯⋯⋯⋯⋯⋯Thesis Advisor

(Professor Anchalee Tassanakajon, Ph.D.)

⋯⋯⋯⋯⋯⋯⋯⋯⋯⋯⋯⋯⋯⋯Thesis Co-Advisor

(Assistant Professor Kuakarun Krosong, Ph.D.)

⋯⋯⋯⋯⋯⋯⋯⋯⋯⋯⋯⋯⋯⋯Examiner

(Kittinan Komolpis, Ph.D.)

⋯⋯⋯⋯⋯⋯⋯⋯⋯⋯⋯⋯⋯⋯External Examiner

(Kallaya Sritunyalucksana-Dangtip, Ph.D.)

โศภชา อารยเมธากร : การวิเคราะห์โครงสร้างและหน้าที่ของ crustin*Pm*1 และ crustin*Pm*7 จากกุ้งกุลาดำ *Penaeus monodon*. (STRUCTURE AND FUNCTION ANALYSIS OF crustin*Pm*1 AND crustin*Pm*7 FROM BLACK TIGER SHRIMP *Penaeus monodon*) อ.ที่ปรึกษาวิทยานิพนธ์หลัก: ศ. ดร.อัญชลี ทัศนาขจร, อ.ที่ปรึกษาวิทยานิพนธ์ ร่วม: ผศ. ดร.เกื้อการุณย์ ครูส่ง, 147 หน้า.

เปปไทด์ต้านจุลชีพมีบทบาทสำคัญในระบบภูมิคุ้มกันโดยสารน้ำ ซึ่งมีฤทธิ์การยับยั้งการเจริญ ของเชื้อจุลชีพ ครัสตินไอโซฟอร์ม 1 (crustin*Pm*1) และครัสตินไอโซฟอร์ม 7 (crustin*Pm*7) เป็นสองไอ โซฟอร์มซึ่งพบมากในเม็ดเลือดของกุ้งกุลาดำ งานวิจัยนี้สนใจศึกษา (1) ฤทธิ์การยับยั้งการเจริญของ แบคทีเรีย และสมบัติการจับของโปรตีนรีคอมบิแนนท์ crustin*Pm*1 และ crustin*Pm*7 (2) โครงสร้าง ทุติยภูมิของโปรตีนรีคอมบิแนนท์ครัสตินทั้งสองไอโซฟอร์ม (3) การตกผลึกของโปรตีนรีคอมบิแนนท์ crustin*Pm*1 และ (4) การควบคุมการแสดงออกของยีน crustin*Pm*1 และ crustin*Pm*7 จากการศึกษา โปรตีนรีคอมบิแนนท์ crustin*Pm*1 และ crustin*Pm*7 มีการแสดงออกอย่างมากในยีสต์ *Pichia pastoris* และเมื่อทดสอบฤทธิ์การยับยั้งเชื้อแบคทีเรีย พบว่า crustin*Pm*1 มีฤทธิ์ยับยั้งแบคทีเรียแกรม บวกเท่านั้น ในขณะที่ crustin*Pm*7 สามารถยับยั้งได้ทั้งแบคทีเรียแกรมบวก และแบคทีเรียแกรมลบ อีก ทั้งศึกษาฤทธิ์การยับยั้งการทำงานของเอนไซม์โปรติเนส พบว่า โปรตีนรีคอมบิแนนท์ crustin*Pm*1 และ crustin*Pm*7 ไม่มีแอคทิวิตีในการยับยั้งการทำงานของเอนไซม์โปรติเนสทางการค้า และเอนไซม์โปรติ เนส จาก *Bacillus subtilis* จากการศึกษาการจับกันระหว่างลิพิดและโปรตีน แสดงให้เห็นว่า ครัสตินทั้ง สองไอโซฟอร์มสามารถจับได้อย่างจำเพาะกับกรดฟอสฟาทิดิก (Phosphatidic acid, PA) และจากผล ของ Enzyme-linked immunosorbent (ELISA) assay พบว่า ครัสตินทั้งสองไอโซฟอร์มสามารถจับ กับกรดฟอสฟาทิดิก แบบ Positive cooperative โดยมีค่า Hill slope (H) มากกว่า 2 ชี้ให้เห็นว่า ครัส ตินอย่างน้อย 2 โมเลกุล สามารถจับกับกรดฟอสฟาทิดิก 1 โมเลกุล จากการศึกษาโครงสร้างทุติยภูมิ ของครัสตินทั้งสองไอโซฟอร์มโดยวิธีเซอร์คิวลาร์ไดโครอิซึม (Circular Dichroism Spectroscopy) แสดงให้เห็นว่า โปรตีนรีคอมบิแนนท์ crustin*Pm*1 มีองค์ประกอบของ alpha-helix 40.81% และ beta-sheet 22.34% ส่วนโปรตีนรีคอมบิแนนท์ crustin*Pm*7 มีองค์ประกอบของ alpha-helix 32.86% และ beta-sheet 27.53% จากการทดลองตกผลึกโปรตีนรีคอมบิแนนท์ crustin*Pm*1 พบว่า ได้ผลึกของโปรตีนในหลายสภาวะ อย่างไรก็ตาม พบว่าผลึกที่ได้นั้นไม่ให้การเลี้ยวเบนของรังสีเอ็กซ์ จึง ต้องปรับปรุงสภาวะเพื่อให้เหมาะสมสำหรับการเติบโตของผลึก นอกจากนี้ ได้ทำการทดลองลดการ แสดงออกของ *Pm*Relish และ *Pm*MyD88 ถูกทำให้ไม่มีการแสดงออก เพื่อศึกษาวิถีการควบคุมการ แสดงออกของ crustin*Pm*1 และ crustin*Pm*7 ซึ่งพบว่า crustin*Pm*1 ถูกควบคุมผ่านวิถี Toll ในขณะ ที่ crustin*Pm*7 ถูกควบคุมผ่านทั้งวิถี Toll และ Imd

สาขาวิชา   เทคโนโลยีชีวภาพ   ลายมือชื่อนิสิต ....

ปีการศึกษา 2556   ลายมือชื่อ อ.ที่ปรึกษาวิทยานิพนธ์หลัก ....

                                                ลายมือชื่อ อ.ที่ปรึกษาวิทยานิพนธ์ร่วม ....

5472260423 : MAJOR BIOTECHNOLOGY

KEYWORDS: CRUSTINPM1 / CRUSTINPM7 / PENAEUS MONODON / TOLL PATHWAY / IMMUNE DEFICIENCY PATHWAY

SOPACHA ARAYAMETHAKORN: STRUCTURE AND FUNCTION ANALYSIS OF crustin*Pm*1 AND crustin*Pm*7 FROM BLACK TIGER SHRIMP *Penaeus monodon*. ADVISOR: PROF. ANCHALEE TASSANAKAJON, Ph.D., CO-ADVISOR: ASST. PROF. KUAKARUN KROSONG, PH.D., 147 pp.

Antimicrobial peptides (AMPs) are considered to play an important role in humoral defense against pathogen infection. Crustin*Pm*1 and crustin*Pm*7 are two of most abundant crustin identified from the hemocytes of the black tiger shrimp, *Penaeus monodon*. This research aims to study (1) activities and binding properties of the recombinant crustin*Pm*1 (rcrustin*Pm*1) and recombinant crustin*Pm*7 (rcrustin*Pm*7), (2) the secondary structure of both crustins, (3) crystallization of the rcrustin*Pm*1, and (4) the regulation of crustin*Pm*1 and crustin*Pm*7 gene expressions. In this study, crustin*Pm*1 and crustin*Pm*7 were overexpressed in *Pichia pastoris*. Antimicrobial assays demonstrated that rcrustin*Pm*1 was active against Gram-positive bacteria only but rcrustin*Pm*7 inhibited both Gram-positive and Gram-negative bacteria. The rcrustin*Pm*1 and rcrustin*Pm*7 showed no proteinase inhibitory activity against the commercial proteinases and proteinase from *Bacillus subtilis*. Study of lipid-protein interaction showed that both crustins could specifically bind phosphatidic acid (PA). Enzyme-linked immunosorbent assay suggested that crustins bind to PA with positive cooperativity of Hill slope (H) > 2. This indicates that at least two molecules of crustins interact with one PA molecule. In addition, circular dichroism spectroscopy was used to determine secondary structure of crustin*Pm*s. Crustin*Pm*1 contained 40.81% of alpha-helix and 22.34% of beta-sheet, whereas crustin*Pm*7 contained 32.86% of alpha-helix and 27.53% of beta-sheet. Crystallization of rcrustin*Pm*1 was performed and crystals were obtained in some crystallization conditions. However, these crystals gave no diffraction. Therefore, crystallization conditions will be optimized for further crystal growth. Regulatory pathways of crustin*Pm*1 and crustin*Pm*7 were investigated by *Pm*Relish and *Pm*MyD88 knockdown. It is likely that crustin*Pm*1 was mediated through Toll signaling pathway, while crustin*Pm*7 was related with both Toll and Imd pathways.

Field of Study: Biotechnology

Academic Year: 2013

Student's Signature ....

Advisor's Signature ....

Co-Advisor's Signature ....

ACKNOWLEDGEMENTS

CONTENTS

LIST OF TABLES

LIST OF FIGURES

Page

LIST OF ABBREVIATIONS

A	absorbance
bp	base pair
dATP	deoxyadenosine triphosphate
dCTP	deoxyadecytosine triphosphate
DEPC	diethylpyrocarbonate
dGTP	deoxyguanosine triphosphate
DNA	deoxyribonucleic acid
dTTP	deoxythymidine triphosphate
ELISA	enzyme-linked immunosorbent assay
EMS	early mortality syndrome
EtBr	ethidium bromide
h	hour, hours
His	histidine
imd	immune deficiency
Kb	kilobase
KDa	kilodalton
LGBP	lipopolysaccharide and beta-1,3-glucan binding protein
LPS	lipopolysaccharide
LTA	lipoteichoic acid
M	molar
mA	milliampere
mg	milligram
min	minute
ml	millilitre
mM	millimolar
ng	nanogram

nm	nanomolar
O.D.	optical density
ORF	open reading frame
PA	Phosphatidic acid
PCR	polymerase chain reaction
Pm	Penaeus monodon
PPAE	prophenoloxidase activating enzyme
rcrustin*Pm*s	Recombinant crustinPms
RNA	ribonucleic acid
RT	reverse transcription
sec	second
TCBS	thiosulfate-citrate-bile-sucrose
TMB	Tetramethylbenzidine
TSB	tryptic soy broth
WSSV	white spot syndrome virus
YHV	yellow head virus
°C	degree celcius
µg	microgram
µl	microliter
µM	micromolar

CHAPTER I

INTRODUCTION

For over 20 years, shrimp is one of the economically important animals in Thailand. Improvement of shrimp production and logistics system made them become a valuable export product to many countries around the world. In Thailand, 80% of all farmed shrimps are the two species of the *Penaeus monodon* (Black tiger shrimp) and *Litopenaeus vannamei* (Pacific white shrimp).

According to the graph (Figure 1.1), black tiger shrimp farming started in the late 1980s in Thailand and the country has become the largest exporting shrimp production in forms of frozen and value-added products to the market world. Its production increased sharply in the first 10 years and reached a peak of about 260,000 metric tons in 2002 providing the income of approximately 85,000 million baht per year (Source: Office of Agriculture Economics in cooperation with the Customs Department). In 2003, the black tiger shrimp production was susceptible to bacterial and viral diseases, resulting in a dramatic reduction of 10,000 metric tons per year and never regain its pre-recession level. Pacific white shrimp become a popular species since it grows rapidly, disease resistant, temperature tolerant and requires low salinity. *L. vannamei* farming has been helped the country to maintain the farmed shrimp production by rapidly increasing the whiteleg shrimp output from 45,000 metric tons in 2002 to more than 500,000 metric tons in 2006 and a peak of 650,000 metric tons in 2010. However, the whiteleg shrimp production in Thailand started to decline in 2011 and is expected to drop due to the early mortality syndrome (EMS).

P. monodon is a native species in Thailand. Thus, study of its immune system is important in fighting the shrimp diseases and this could lead to an increase in *P. monodon* aquaculture.
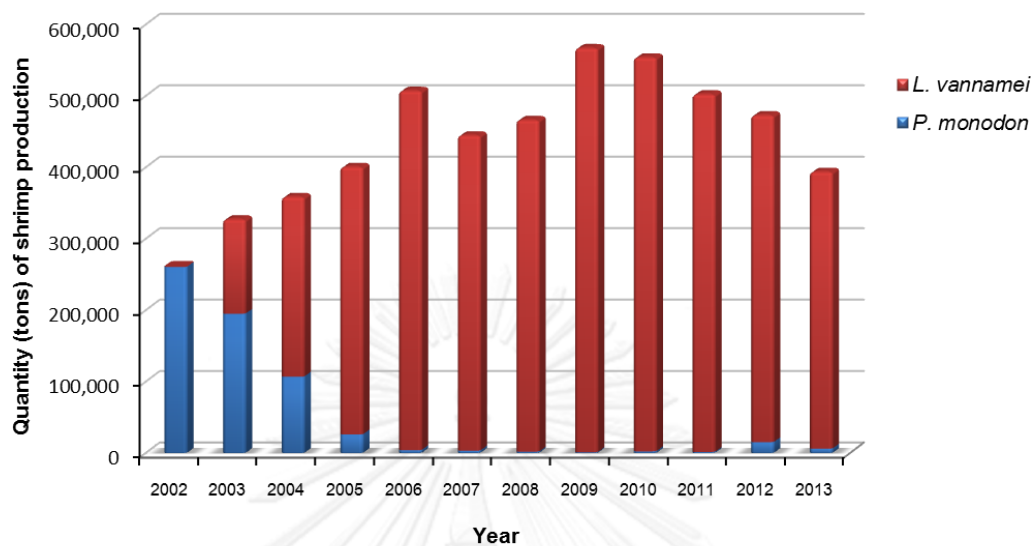
Source: http://www.thai-frozen.or.th/news_45.php

Figure 1.1 The black tiger shrimp and white shrimp export of Thailand during 2002 to 2013

1.1 The black tiger shrimp *Penaeus monodon*

Source : http://www.shiau.ntou.edu.tw/member-9.htm

Figure 1.2 The black tiger shrimp *Penaeus monodon*

The taxonomy of the black tiger shrimp, *Penaeus monodon* classified into the kingdom, Animalia (Linnaeus 1758) as follows (Baily-Brock and Moss 1992)

Phylum Arthropoda

Class Crustacea

Subclass Malacostraca

Order Decapoda

Suborder Natantia

Family Penaeidae (Rafinesque 1815)

Genus *Penaeus*   (Fabricius 1798)

Subgenus *Penaeus*

Species *monodon*

The black tiger shrimps (Figure 1.2) have typical body containing a head (cephalon), tail (abdomen), five pairs of swimming legs (pleopods) and five pairs of walking legs. (pereopods). The particularities of the black tiger shrimp are brown color with the black and white band across their back and tail. When they were cultured in the pools, their color changed to dark brown. The important various parts of *P. monodon* were shown in Figure 1.3.
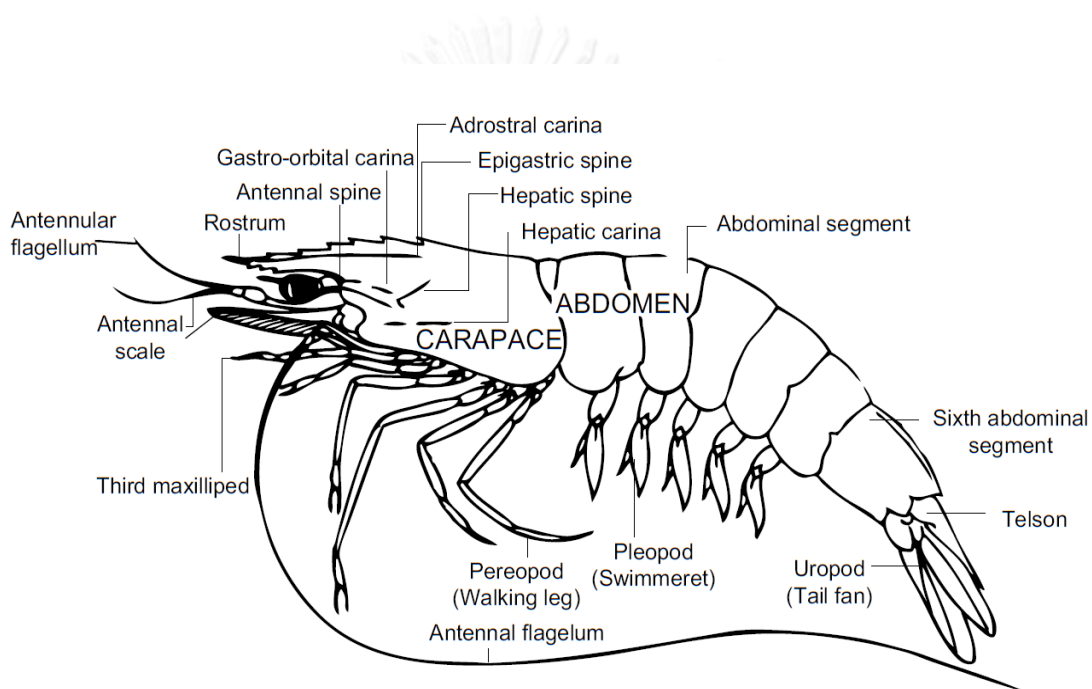
Figure 1.3 The important parts of *P. monodon* (Motoh 1981)

1.2 Major shrimp diseases

1.2.1 Bacterial diseases

The species of Vibrio have been associated with shrimp diseases in Thailand. They are *Vibrio harveyi* and *Vibrio parahaemolyticus*.

1.2.1.1 Vibriosis

Vibriosis, one of a major disease in shrimp aquaculture, is caused of shrimp mortality by gram-negative bacteria, *Vibrio harveyi*. This luminous bacteria can emit a blue-green color light through the luciferase catalysis reaction. The luminescent shrimp caused by *V. harveyi* infection is shown in Figure 1.3. Vibrio species are part of the natural microflora of cultured shrimps (Sinderman 1977) and become opportunistic pathogens when natural defence mechanisms are suppressed (Brock and Lightner 1990). Vibriosis mortalities occurred when shrimps are under stress conditions by malnutrition, extreme fluctuations in water temperature, parasitic infections, poor water quality, crowding, low dissolved oxygen and low oxygen exchange etc. (Lewis 1973, Brock and Lightner 1990). The symptoms are necrosis, weak body, slow swim, appetite loss, red spots on the pleopod and abdominal as well as visible light at night.

Source : http://www.thailandshrimp.org/agriculture_tiger8.html

Figure 1.4 The luminescent shrimp from *Vibrio harveyi*

1.2.1.2 Early mortality syndrome (EMS)

Early mortality syndrome (EMS) has caused large-scale die-offs of shrimps in several countries in Asia. EMS was first discovered in China in 2009 and it also hit to Vietnam, Malaysia and Thailand. EMS affects two species of shrimp, which are the black tiger shrimp and the whiteleg shrimp. Donald Lightner identified a unique bacterial strain of *Vibrio parahaemolyticus* that caused the high virulent of shrimps (Lightner *et al.* 2012). The symptoms of EMS disease are swollen body, slow growth rate, corkscrew swimming, colonization of the shrimp gastrointestinal tract and production of a toxin that cause tissue destruction and dysfunction of the shrimp digestive organ (the hepatopancreas). *V. parahaemolyticus* does not affect humans (Lightner *et al.* 2012). EMS outbreaks occur within 30 days after farming a new shrimp pond, and the dead rate is as high as 70% (Figure 1.5).

Source : http://www.dw.de/thai-shrimp-death-scientists-still-baffled-by-southeast-asian-disease/a-17301496

Figure 1.5 Shrimps died by Early Mortality Syndrome (EMS)

1.2.2 Viral diseases

Two major viral pathogens that have been identified in shrimp farms around the world are White Spot Syndrome Virus (WSSV) and Yellow Head Virus (YHV).

1.2.2.1 White spot syndrome (WSS) disease

White spot syndrome (WSS) is a viral infection of penaeid shrimp which was first reported in Taiwan in 1992 (Chou *et al.* 1995), however, this disease was severely spread in many countries including Thailand (Lo 1996). The disease is caused by a family of related viruses as the Whitespot Syndrome Baculovirus complex (WSSV). WSSV is a rod shape and envelope with double-stranded DNA virus which is highly virulent and leads to mortality rates of 100% within days. The symptoms of this disease are red or pink body surface and appendages, loose cuticle, white spots of 0.5-2.0 mm in diameter on the inside surface of the carapace, appendages and cuticle over the abdominal segments, lack of appetite and slow movement (Figure 1.6).

Source : http://vietnamseafoodnews.com/wp-content/uploads/2011/10/WSSV2.jpg

Figure 1.6 White spot after WSSV infection in shrimp

1.2.2.2 Yellow Head Disease (YHD)

Yellow Head Disease is a viral infection of shrimp such as the black tiger shrimp and the whiteleg shrimp. The disease was first reported in Thailand in 1990 and caused a reduction of shrimp export value. YHD is caused by the yellow head virus (YHV), a pleomorphic and positive-sense single-stranded RNA virus which localized in the cytoplasm of infected cells (Cowley *et al.* 1999). The clinical signs of YHD include the cephalothorax and hepatopancreas of infected shrimp turning yellow light discoloration (Figure 1.7). Cumulative mortalities after YHV infected reaches 100% within two to four days (Chantanachookin *et al.* 1993).

Source : http://library.enaca.org/Health/FieldGuide/html/cv010yhd.htm

Figure 1.7 Yellowhead disease in shrimp presenting by yellow heads of infected shrimps on left, comparing to normal shrimps on right.

1.3 The crustacean immunity

The crustaceans have the innate defense mechanisms as non-specific mechanism. Crustaceans have mechanisms to protect themselves from injuries or foreign matter. These defense can be divided into two groups as cellular and humoral immune responses (Jiravanichpaisal *et al.* 2006). Hemocytes are important defense responses by cellular and humoral responses. Cellular immune responses associate the activation by hemocytes; for example phagocytosis, nodule formation, coagulation system, melanization, encapsulation and cell-mediated cytotoxicity. On the other hand, the humoral immune responses refers to the body protects itself from the foreign material infection in the bloodstream by producing antibodies and marking it for destruction. The fluid substances such as secreted antibodies, enzymes and proteins are found in prophenoloxidase activating system, coagulation system, agglutinin, prophenoloxidase (proPO) and antimicrobial peptides (Holmbald and Söderhäll 1999, Jiravanichpaisal *et al.* 2006). The knowledge of crustacean immunity was described in Figure 1.8 (Jiravanichpaisal *et al.* 2006).
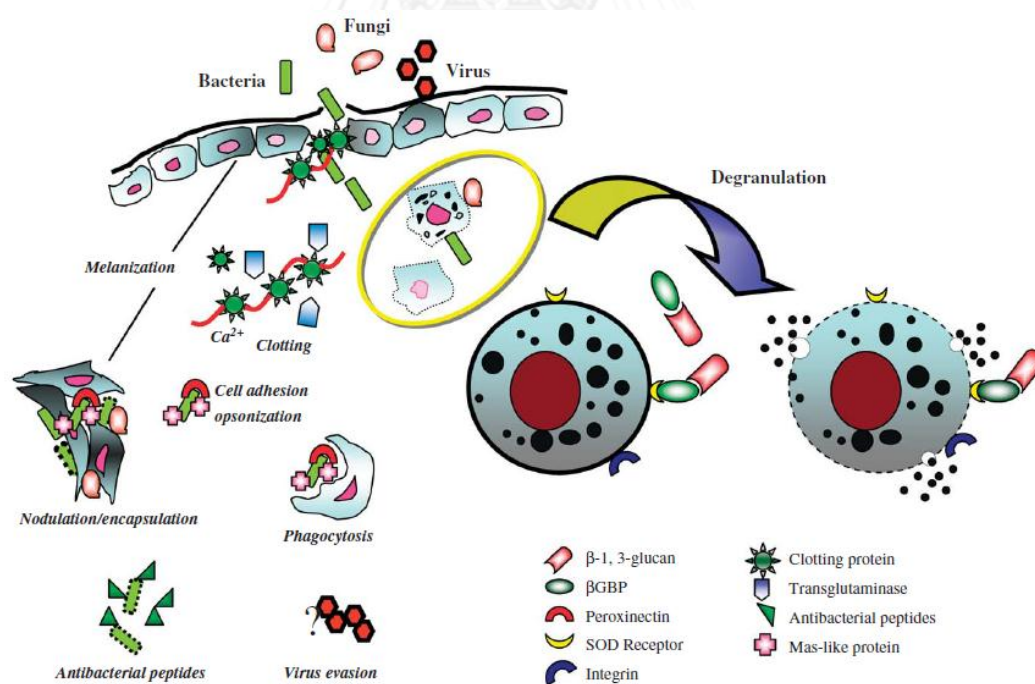
Figure 1.8 Overview of the innate defense mechanism

(Jiravanichpaisal *et al.* 2006)

1.3.1 Cell-mediated immune response

Cell-mediated immune responses are important in defense against pathogens including phagocytosis, encapsulation and nodule formation (Millar, 1994). In crustacean immunity, the hemocytes are mainly immune related cells and can be separated into three type: hyaline cells (the smallest hemocytes with cytoplasmic granule), semi-granular cells (the small granules in cytoplasm), and granular cells (the biggest hemocytes with large cytoplasmic granules).

Phagocytosis is a major mechanism that removes pathogens and cell debris. It can be divided into three processes that are recognition pathogenic microorganisms, ingestion, and destroying. The cell engulfs microbes and traps them in the internal phagosome. Enzyme in phagosome then digests the microbes and kills them (Reviewed in Sharon and Lis 2004).

Cell encapsulation is a process that layers of cells surround the foreign material to prevent spreading of the pathogen. This process occurs when foreign matter is too large to ingest by phagocytosis (Gillespie *et al.* 1997). This process occurs to protect host cell by approaching host hemocytes to pathogens and parasites and forming on a surface. The microbes in capsule that come from cell encapsulation process were destroyed by the action of hydrolases and the decrease in oxygen concentration (Söderhäll *et al.* 1984).

Nodule formation appears when the number of invading pathogens is high. It involves in cell-cell co-operation. The entrapped foreign matter is in the center of the forming nodules. The nodule traps microorganisms to destroy by secretory humoral defense molecules from the cell in stress condition such as low oxygen and nutrients produced by the prophenoloxidase activating system (Jiravanichpaisal *et al.* 2006).

1.3.2 Humoral responses

1.3.2.1 Coagulation system / Clotting system

The hemolymph coagulation in crustacean is a process that prevents dissemination of bacteria throughout the body and loss of hemolymph through breaks in the exoskeleton (Martin *et al.* 1991). It is a proteolytic cascade which is activated by microbial cell wall components.

The coagulation process in crayfish and horseshoe crab has been reported in different mechanisms. In crayfish (*Pacifastacus leniusculus*), coagulation is depended on the transglutaminase (TGase)-mediated crosslinking of a clotting protein in plasma (Hall *et al.* 1999). The crayfish clotting protein (CP) is a dimeric lipoprotein containing both glutamine and lysine side chains, that are recognized and covalently linked to each other Ca^{2+} dependent TGase. In crustacean, CP is synthesized in hepatopancreas and released into hemolymph. They were found in many species such as the lobster (*Panulirus interruptus*), the freshwater crayfish and *P. monodon*. On the other hand, coagulation in horseshoe crab (*Tachpleus tridentatus*) is regulated by proteolytic cascade and activated by the elicitors through specific recognition proteins (Muta *et al.* 1993).

1.3.2.2 Prophenoloxidase (proPO) system

The proPO activating system or melanization is a major innate defense system in invertebrates. The proPO activating system is composed of several proteins involved in melanin production, cell adhesion, encapsulation, and phagocytosis (Söderhäll and Cerenius 1998). The proPO cascade is controlled by phenoloxidase (PO) and produce melanin as a final product. This cascade is activated by very low amounts of bacterial cell wall components such as peptidoglycans, lipopolysaccharides and β-glucans from microorganisms via pattern recognition proteins (PRPs) (Hernández-López et al. 1996; (Söderhäll and Cerenius 1998).

Briefly, activation of a serine protease cascade leads to the conversion of the proPO-activating enzyme (PPAE) to an active proteinase that converts the inactive proPO into active PO, a key enzyme in melanin synthesis. PO catalyzes the oxidation of tyrosine to produce toxic quinone substances that lead to the formation of melanin. The melanin can bind to the surface of bacteria and increase the adhesion of hemocytes to bacteria, leading to bacterial removal by nodule formation (D. 2002, Cerenius *et al.* 2008) (Figure 1.9).

The proPO system is controlled by serine protease inhibitors. In crayfish, ppA is a trypsin-like proteinase presenting as an inactive form in the hemocyte granules. After degranulation, the enzyme is released together with proPO and becomes an active form in the presence of microbial elicitors. The active ppA can convert proPO to an active form, phenoloxidase (PO) (monophenyl L-dopa: oxygen oxidoreductase; (Aspan *et al.* 1995)

PO is a copper-containing protein and a key enzyme in melanin synthesis (Söderhäll and Cerenius 1998, Shiao *et al.* 2001). It catalyses o-hydroxylation of monophenols to diphenols and oxidizes diphenols to quinones, which can polymerize nonenzymatically to melanin as a toxic to microorganisms (Söderhäll *et al.* 1986).

Melanization is usually observed by blackening of the parasite in the hemolymph or black spots on the cuticle. The melanin and intermediates in the melanin formation can inhibit growth of microbial parasites such as crayfish plague fungus, *Aphanomyces astaci* (Söderhäll and Ajaxon 1982).

In the black tiger shrimp, *P. monodon*, proPO localizes in the hemocytes. Gene silencing studies of proPO activating enzyme (*Pm*PPAE1 and *Pm*PPAE2), showed that the significant reduction of the PO activity resulted in the higher mortality rate and bacterial counted in the *V. harveyi* infection (Amparyup *et al.* 2009, Charoensapsri *et al.* 2009, 2011).
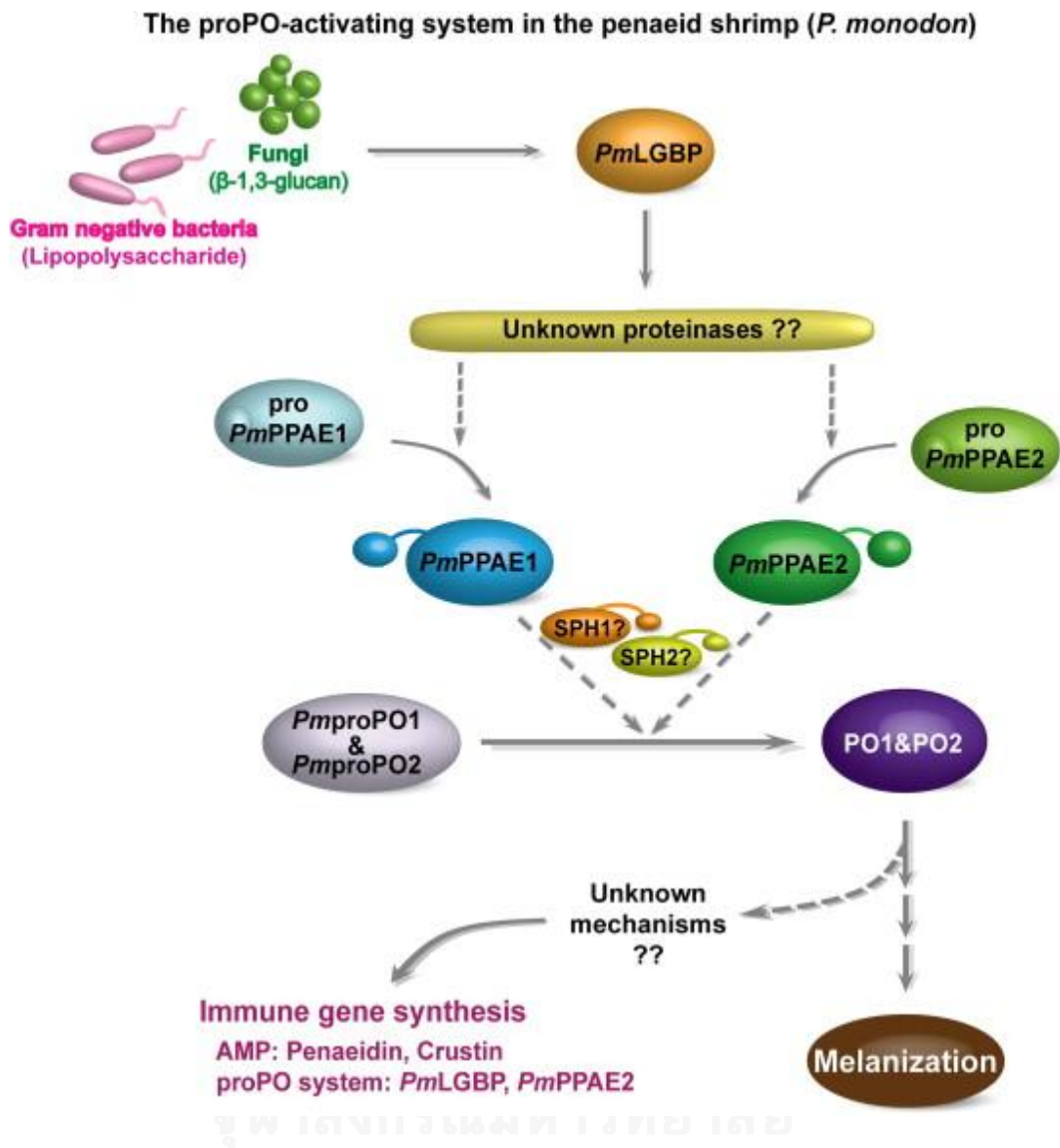
Figure 1.9 Overview of shrimp prophenoloxidase activating system

(Amparyup *et al.* 2012)

1.3.2.3 Proteinase inhibitors

Proteinase inhibitors are necessary to regulate the proteinase cascades, for example, in prophenol oxidase and coagulation systems. Some of proteinase inhibitors produced in the hemolymph may inhibit the proteinases from pathogens such microbial proteinases.

In vertebrates, the microbial infection leads to activation of the blood clotting and proPO systems. Both systems operate the cascade of serine proteinases to amplify the presence of microbial polysaccharides or wounded tissue (O'Brien and McVey 1993, Whaley and Lemercier 1993). The proteinases are regulated by proteinase inhibitors because these systems can be harmful to host if they are not limited as local and transient reactions.

In invertebrates, the blood clotting and phenoloxidase activation are regulated by serine proteinases inhibitor, for example, Serpin-1J from hemolymph of *Manduca sexta* inhibits the activity of a serine proteinase linked to prophenoloxidase activation (Jiang and Kanost 1997). Recently, the *M. sexta* serpin-6 was isolated from hemolymph of the bacteria-challenged larvae, which selectively inhibited proPO-activating proteinase-3 (PAP-3) (Wang and Jiang 2004). The results indicated that serpin-6 plays important roles in the regulation of immune proteinases in the hemolymph. It is likely that each proteinase in the PPO cascade is regulated by one or more specific inhibitors present in plasma or in hemocyte granules.

Moreover, serine proteinases inhibitors from the Kazal, Kunitz, α-macroglubulin, and serpin families have been identified and characterized in arthropod hemolymph.

Kazal-type serine proteinase inhibitors (KPIs) can be a single or multiple domain protein that linked by peptide spacers. KPIs played a potential role in immune response as a regulator of serine proteinase in several biological processes in invertebrates (Rimphanitchayakit and Tassanakajon 2010).

Kunitz-type domains are common functional constituent that found in the extracellular protein. Kunitz domains appear as multiple tandem repeats. The proteinase inhibitors in Kunitz family have been characterized from lepidopteran, dipteran, and horseshoe crab (Kanost 1999).

α-Macroglubulins (αMs) are a family of serine proteinase inhibitors. They have been identified in vertebrate and invertebrate. Clevage of the protein inhibitor bait region leads to a conformation change that traps the proteinase into inhibitor cavity

by forming **α**-Macroglubulins dimer. The conformational change also leads to covalent crosslink between proteinase and **α**-Macroglubulins (Sottrup-Jensen 1989), (Kanost 1999). The **α**-macroglobulin were found in various shrimps such as *Metanephrops japonicas*, *Fennerpenaeus chinensis*, *Farfantepenaeus paulensis*, and *P. monodon*, they are expressed in hemocytes and stored in the large granules (Rattanachai *et al.* 2004, Ma *et al.* 2010, Perazzolo *et al.* 2011, Chaikeeratisak *et al.* 2012).

Serpin-type serine proteinase inhibitors have been found in several organisms such as *Homo sapien* and other mammalians. Previously, in mammalian, serpins have functions in inflammation and blood coagulation (Marshall 1993). In insects such as *M. sexta*, *Bombyx mori*, *Drosophila melanogater*, and *Ixodes Scappularis*, serpins in hemolymph have roles in regulating innate immune pathways, including proPO activation system and Toll pathway (Zou *et al.* 2009). From previous reports, the *Pm*SERPINB3 from *P. monodon* hemocyte of *V. harveyi* infected shrimp was identified (Somboonwiwat *et al.* 2006). *Pm*SERPIN6 responds to bacterial and viral infections, implicating its roles in regulation of shrimp immune response (Homvises *et al.* 2010). Recently, *Pm*SERPIN8 was found to be up-regulated after *V. harveyi* infection and can inhibit proPO activation (Somnuk *et al.* 2012).

1.3.2.4 Antimicrobial peptides

Antimicrobial peptides (AMPs) are the part of innate immunity and play as a first line of defense against microorganisms. AMPs have unique structural properties that allow the permeation and disruption of target membranes (Hancock *et al.* 2006). Some antimicrobial peptides are produced constitutively while others are induced in response to infection or inflammation. They found in many microorganisms such as bacteria, virus, yeast, eukaryotic parasites, and fungi including human (Boman 2003, Hancock *et al.* 2006). The AMPs are diverse and ubiquitous. They tend to be small molecules (<30 kDa) less than 150-200 amino acid residues, and have amphipathic structure and cationic property specialized at attacking particular microbial classes. Most AMPs adopt an amphipathic secondary structure that is essential for their antimicrobial action (Bulet *et al.* 2004). They are active in broad spectrum antimicrobial activity against microorganisms. Moreover, the highest concentrations of antimicrobial peptides are found in animal tissues exposed to microbes or cell types that are involved in host defense (Zasloff 1987, Diamond *et al.* 1991). For example, epithelial surfaces secrete antimicrobial peptides from both barrier epithelia and

glandular structures (Jones and Bevins 1992, Ouellette and Selsted 1996). Phagocytic cells contain several types of storage organelles (granules) for microbicidal substances and digestive enzymes (Levy 1996, Ganz and Lehrer 1997). In the process of phagocytosis, granules fuse to phagocytic vacuoles that contain ingested microbes, thereby exposing the microbes to very high concentrations of microbicidal and digestive substances. Other granules are secreted into the extracellular fluid where their contents kill microbes or inhibit their multiplication. Both types of granules contain abundant antimicrobial peptides (Selsted *et al.* 1984, Ganz *et al.* 1985, Cowland *et al.* 1995).

The AMPs are divided into four sub-groups on the basis of their amino acid composition and structure. The first sub-group is small anionic antimicrobial peptide rich in glutamic and aspartic acid that are required zinc as a cofactor for antimicrobial activity and can act against Gram-positive and Gram-negative bacteria such as Maximin H5 from amphibians, Dermcidin from humans. The second sub-group is linear cationic **α**-helical peptides that contain ~290 short cationic peptides that lack in cysteine residues and sometimes have a hinge in the middle such as ceropin, magainin, CAP18, LL37, and pleurocodin (Tossi *et al.* 2000). The third sub-group is cationic peptides which are rich in specific amino acid (Otvos 2002) such as bactenecins, hymenoptaecin, coleoptercin and indolicidin. The fourth sub-group is anionic and cationic peptides (~380 members) containing cysteine residues and form disulphide bonds and stable **β**-sheet such as a diverse family of defensins, protegrin and brevinin (Brogden 2005).

Mechanisms of antimicrobial peptide

Antimicrobial mechanism studies showed that AMPs kill bacteria by disrupting membranes, interfering the metabolism and acting on the cytoplasmic components (Brogden 2005).

Antimicrobial activity can be divided into two modes of action which are intracellular antimicrobial peptide activity and transmembrane pore-forming mechanism.

Intracellular killing is the mechanism that antimicrobial peptides penetrate into the cell and bind the intracellular molecules that crucial to cell living. The peptides can inhibit cell wall synthesis, nucleic acid synthesis, protein synthesis, enzymetic activity or alter cytoplasmic membrane septum formation (Figure 1.10).
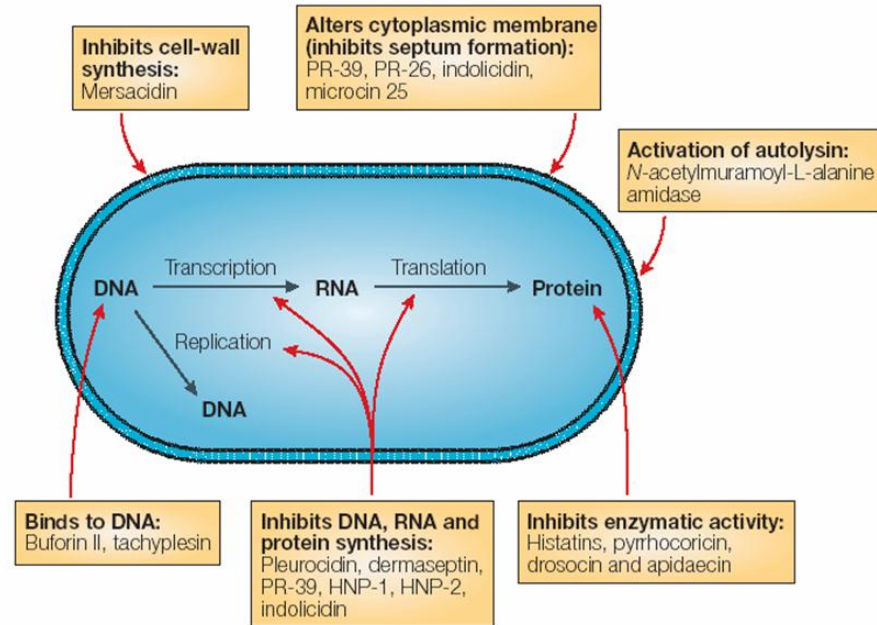
Figure 1.10 Mode of action for intracellular antimicrobial peptide activity (Brogden 2005)

On the other hand, the transmembrane pore-forming mechanism can disrupt membrane and kill the target microbes via various modes of action (Figure 1.11).

The first model is the barrel-stave that peptides insert in the bilayer, associate and form a pore. The peptides line the pore lumen in a parallel direction relative to the phospholipid chains, which remain perpendicular to the bilayer plane (Figure 1.11A). The second model is carpet-like model which peptides adsorb parallel to the bilayer and, after reaching sufficient coverage, produce a detergent-like effect that disintegrates the membrane. In this model, specific peptide–peptide interactions are not required (Figure 1.11B). The Third model is toroidal model which peptides insert perpendicularly in the bilayer, but instead of packing parallel to the phospholipid chains, peptides induce a local membrane curvature in such a way that the pore lumen is lined partly by peptides and partly by phospholipid head groups. A continuity between inner and outer leaflets is established (Figure 1.11C).
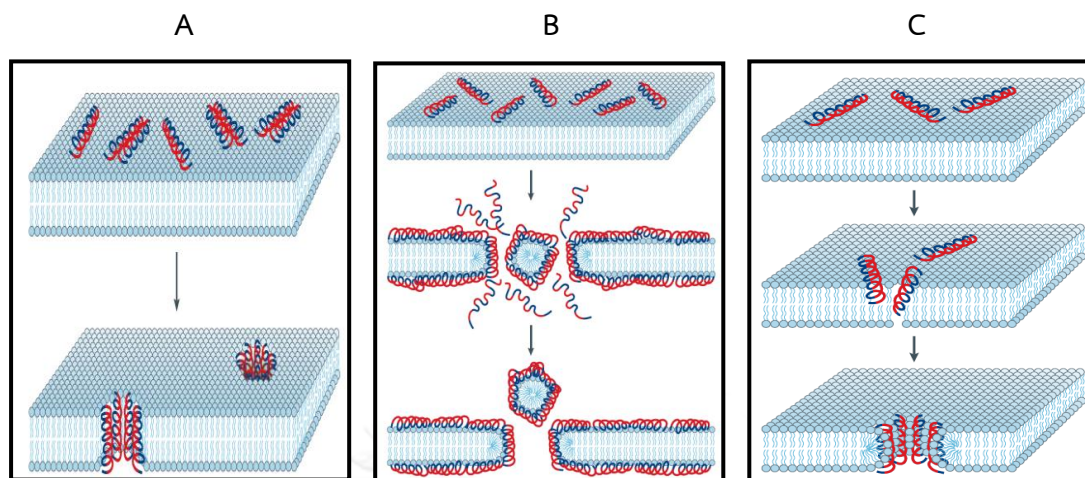
Figure 1.11 Transmembrane pore-forming mechanisms of AMPs. (A) The barrel-stave model, (B) The carpet model, and (C) The toroidal model (Brogden, 2005).

In many cases, the mechanism of killing bacteria is not known. In general, the antimicrobial activity of these peptides is determined by measuring the minimal inhibitory concentration (MIC), which is the lowest concentration of antimicrobial peptide that inhibits bacterial growth. These peptides appear to be bacteriocidal (bacteria killer) or bacteriostatic (bacteria growth inhibitor).

Several antimicrobial peptides from crustaceans have been reported. In 1997, the calliectin in the hemolymph of blue crab (*Callinectes sapidus*) was reported to have antimicrobial activity (Khoo *et al.* 1999). Many antimicrobial peptides have been identified in shrimps such as penaeidins, stylicin, lysozyme, anti-lipopolysacchasride factor (ALFs) and crustins (Rolland *et al.* 2010, Tassanakajon *et al.* 2011).

Penaeidin is the first reported shrimp AMPs found in Pacific white shrimp *L. vannamei* (Destoumieux *et al.* 1997) and exhibited antifungal and Gram-positive antibacterial activities. Later, penaeidin were found in the Atlantic white shrimp *L. setiferus* (Cuthbertson *et al.* 2004), the chinese shrimp *F. chinesis* (Kang *et al.* 2004) and the black tiger shrimp *P. monodon* (Supungul *et al.* 2004).

Anti-lipopolysacchasride factor (ALF) was found in hemocytes of horseshoe crabs, *Limulus polyphemus* (LALF) and *Tachyoleus tridentatus* (TALF) (Tanaka *et al.* 1982, Morita *et al.* 1985). ALFs exhibited the lipopolysaccharide (LPS)-mediated activation of *Limulus* coagulation system (Morita *et al.* 1985). So far, ALFs have been

identified in many shrimp species such as *L. vannamei* (Gross *et al.* 2001), *F. chinesis* (Liu *et al.* 2005) and *P. monodon* (Somboonwiwat *et al.* 2005). ALF has antiviral and antibacterial activity against both Gram-positive and Gram-negative bacteria.

Other AMPs such as lysozyme, histones, C-type lectin, peritropins, anionic hemocyanins, etc., have been isolated and characterized in penaeid shrimp (Destoumieux *et al.* 1997).

1.4 Crustin

Crustin is an antimicrobial peptide that was identified in many crustacean species including *L. vannamei, L. setiferus* (Bartlett *et al.* 2002), *F. chinesis* (Zhang *et al.* 2007) and *P. monodon* (Supungul *et al.* 2004, Amparyup *et al.* 2008, Supungul *et al.* 2008). The first identified crustin was an 11.5 kDa cationic and hydrophobic protein that found in the hemocytes of shore crab, *Carcinus maenas* (Relf *et al.* 1999) named as carcinin. The activities of carcinin were characterized against Gram-positive bacteria. Recently, there are more than 50 crustins or crustin-like peptides were reported in dacapods such as crabs, crayfish, lobsters, and shrimp (Brockton and Smith 2008).

Crustin is mainly found in the plasma and hemocyte granules of shrimps. In previous review, crustin is a cationic cysteine-rich antimicrobial peptide that contains a single whey acidic protein (WAP) domain at the carboxyl terminus and 50 amino acid residues with eight cysteine residues and forms a four-disulphide core (4-DSC) tightly packed structure (Valerie *et al.* 2008). The WAP domain functions as proteinase inhibition (Sallenave 2000) and antimicrobial activity (Wiedow *et al.* 1998, Shugars 1999). The WAP discovered in whey fraction of mammalian milk. Analysis of numerous WAPs in vertebrates reveals a high degree of similarity between the WAP domain structures (Ranganathan *et al.* 1999). The region between the signal sequence and WAP domain is variable but conforms to one of a small number of distinct structural patterns with regard to the presence or absence of other domains.

From the review (Smith et al., 2008), they classified crustin into three subgroups based on the structure of the central region (Figure 1.12). Type I crustin contains cysteine-rich region and the WAP domain which is an incomplete four-disulphide core (4-DSC). Type I crustins were found in crabs, lobsters, and crayfish (Stoss *et al.* 2004, Hauton *et al.* 2006, Brockton *et al.* 2007, Christie *et al.* 2007, Jiravanichpaisal *et al.* 2007). Type II crustin contains a long glycine-rich region between signal sequence and cysteine-rich region and the WAP domain. These crustins mainly present in shrimps. They are often arranged as repeat VGGGLG motifs that vary in number from 5 to 8. However, some Type II crustin from *P. monodon* (Amparyup *et al.* 2008) contains 22 glycine residues, and do not show the same VGGGLG repeat. Type III crustin contains only the WAP domain called single-whey acidic domain (SWD) protein. Type III crustins are also present in shrimp.
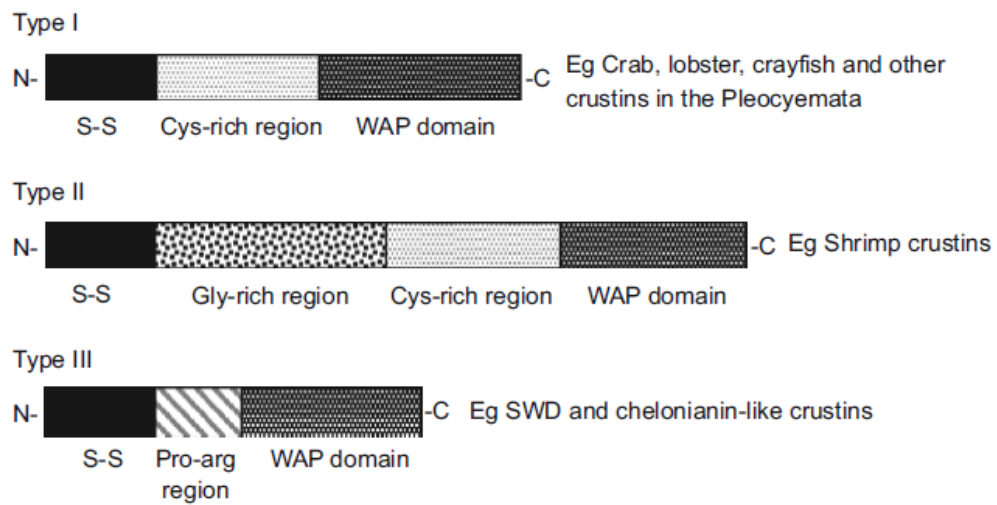
Figure 1.12 Schemetic representation of domain organization of the three main crustin types from decapods (Brockton and Smith 2008).

Crustin homologs have been identified from Expressed Sequence Tag (EST) database of cDNA libraries from *L. vannamei* and *L. setiferus* (Bartlett *et al.* 2002), the kuruma shrimp, *M. japonicas* (Rattanachai *et al.* 2004) and *P. monodon* (Supungul *et al.* 2004, Supungul *et al.* 2008, Tassanakajon *et al.* 2008). The previous study, reported that most crustins exhibit strong antimicrobial activity against Gram-positive bacteria.

Crustins in *P. monodon* have been identified in different isoforms (Supungul *et al.* 2004, Tassanakajon *et al.* 2008) including crustin*Pm*1, crustin*Pm*2, crustin*Pm*3-4, crustin*Pm*5, crustin*Pm*6 and crustin*Pm*7 or crustin-like antimicrobial peptide (Figure 1.13). Crustin*Pm*1 and crustin*Pm*7 are two most abundant isoforms in black tiger shrimp. Recombinant crustin*Pm*1 and crustin*Pm*7 were produced in *Escherichia coli* and characterized the functions of their antimicrobial activities (Amparyup *et al.* 2008, Supungul *et al.* 2008).

Crustin*Pm*1 contains an open reading frame of 435 bp encoding a precursor of 145 amino acids that comprises 17 amino acid signal peptides and 128 amino acid mature peptides. The peptides contain a Gly–Pro rich region at the amino-terminus and a WAP domain at the carboxyl-terminus. The recombinant crustin*Pm*1 has a molecular mass of 14.7 kDa with a predicted pI of 8.3. Crustin*Pm*1 displays

antimicrobial activity against only Gram-positive bacteria such as *Staphylococcus aureus* and *Streptococcus iniae*. The antimicrobial activity of crustin*Pm*1 was reported to be bactericidal effect (Supungul *et al.* 2008). In addition, the study of binding properties suggested that crustin*Pm*1 can bind to both Gram-positive and Gram-negative bacteria, as well as cell wall components LTA and LPS. In addition, crustin*Pm*1 can induce bacterial agglutination in some strains of bacteria. It can also change inner membrane permeability of *E. coli* strain MG1655 and induced physical change on cell surface (Krusong *et al.* 2012).

Crustin*Pm*7 contains 124 amino acid residues of the mature peptide and a signal peptide of 17 amino acid residues. The mature peptide contains a glycine-rich domain at the N-terminus and 12 conserved cysteine residues containing a single WAP domain at the C-terminus. The recombinant crustin*Pm*7 has a molecular mass of 12.96 kDa with a predicted pI of 7.81. The recombinant crustin*Pm*7 acts against both Gram-positive and Gram-negative bacteria including *V. harveyi*, a major pathogenic bacteria in shrimp aquaculture (Amparyup *et al.* 2008). In addition, the study of binding properties suggested that crustin*Pm*7 can bind to both Gram-positive and Gram-negative bacteria, as well as cell wall components LTA and LPS. Crustin*Pm*7 can induce bacterial agglutination and changes inner membrane permeability of *E. coli* strain MG1655. Scanning Electron Microscopy (SEM) presented that the change on the cell surface of *S. aureus*, *V. harveyi* and *E. coli* after treated with the recombinant crustin*Pm*7 (Krusong *et al.* 2012).

```
crustinPm1    MKGLGVILFC-VLAMASA------------------------------------------   17
crustinPm3,4  MKGVKAVILCSLLATALA-GKFRGSGTYGGGGSYGGGGSYGGGLGGGVSGGGLGGGVNGG   59
crustinPm5    MRVAGYLVVAVASVAVTDG------------------------------------------   19
crustinPm6    MKGVSVAILCCVLAAASA------------------------------------------   18
crustinPm7    MLKFVVLSVVAVAVVHA-------------------------------------------   17
              *          .   .

crustinPm1    -------------------------------------------------------      17
crustinPm3,4  GLGGGVNGGGLGGGLGGGVNGGGLGGGGAYGGGLGGGLGGGGVNGGGLGGGLGGGVQGGG    119
crustinPm5    -------------------------------------------------------QY      21
crustinPm6    -------------------------------------------------------      18
crustinPm7    -------------------------------------------------------      17

crustinPm1    ----------QSWHGGRPG----GFPG---GGRP---GGFPGGG--RPGGRP--GGFP-    51
crustinPm3,4  LGGGLGGGVHGGGLGGGLGGGVHGGGLGGGLGGGLS-GGLGGGLG--RPGGGLGRPGGGL   176
crustinPm5    IGFGVPGQGLVDSLNGLISGG---GFPG---GHFPGQGGHFPGQGGHFPGQGGNFPGQG-   74
crustinPm6    ----NERQGSNRFFNGGFGGGVNSGFGGGFGGGFPG-AGGFQGGG--FPGGFGGIGGFPG   71
crustinPm7    -------QDKGNADTRFLGG---LGVPG---GGVPGVGGGFLPGV---PGHGGVVPGGGG   61
                           *     *   *   *     *       **     *

crustinPm1    -SVTAPPASCRRWCETPENAFYCCE---SRYEPEAPVGTKILDCPKVRDTCPPVRFLAVE   107
crustinPm3,4  SPGSRGPSTCRYWCTTPEGKQYCCE---DKNEPEIPVGTKPLDCPQVRPTCP--RFQG--   229
crustinPm5    -GNYPGQGSCKYWCRSPENQYYCCDRGNNQGQGNYP-GSKPGFCPAVRDVCPPTRFGVG-   131
crustinPm6    AGISOGSSQCRYWCRNPENQVYCCE---TDLEPEGPVGTKPLDCPIVRPTCP-VSVRG-L   126
crustinPm7    -LLPGGQFBCN-YCRT-RYGYVCC--------------KPGRCPQIRDTCPGLRKGVP-   102
                       *. :* . .     **               *   ** :* .**

crustinPm1    QPVPCSSDYKCGG-LDKCCFDRCLGQHVCKPPSFY--EFFA  145
crustinPm3,4  PPVTCSHDFKCAG-LDKCCFDRCLGEHVCKPPSFYGRNVKG  269
crustinPm5    RPIQCAHDGQCYASNDKCCFDRCLGEHVCKPATYYNGR---  169
crustinPm6    RPITCSNDYKCGG-VDKCCYDRCLQENVCKPPS-----FFG  161
crustinPm7    ---ICRQDTCFG-SDKCCFDTCLNDTVCKPIV---AGSQG  136
                *   *  .    ****:  ** : ****
```

Figure 1.13 Multiple alignment of crustin amino acid sequences of *P. monodon*. (*) indicates amino acid identify and (.) and (:) indicate amino acid similarity. The signal peptides, glycine-rich regions, cysteine rich regions, and WAP domains are indicated by blue, pink, green and yellow, respectively.

1.5 Regulators of the Toll and Immune deficiency (Imd) pathways in innate immune response

The innate immune response is the first line of defense against microbial infections, found in insects and mammal. Drosophila has been developed as an attractive model organism for studying the innate immune response in order to understand the basic mechanisms of pathogen recognition and activation of response (Hoffmann and Harshman 1999). Drosophila was chosen as a model organism because it does not have adaptive immunity. Two separated intracellular signal transduction pathways, Toll and immune deficiency (IMD) are responsible for controlling the antibacterial and antifungal responses in *Drosophila melanogaster* (Lemaitre *et al.* 1995, Lemaitre *et al.* 1996). The Toll and Imd pathways were stimulated by recognition of pathogen associated molecules, such as peptidoglycans to induce antimicrobial responses. These two pathways are homologous to the mammalian Toll-like receptor (TLR) and tumor necrosis factor receptor (TNFR) signaling pathways, respectively, and are essential for Drosophila to survive infection. Toll pathway involves in Fungal and Gram-positive bacterial infections, while the signaling cascade of Imd pathway was stimulated by Gram-negative bacterial infections but not the fungal infections. The genetic requirements of the signaling components in these two pathways are independent (Lemaitre *et al.* 1995) (Figure 1.14).
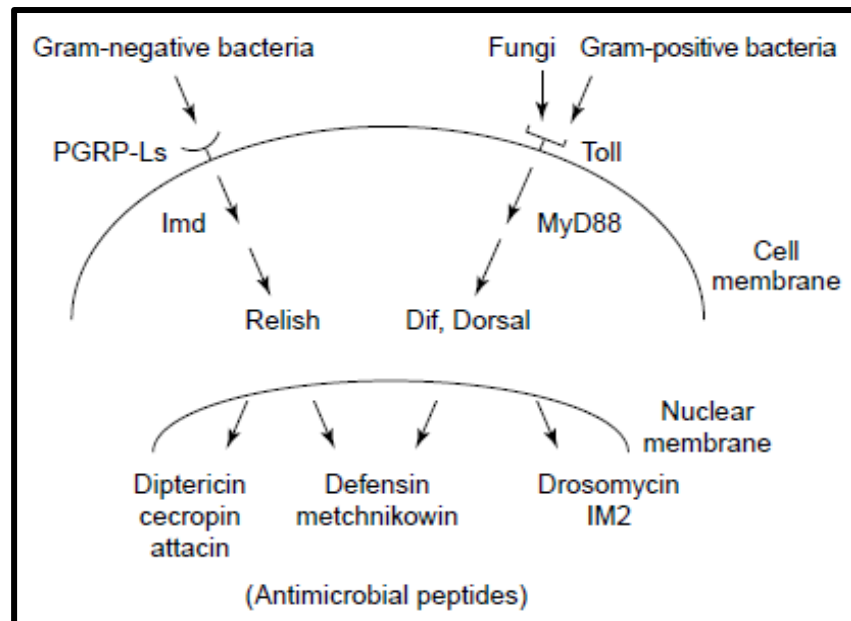
Figure 1.14 The two pathway model for the inducible expression of antimicrobial peptide genes in Drosophila (Tanji and Ip 2005).

1.5.1 Toll pathway

In *D. melanogaster*, the Toll pathway is stimulated by Gram-positive bacteria and fungi. Gram-positive bacteria is mediated through the extracellular peptidoglycan recognition protein (PRGP)-SA (Michel *et al.* 2001), PGRP-SD (Bischoff *et al.* 2004), and Gram-negative binding protein-1 (GNBP-1) (Gobert *et al.* 2003, Wang *et al.* 2006) (Figure 1.15). High-level expression of PGRP-SA and GNBP-1 leads to constitutive activation of the Toll pathway (Gobert *et al.* 2003). The study suggested that Gram-positive bacteria-associated molecules are recognized by multiple host proteins, which then work cooperatively to stimulate the Toll pathway. Fungi activate the Toll pathway via a serine protease, and a protease inhibitor (Levashina *et al.* 1999, Ligoxygakis *et al.* 2002). A Gram-positive or fungal infection triggers the activation of the Toll pathway, which leads to the production of antimicrobial peptides (AMPs) (Aggarwal and Silverman 2008, Hetru and Hoffmann 2009). The Toll pathway plays a role in the cellular immune response, which includes the phagocytosis, and the encapsulation and killing of parasites (Hultmark 2003).

The upstream regulatory cascades, the Gram-positive bacterial and fungal responses lead to the processing Spätzle. Previous report showed that cleavage of Spätzle as a ligand can bind to Toll and triggers Toll pathway. They suggested that a function of Spätzle is to induce the dimerization of Toll (Weber *et al.* 2003, Hu *et al.* 2004). Three cytoplasmic proteins including MyD88, Tube and Pelle were found under the cell membrane, when Toll was stimulated MyD88 and Tube are adaptor proteins and Pelle is serine–threonine kinase. These three proteins form the signaling complex under the cell membrane. When the receptor is active, the Toll–interleukin-1 (IL-1) receptor domain (TIR) of Toll can bind to the TIR domain of MyD88 (Horng and Medzhitov 2001, Tauszig-Delamasure *et al.* 2002, Sun *et al.* 2004). The activated Pelle causes a formation of Dorsal–Cactus and Dif–Cactus complexes. Dif and Dorsal are NF-kB homologs. After degradation of Cactus, Dif and Dorsal translocate to the nucleus and bind to the kB-related sequence of antimicrobial peptide genes (Reichhart *et al.* 1993).
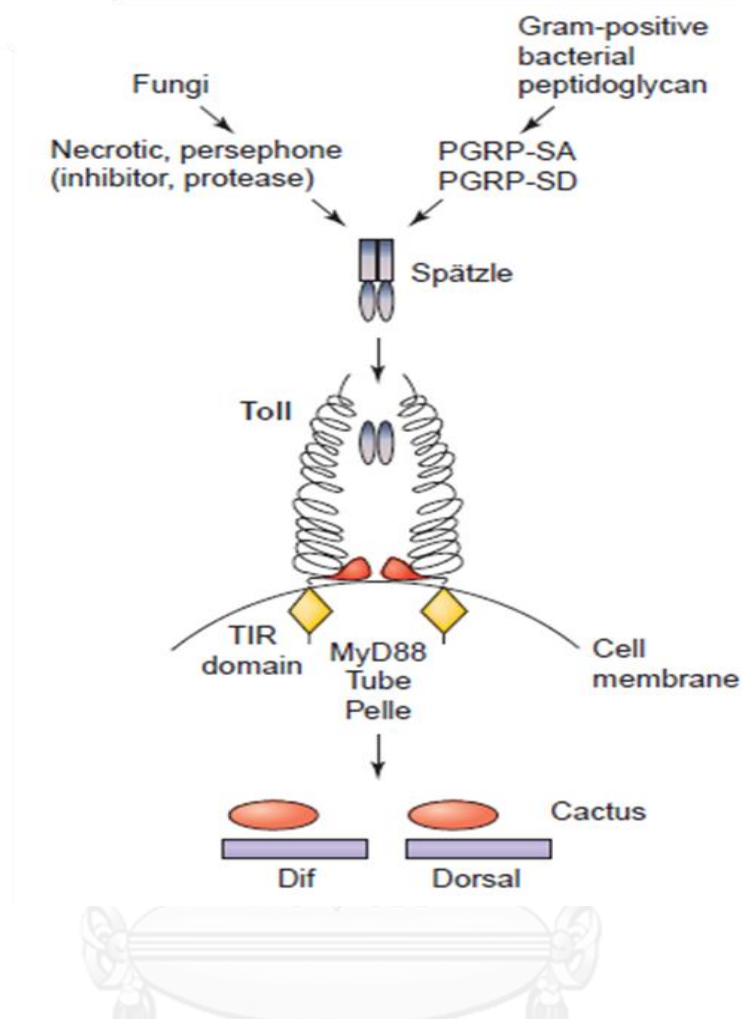
Figure 1.15 Stimulation of the Toll pathway in Drosophila by two upstream pattern-recognition mechanisms. Abbreviations: IRAK, IL-1R-associated kinase; LBP, LPS binding protein (Tanji and Ip 2005).

1.5.2 Immune deficiency (Imd) pathway

The Immune deficiency (Imd) pathway is activated mainly by Gram-negative bacteria but not fungi. Recognition of an infection leads to a signaling cascade that typically results in the activation of antimicrobial peptides (AMPs) genes. Imd is an adaptor protein homolog to the TNFR interacting protein receptor interacting protein (RIP) (Georgel *et al.* 2001). In Drosophila, Imd pathway is triggered by pattern-recognition receptor of Gram-negative bacteria by the receptor peptidoglycan recognition protein (PGRP-LC) (Choe *et al.* 2002, Gottar *et al.* 2002). Binding of peptidoglycan of Gram-negative bacteria to PGRP-LC or PGRP-LE stimulates the Imd pathway.

Stimulation of Imd pathway results in at least three downstream events (figure 1.16). First, TAK1 (transforming growth factor-β activated kinase 1) stimulates IKK complex-dependent cleavage and activation of Relish that induce NF-kB activation. Second pathway is the FADD (Fas-associated protein with death domain) – Dredd pathway that also activates Relish (Leulier *et al.* 2000, Balachandran *et al.* 2004). This branch also has a negative regulatory loop that involves the caspase inhibitor Dnr-1. Dnr-1 keeps the FADD–Dredd branch inactive until infection occurs. Previous work showed that Dnr-1 can inhibit the caspase Dredd in an S2 cell assay (Foley and O'Farrell 2004). Third pathway is the activation through TAK1 of the JNK (c-Jun N-terminal kinase) pathway. The JNK cascade is one branch of the Imd pathway. This pathway regulates immune-induced genes, such as puckered, flightin, punch, and relish, wound healing and melanization (Boutros *et al.* 2002, Park *et al.* 2004). The JNK pathway is also negatively regulated by Relish. The protein level of Relish, and thus the responsiveness of the Imd pathway, might also be regulated by an ubiquitin–proteasome complex.
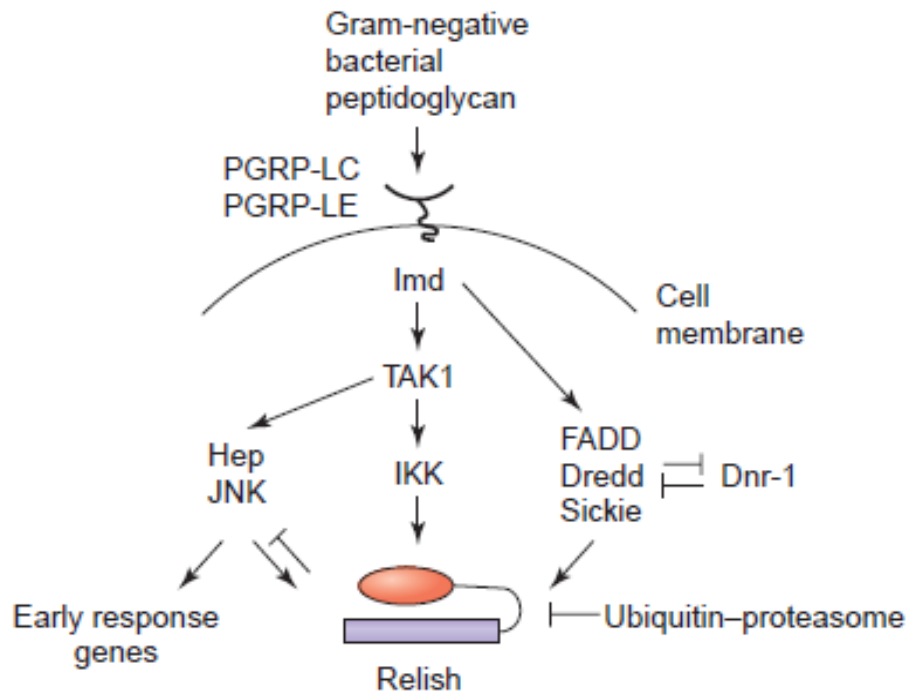
Figure 1.16 Activation and branching of the Imd pathway (Tanji and Ip 2005).

1.6 Bacterial cell wall components

Bacteria contain a variety of cell-surface structures. The cell wall is responsible for unique biological properties. It is an essential structure that protects the cells from attack by antibiotic or the immune system. Prokaryotes usually live in dilute environments such that the accumulation of solutes inside the prokaryotic cell cytoplasm greatly exceeds the total solute concentration in the outside environment. Thus, the osmotic pressure against the inside of the plasma membrane may be the equivalent. Since the membrane is a delicate, plastic structure, it must be restrained by an outside wall made of porous, rigid material that has high tensile strength. The major component of the bacterial cell wall is peptidoglycan or murein. Peptidoglycan is a large polymer of disaccharides (glycan) cross-linked by short chains of amino acids (peptide). Bacterial peptidoglycans are composed of two derivatives of glucose, that are N-acetlymuramic acid (NAM) and N-acetylglucosamine (NAG). They are synthesized in the cytosol of the bacteria and transported across the cytoplasmic membrane by a carrier molecule. There are two main types of bacterial cell walls, those of Gram-positive bacteria and Gram-negative bacteria (Demchick and Koch 1996).

1.6.1 Gram-positive bacteria

Gram-positive cell walls consist of almost 95% peptidoglycan layers and may also include other components such as teichoic and lipoteichoic acids and complex polysaccharides. Teichoic acids are important factors in virulence and water-soluble polymers of ribitol and glycerol phosphates, which are covalently connected to the peptidoglycan. However, a unique component of the gram-positive cell wall is lipoteichoic acid. It has a fatty acid and its adhesive properties assist in its anchoring to the cytoplasmic membrane (Figure 1.17).
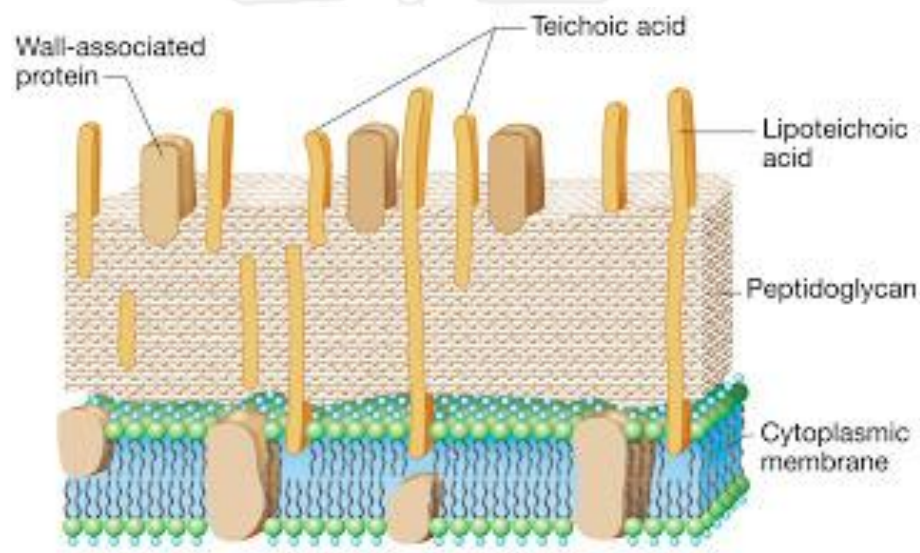
Figure 1.17 Structure of the Gram-positive bacterial cell wall. The wall is relatively thick and consists of many layers of peptidoglycan interspersed with teichoic acids that run perpendicular to the peptidoglycan sheets (Woese 1987).

1.6.2 Gram-negative bacteria

Gram-negative cell walls contain a peptidoglycan layer surrounded by a membranous structure called the outer membrane, which is unique component to Gram- negative bacteria such as lipopolysaccharide (LPS). It is toxic to animals. There are no teichoic or lipoteichoic acids in the Gram- negative cell wall. The area between the external surface of the cytoplasmic membrane and the internal surface of the outer membrane is referred to as the periplasmic space. This space is a compartment containing a variety of hydrolytic enzymes including proteases, phosphatases, lipases, nucleases, and carbohydrate-degrading enzymes, which are important to the cell for the breakdown of large macromolecules for metabolism (Figure 1.18).
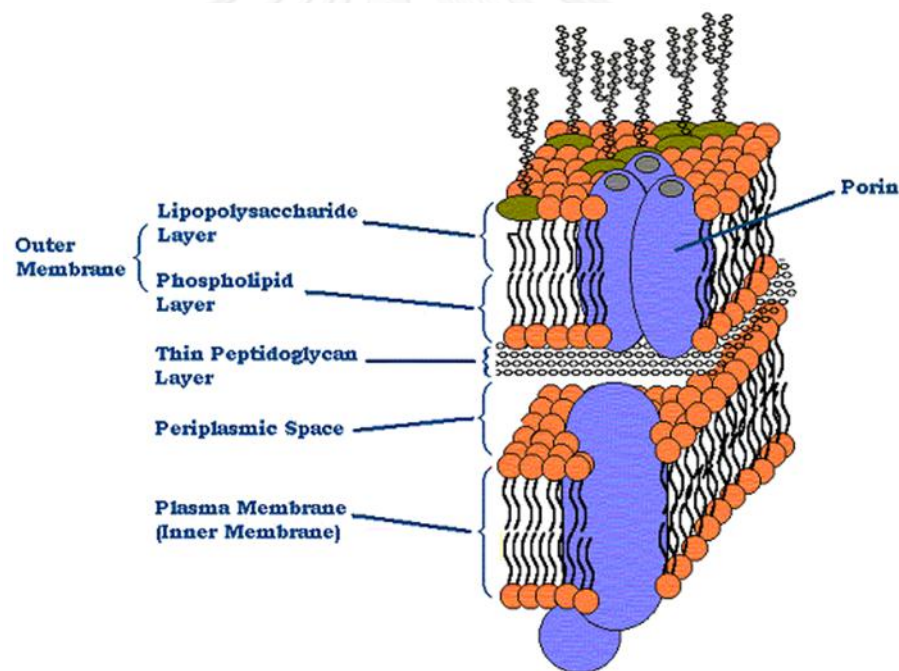
Figure 1.18 Structure of the Gram-negative cell wall. The Gram negative cell wall consists of an outer membrane that is outside of the peptidoglycan layer. The outer membrane is attached to the peptidoglycan sheet by a unique group of lipoprotein molecules (Woese 1987).

1.7 Objective of this thesis

On one hand, this work aims to study activities and binding properties of the recombinant crustin*Pm*1 and crustin*Pm*7, as well as determine the secondary structure of the two crustins and crystallize the recombinant crustin*Pm*1. On the other hand, this research aims to understand regulation of crustin*Pm*1 and crustin*Pm*7 gene expression.

In this work, crustin*Pm*1 and crustin*Pm*7 were cloned and produced in *Pichia pastoris* expression system in order to obtain the recombinant proteins in soluble form. Antibacterial activity and proteinase inhibitor activity of rcrustin*Pm*1 and rcrustin*Pm*7 were tested. Binding properties of the two crustin isoformed to bacterial cell wall components and lipid were performed. Secondary structure of rcrustin*Pm*1 and rcrustin*Pm*7 was determined by circular dichroism spectroscopy. In addition, screening of crystallization conditions of rcrustin*Pm*1 was carried out in order to obtain a crystal for three dimensional structure determination by X-ray crystallography. To investigate regulatory pathways of crustin*Pm*1 and crustin*Pm*7, expression levels of several genes in shrimp immunity were measured by quantitative real time RT-PCR after *V. harveyi* and *S. aureus* challenges. Effect of such immune pathway on expression levels of crustin*Pm*1 and crustin*Pm*7 were confirmed by RNA interference experiment.

CHAPTER II

MATHERIALS AND METHODS

2.1 Equipments and Chemicals

2.1.1 Equipments

-80 °C Freezer (Thermo Electron Corporation)

-20 °C Freezer (Whirlpool)

4 °C Freezer (Whirlpool)

96-well cell culture cluster, flat bottom with lid (Costar)

96-well flat bottom, certified RNase/DNase Free, Polypropylene (Costar)

96- Well Hanging Drop Vapor Diffusion Plate (Hampton Research)

Amicon Ultra-15 10K concentrators (Millipore)

Autoclave model # MLS-3020 (SANYO E&E Europe (UK Branch) UK Co.)

Autoclave model # MLS-3750 (SANYO E&E Europe (UK Branch) UK Co.)

Automatic micropipette P10, P20, P200 and P1000 (Gilson Medical Electronic S.A. France)

Automatic micropipette SL-5000XLS (Mettler Toledo)

Balance PB303-S (Metter Toledo)

Biophotometer (Eppendorf)

Centrifuge JA-14 (Beckman)

Centrifuge 5417C (Eppendorf)

Centrifuge 5804R (Eppendorf)

Gel documention System (GeneCam FLEX1, SYNGENE)

GelMate2000 (Toyobo)

INNOVA44, Incubator shaker 4080 (New Brunswick Scientific)

Incubator shaker 4080 (New Brunswick Scientific)

Incubator 30 °C (Heraeus)

Incubator 37 °C (Memmert)

JASCO J-715 CD Spectropolarimeter

Laminar Airflow Biological Safety Cabinet Class II Model NU-440-400E (NuAire, Inc., USA)

Microcentrifuge tube 0.6 and 1.5 ml (Axygen® Scientific, USA)

Minipulser electroporation system (Bio-RAD)

PCR Mastercycler (Eppendorf AG, Germany)

PCR thin wall microcentrifuge tube 0.2 ml (Axygen® Scientific, USA)

pH meter, pH 900 (Precisa, USA)

Pipette tips 10, 20, 100, 1000 µl (AxygenMCT-150-C, USA)

Power supply, Model Power PAC 300 (Bio-RAD Laboratories)

SpectraMax M5 Multi-Mode Microplate Reader (Molecular Devices)

Trans-Blot® SD (Bio-RAD Laboratories)

VDX™ Plate (Hampton Research)

Water bath (Memmert)

Whatman® 3 MM Chromatography paper (Whatman International Ltd., England)

2.1.2 Chemicals

1,2-dipalmitoly-sn-glycero-3-phosphate sodium salt (Sigma)

2-Mercaptoethanol, C_2H_6OS (Fluka)

5-Bromo-4-chloro-indolyl phosphate (BCIP) (Fermentas)

Absolute ethanol, C_2H_5OH (Hayman)

Absolute methanol, CH_3OH (Scharlau)

Acetic acid glacial, CH_3COOH (Merck)

Acrylamide, C_3H_5NO (Merck)

Agar powder, Bacteriological (Hi-media)

Agarose, (low EEO, Molecular Biology Grade (Research Organics)

Alkaline phosphatase-conjugated goat anti-mouse IgG (Millipore)

Anti-Histidine Tagged Antibody, clone HIS.H8 | 05-949 (Millipore)

Anti-Mouse IgG (Fab specific)–Peroxidase antibody produced in goat (sigma)

Albumin from bovine serum, fatty acid free (Sigma)

Ammonium persulfate, $(NH_4)_2S_2O_8$ (USB)

Bacto yeast extract (Hi-media)

Biotin (Sigma)

Bovine Serum Albumin (BSA)

Chloroform, $CHCl_3$ (Merck)

Coomasie brilliant blue R-250 (Sigma)

Diethyl pyrocarbonate (DEPC), $C_6H_{10}O_5$ (Sigma)

Difco Yeast Nitrogen Base w/o Amino Acids (Becton)

Dipotassium hydrogen phosphate, K_2HPO_4 (Merck)

Ethylene diamine tetraacetic acid disodium salt dehydrate (EDTA) (Ajax)

GeneRuler™ 100 bp DNA ladder (Fermentas)

Glycine, USO Grade, NH_2CH_2COOH (Research organics)

Hydrochloric acid (HCL) (Merck)

Imidazole (Fluka)

Isopropanol, C_3H_7OH (Merck)

Lipopolysaccharides from *Escherichia coli* 0111:B4 (Sigma)

Lipoteichoic acid from *Staphylococcus aureus* (Sigma)

Lithium sulfate monohydrate (Hampton Reserch)

MES, Free acid monohydrate (Biobasic INC.)

Millipore membrane filter 0.22 and 0.45 µm (Millipore)

Nitro blue tetrazolium chloride (NBT), $C_{40}H_{30}Cl_2N_{10}O_6$ (Fermentus)

Ni Sepharose 6 Flas Flow (GE Healthcare)

N,N,N',N'-Tetramethylethylenediamine (TEMED) (BDH)

Peptone from meat (Merck)

Prestain protein molecular weight marker (Fermentas)

Polyethylene glycol (PEG) (Hampton Reserch)

Potassium dihydrogen phosphate, KH_2PO_4 (Merck)

Skim milk powder (Hi-media)

Sodium chloride, NaCl (Ajax)

Sodium dodecyl sulfate, $C_{12}H_{25}O_4SNa$ (Sigma)

Tris (Vivantis)

Tween™-20 (Fluka)

2.1.3 Kits

Additive Screen (Hampton Research)

Geneaid High-speed Plasmid Mini Kit

Index (Hampton Research)

PCT™ Pre-Crystallization Test (Hampton Research)

Pierce® BCA Protein Assay Kit (Thermo scientific)

PIP Strips™ (Echelon)

Qiaprep® Spin Miniprep Kit (QIAGEN)

SaltRx I&II (Hampton Research)

Tissue Total RNA Purification Mini Kit (Favogen)

Wizard III, and IV random sparse matrix crystallization screen (Emerald

Biosystems)

2.1.4 Proteinases and Substrates

N-succinyl-Ala-Ala-Ala-*p*-nitroanilide (Sigma)

N-succinyl-Ala-Ala-Pro-Phe-*p*-nitroanilide (Sigma)

N-benzoyl-Phe-Val-Arg-*p*-nitroanilide (Sigma)

Trypsin (Sigma)

Chymotrypsin (Sigma)

Subtilisin A (Sigma)

Elastase (USBiology)

2.1.5 Enzymes

*Eco*R I (Biolabs)

Not I (Biolabs)

Taq DNA polymerase (Fermentas)

T4 DNA ligase (Fermentas)

SsoFast™ EvaGreen® Supermix (BIO-RAD)

2.1.6 Vector

pPIC9K (Invitrogen)

2.1.7 Bacterial strains

Bacillus subtilis

Escherichia coli strain 363

Micrococcus luteus

Pichia pastoris

Staphylococcus aureus

Vibrio harveyi 1526

2.2 Software

CFX Manager™ software (BIO-RAD)

ClustalW (http://www.ebi.ac.uk/Tools/msa/clustalw2/)

Graphpad Prism® version 6.0 (Graphpad software, USA Inc.)

K2D3 software (Proteins (2012) Vol 80-2)

SECentral (Scientific & Education Software)

2.3 Expression and purification of recombinant crustin*Pm*7

2.3.1 Construction of the recombinant pPIC9K_crustin*Pm*7

To obtain the complete nucleotide sequence of crustin*Pm*7 cDNA (Genbank accession no. EF654658) was cloned into *Pichia pastoris* expression vector, pPIC9K (Figure 2.1). The specific primers (forward : 5' GATGAATTCCATCATCATCATCATCACCAG GATAAAGGCAATGCCGA 3', which introduced an *Eco*R I site and a 6 x His-Tag at N-terminus, and reverse : 5' CTGCGGCCGCCTATCCCTGAGAACCTGCCA 3'), which introduced a *Not* I site at C-terminus were designed and used for PCR amplification. An open reading frame (ORF) of crustin*Pm*7 was amplified by PCR from unchallenged shrimp cDNA. PCR reaction was performed by incubating the reaction mixtures at 94°C for 2 min, followed by successive cycles at 94°C for 30 sec, 55°C for 30 sec, and 72°C for 1 min for 30 cycles. PCR product of crustin*Pm*7 gene (426 bp) was analyzed through 1.5% agarose gel electrophoresis. The crustin*Pm*7 DNA fragment was purified using NucleoSpin® Extract Kit (Macherey-Nagel). The crustin*Pm*7 DNA fragment and pPIC9K vector were digested with *Eco*R I and *Not* I for gene insertion. Then, crustin*Pm*7 fragment was ligated into pPIC9K vector with the same restriction enzymes at room temperature for 3 h and transformed into the *E. coli* strain XL-1 Blue competent. The single colony was verified by sequencing (Macrogen Inc., Korea). After that, plasmid DNA was linearized by *Sac* I and about 5-10 μg of linearized DNA was transformed into *P. pastoris* strain GS115 competent and incubated the plates at 30°C until colonies appear on plates of His$^+$ GS115 transformants. Then, screen for Mut$^+$/Mut^S phenotypes. Two different phenotypes of His$^+$ recombinant strains can be generated: Mut$^+$ (Methanol utilization plus) and Mut^S (Methanol utilization slow). Transformation of strain GS115 can yield both classes of transformants, His$^+$ Mut$^+$ and His$^+$ Mut^S, while strain KM71 yields only His$^+$ Mut^S. Finally, colonies containing crustin*Pm*7 gene were checked by direct PCR screening. The single colony was picked and dissolved in 10 μl sterile water. Glass beads (0.45 mm) were added in the solution, vortexed for 10 min, boiled for 3 min and placed on ice for 1 min. The solution was them taken for hot start PCR. PCR reaction was set up at 95°C for 2 min, followed by successive cycles at 95°C for 1 min, 54°C for 1 min, and 72°C for 1 min for 35 cycles.
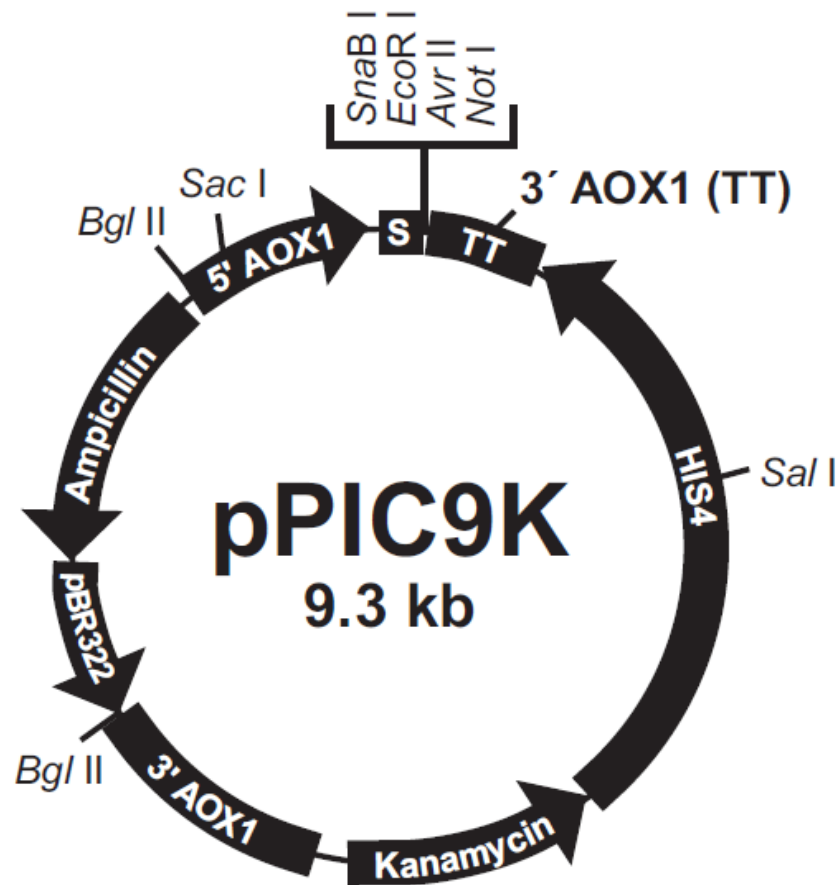
Figure 2.1 The pPIc9K vector map (Invitrogen™)

2.3.1.1 Primer design

PCR primers were designed based on based on nucleotide sequences of template DNA using SECentral program (Scientific & Educational Software). These primers should have a length of about 20 bases and considered the melting temperature, minimal self-priming, GC content and primer dimer formation.

2.3.1.2 DNA fragment extraction from agarose gel

The DNA fragment containing crustin*Pm*7 gene was eluted from the agarose gel using NucleoSpin® Extract Kit (Macherey-Nagel). The DNA band was cut from the agarose gel in minimal volume and then added 200 µl NT buffer per 100 mg gel and

melted at 55°C for 5-10 min. The solution was added into NucleoSpin® extract column and centrifuged at 11,000 rpm for 1 min for binding DNA. 600 µl of NT3 buffer was added in column and centrifuged at 11,000 rpm for 1 min 2 times for washing silica membrane. The membrane was dried by centrifuged at 11,000 rpm for 3 min. Then, the column was transferred into a new 1.5 ml microcentrifuge tube, added 15-50 µl of ultrapure water, incubated at room temperature for 10 min and centrifuged for eluting DNA at 11,000 rpm for 1 min.

2.3.1.3 Competent cell preparation and transformation

- *E. coli* competent cell preparation and transformation

The *E. coli* strain XL-1-Blue competent cells used in this study were prepared by $CaCl_2$ treatment. Briefly, the *E. coli* strain XL-1-Blue was streaked in LB agar plate and incubated at 37°C for 16-18 h. A single colony was picked into LB broth and incubated overnight at 37°C with shaking at 250 rpm as starter. The culture was inoculated in 1:100 dilution into 100 ml of LB broth and grown until OD_{600} reach 0.4-0.6. The cells were chilled on ice for 30 min. Then, cells were centrifuged at 4,000 rpm for 15 min at 4°C and washed once with 0.5 volume of cold 10 mM $CaCl_2$ solution. The pellet was resuspended in 0.1 volume of cold 100 mM $CaCl_2$ solution containing 10% (v/v) glycerol and placed on ice for 30 min. The 100 µl of competent cells were aliquoted and immediately stored at -80°C until used. For transformation, the 10 µl of ligation mixture was mixed with the 100 µl of competent cell and placed on ice for 30 min, and then the ligation mixture was heat-shocked at 42°C for 1 min and added 1ml of cold LB broth. The cell suspension was incubated at 37°C with 250 rpm shaking for 1 h, then spread on LB agar plate and incubated at 37°C for 16-18 h.

- *P. pastoris* competent cell preparation and transformation

The *P. pastoris* strain GS115 competent cells used in this study was prepared as electrocompetent cell. In brief, the *P. pastoris* strain GS115 was streaked onto YPD agar plate and incubated at 30 °C for 2-3 days. A single colony was picked into 5 ml of YPD media and incubated overnight at 30 °C with 280-300 rpm shaking. The overnight culture was diluted 1:1000 in a volume of 100 ml YPD media, and then grown at 30°C with 280 rpm for 16-18h until OD_{600} reach 1.3-1.5 and centrifuged the cells at 5,000 rpm for 5 min at 4 °C. The supernatant was discarded and the cell

pellet was resuspended with 100 ml of cold water and centrifuged again. The cell pellet was resuspended with 50 ml of cold water and centrifuged. The supernatant was discarded and the cell pellet was washed with 4 ml of 1 M cold sorbital and centrifuged as previously described. Finally, the cell pellet was washed with 200 μl of 1 M cold sorbital and aliqouted 80 μl of the fresh competent cell. For electro-transformation, the approximately 10 μl (5-20 ng) linearized plasmid was mixed with fresh competent cell and chilled on ice for 5 min. The mixture was added in 0.2 cm cold electroporation cuvette and incubated on ice for 5 min. The mixture was pulsed using Gene Pulser$^{®}$ electroporator (BIO-RAD) at constant voltage 1.5 kV. One milliliter of 1 M cold sorbital was immediately resuspended and transferred the cell mixture in a new tube. The resuspended cell was plated on selective media or MD plate and incubated at 30ºC for 3 days.

2.3.1.4 Selection of His^{+} transformants

The plates containing His^{+} transformants were screened with Geniticin$^{®}$. The His^{+} transformants on each MD plate were resuspended with 2 ml sterile water, pooled the cell suspension into a sterile centrifuge tube and vortex about 5-10 second and measured the cell density (1 OD$_{600}$ = 5×10^{7} cells/ml). The 10^{9} cells were plated onto 1 and 2 mg/ml YPD-Geniticin$^{®}$ plate and incubated at 30ºC for 2-5 days.

2.3.1.5 Screen for Mut^{+} and Mut^{s} phenotype

P. pastoris has two strains such a GS115 and KM71 strains. *P. pastoris* strains GS115 competent was used in this study, Transformation of strain GS115 can yield both classes of transformants, His^{+} Mut^{+} and His^{+} Mut^{s}, while KM71 yields only His^{+} Mut^{s} since the strain itself is Mut^{s}. Both Mut^{+} and Mut^{s} recombinants are useful to have as one phenotype may better expression of your protein than the other. Therefore we would to screen Mut^{+} and Mut^{s} phenotype. The colonies were picked by sterile capillary tube and streaked onto MM and MD agar plate respectively. Then, plates were incubated at 30 ºC for 2 days.

2.3.2 Expression of the recombinant crustin*Pm*1 and crustin*Pm*7 protein

Recombinant crustin*Pm*1 and crustin*Pm*7 was expressed in *P. pastoris* strain GS115 and the tranformants that displayed the highest expression were selected by Geneticin®. The rcrustin*Pm*1 and rcrustin*Pm*7 were streaked onto YPD agar plate and incubated at 30°C for 3 days. The single colony was picked into 5 ml of Buffered Glycerol-complex Medium (BMGY) media and incubated overnight at 30°C with 280-300 rpm shaking until the culture reaches the optical density at 600 nm approximately 4. The overnight culture was diluted 1:100 in a volume of 100 ml of BMGY at 30 °C with shaking at 280 rpm and cells were harvested by centrifugation at 8,000 rpm for 10 min. Then, the supernatant was discarded and the cell pellet was resuspended in 1/5 of the original volume of Buffered Methanol-complex Medium (BMMY) and incubated at 30 °C with shaking. Expression of crustin*Pm*s were induced by adding 100% methanol to a final concentration of 0.5% every 24 h for 3 days. The cells were centrifuged and the supernatant was kept for purification.

2.3.3 Purification of the recombinant crustin*Pm*1 and crustin*Pm*7 protein

The rcrustin*Pm*1 and rcrustin*Pm*7 protein were expressed with His-tags fusion, so Ni-NTA affinity chromatography column (GE Healthcare) was used for protein purification.

Firstly, the soluble protein was filtered with membrane filter 0.45 μm and added binding buffer (50 mM Tris-HCl pH 7.4, 20 mM imidazole and 300 mM NaCl). The soluble protein was equilibrated with Ni-NTA beads with 10 column volume of binding buffer. Protein was loaded onto the column, washed with binding buffer and eluted with elution buffer (50 mM Tris-HCl pH 7.4, 150 mM imidazole and 300 mM NaCl).

Finally, purified protein was dialyzed with 10 mM MES, pH 5.8, and analyzed by SDS-PAGE and Western blot using antibody against 6X His. Protein concentration was determined by Pierce® BCA Protein Assay Kit (Thermo scientific).

2.3.3.1 Sodium dodecyl sulfate-polyacrylamide gel electrophoresis (SDS-PAGE)

For separating the proteins, 15% SDS-PAGE was used to determine protein purity. After the separation gel solution was prepared and added into the gel plate

setting, then the stacking gel solution was prepared and poured on top of the separation gel. When the polymerization was complete, the protein samples were mixed with loading dye and boiled for 5 min before loaded into the gel. Electrophoresis was run at a constant current 25 mA per gel for 50 min. After that the gel was stained in Coomassie blue staining solution or Silver staining solution.

2.3.3.2 Western Blot Analysis

In brief, after the protein was run 15% SDS-PAGE. The gel, nitrocellulose membrane and supports were soaked in transfer buffer (25 mM Tris base, 150 mM glycine and 20% methanol) for 30 min and were put on Trans-Blot$^{®}$ SD (BIO-RAD) (Figure 2.2) before assembling the transfer sandwich blotting. Electroblotting was carried out at 90 mA for 60 min and then membrane was blocked for at least 3 h or overnight in 5% (w/v) skim milk/PBS-Tween-20 solution. After that the membrane was washed for 10 minutes 3 times in PBS/Tween-20 and incubated with 1:3,000 dilution primary antibody (anti-His antibody) in 1% (w/v) skim milk/PBS-Tween-20 at 37°C with shaking for 3 h. The membrane was washed for 10 minutes 3 times in PBS/Tween-20 before incubated with 1:10,000 dilution secondary antibody (alkaline phosphatase-conjugated goat anti-mouse IgG) in 1% (w/v) skim milk/PBS-Tween-20 at 37°C with shaking for 1 h. After that membrane was wash 3 times with PBS/Tween-20. The protein was detected by color development using NBT and BCIP (Fermentas). Positive band is purple and appears in a few minutes and development was stopped by washing with deionized water.
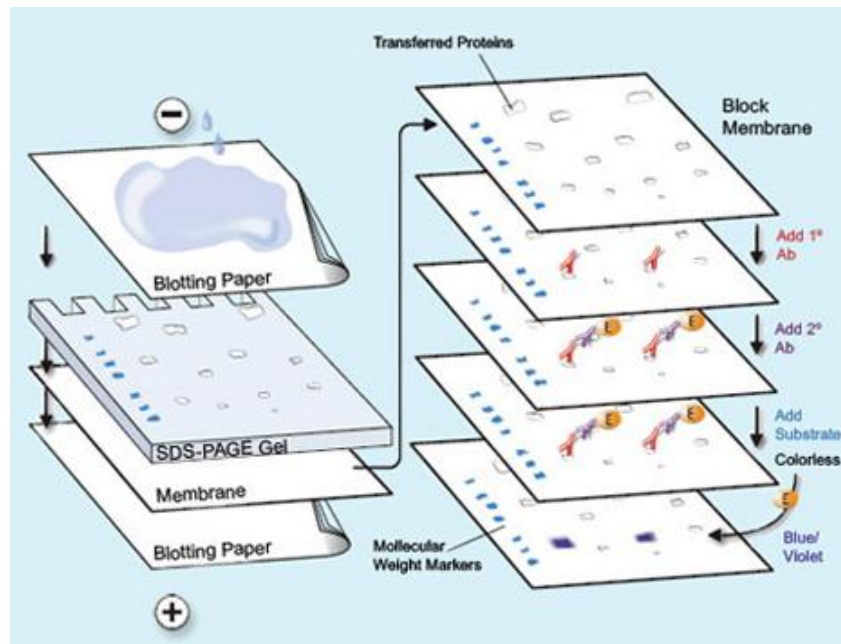
Figure 2.2 Western Blot protocol

2.4 Determination of protein concentration

Protein concentration of purified protein was measured by BCA Protein Assay Kit (Thermo scientific), using bovine serum albumin (BSA) as a protein standard. A sample solution of 25 µl was mixed with 200 µl of BCA working reagent and incubated at 37 °C with gentle shaking for 30 min. After that A_{562} was measured.

2.5 Antimicrobial Assay

Antimicrobial activities of rcrustin*Pm*1 and rcrustin*Pm*7 protein were determined by liquid growth inhibition assay (Destoumieux et al., 1999). The purified rcrustin*Pm*s were tested against Gram-positive bacteria : *Staphylococcus aureus* and *Micrococcus luteus*, and Gram-negative bacteria : *Escherichia coli 363* and *V. harveyi*.

Bacterial strains were grown overnight as a starter, then the culture was inoculated in LB broth and OD_{600} reached to 0.1-0.2. After that, the cell culture was diluted in poor-broth nutrient medium (1% bacto tryptone and 0.5% NaCl, pH 7.5) to obtain starting OD_{600} of 0.001. Then, two-fold serially diluted protein sample was added into a 96-well microtiter plate with 100 µl of bacterial cell. The sample was incubated at 30°C or 37°C according to the optimal grow temperature of each

bacteria with shaking at 150 rpm for 16-18 h. OD_{600} was measured in order to determine the minimal inhibitory concentration (MIC) value which the range between the highest concentration of the protein where bacterial growth was observed and the lowest concentration that kills 100% of bacteria.

2.6 Proteinase inhibitory activity assay

2.6.1 Serine proteinase inhibitor assay

The purified rcrustin*Pm*1 and rcrustin*Pm*7 were determined for their proteinase inhibitory activities according to Hergenhahn et al. (Hergenhahn et al., 1987) against the commercial proteinases such as subtilisin (Bacillus licheniformis, Sigma), trypsin (bovine pancreas, Sigma), α-chymotrypsin (type II bovine pancreas, Sigma) and elastase (porcine pancreas, Pacific Science). The reaction mixture were assayed in 50 mM Tris-HCl pH 7.4 in a total volume of 100 µl, using 110 µM of *N*-benzoyl-Phe-Val-Arg-*p*-nitroanilide hydrochloride as a substrate for trypsin, 80 µM of *N*-succinyl-Ala-Ala-Pro-Phe-*p*-nitroanilide as a substrate for subtilisin and α-chymotrypsin, and 166 µM of *N*-succinyl-Ala-Ala-Ala-*p*-nitroanilide as a substrate for elastase. The final concentrations of trypsin, subtilisin and α-chymotrypsin were 0.04 mM and of elastase was 0.08 mM. The rcrustin*Pm*1 and rcrustin*Pm*7 were diluted in various concentrations as an inhibitor to proteinase ratio of 100:1. The mixture was incubated at 30 °C for 10 min and the reaction was stopped by 50% (v/v) acetic acid. Then, the reaction mixture was measured at A_{405} to analyze the percent of remaining activities comparing to the negative control.

2.6.2 Proteinase inhibition assay by Agar diffusion

Proteinase inhibition of rcrustin*Pm*1 and rcrustin*Pm*7 was determined by using secretory proteinase from *Bacillus subtilis* as described in Chen et al., 2008. *B. subtilis* was grown overnight at 30°C and filtered before used. Crude proteinase and various concentration of protein were added into the well in skim milk agar plate (0.6% skim milk and 0.75% agar) and incubated at 30°C overnight. Crude proteinase with proteinase activity produces clear zone around the well where crude enzyme was added.

2.7 Cell wall components and lipid binding assay

Binding properties of both rcrustin*Pm*s to lipid and cell wall components such as lipopolysaccharide (LPS) from *E. coli* serotype 0111:B4 (Sigma) and lipoteichoic acid (LTA) from *S. aureus* (Sigma) were investigated.

2.7.1 Lipid-protein interaction

Binding of rcrustin*Pm*s to various lipid components was determined using PIP Strips™ (Echelon). First, the strip membrane that has dots of lipid was blocked with PBS-T (0.1% v/v Tween20) + 3% BSA with shaking for 1 h, and then the 0.5 μg/ml of protein was added on membrane in PBS-T (0.1% v/v Tween20) + 3% BSA with shaking at room temperature for 1 h. After that, the membrane was washed with PBS-T (0.1% v/v Tween20) for 5 min 3 times and incubated with 1:3,000 dilution primary antibody (anti-His antibody) for 3 h. The membrane was washed before incubated with secondary antibody (Peroxidase-conjugated goat anti-rabbit IgG antibody) with gentle shaking for 1 h and washed 3 times. Finally, color change of the reaction was observed using 3,3',5,5'-Tetramethylbenzidine (TMB) and H_2O_2.

2.7.2 Enzyme-linked immunosorbent assay (ELISA)

After lipid strip test, ELISA was carried out to quantitatively measure the binding of rcrustin*Pm*1 and rcrustin*Pm*7 to phosphatidic acid (PA), LPS and LTA. Microtiter plate was coated with 100 μl/well of 30 μg/ml PA, LPS or LTA at 37°C for 1 h and washed out with PBS-T (0.1% v/v Tween20) for twice. The plate was blocked with PBS-T (0.1% v/v Tween20) + 5% BSA at 37 °C for overnight and was added and incubated 100 μl of various protein concentration in PBS-T (0.1% v/v Tween20) + 5% BSA at 37°C for 1 h. The plate was washed out and incubated with primary antibody at 1:3000 dilution for 2 h. The plate was washed once before incubated with secondary antibody at 1:10000 dilution for 1 h. After washing step, 100 μl of substrate solution (*p*-nitrophenylphosphate) was added and incubated for 15 min. Then the reaction was stopped with 100 μl of 0.4 N NaOH. Finally, the reaction was measured at A_{405}. The dissociation constants (K_d) and the maximum binding (A_{max}) parameters were calculated with GraphPad Prism version 6.0 for Windows (GraphPad Software, San Diego, Calofornia, USA), using nonlinearly fitting as one site – Specific biding with Hill slope model :

$$Y=B_{max}*X^h/(K_d{}^h + X^h)$$

2.8 Determination of the secondary structure by Circular Dichroism (CD) Spectroscopy

Circular dichroism (CD) spectroscopy is a method in structural biology to examine the structure and conformational changes of proteins, polypeptides, and peptide structures, which by informing on binding and folding properties provides information about their biological functions. It is based on the dependence of the optical activity of the protein in the far ultraviolet (UV) regions (170–240 nm wavelength) with the backbone orientation of the peptide bonds with minor influences from the side chains. Their spectra are reflective of the different types of secondary structures (the ϕ, ψ angles) present (Farman, 1996).

The CD signal occurs when chromophores in an asymmetrical environment interact with polarized light. Some secondary structural such as α-helices and β-sheets produce characteristic CD spectra in the far-UV region (Greenfield, 2006; Kelly et al., 2005). Different types of secondary structure producing characteristic spectra, the spectrum of a given protein can be used to estimate its percentage content on the major secondary structure types. CD spectrometer should be calibrated before used. The asymmetric compound (+)-10-camphorsulfonic acid (CSA) is easily available and provides a convenient two-point calibration with $\triangle\varepsilon$ of +3.71 at 290.5 nm and -8.89 at 192.5 nm (Chen *et al.* 1977).

The secondary structures of rcrustin*Pm*1 and rcrusti*Pm*7 were determined using J-715 CD Spectropolarimeter (JASCO). The purified protein was diluted to 0.8 mg/ml in 10 mM Tris-HCl, pH 7.4. CD machines must be calibrated to check that the ellipticity values and wavelengths are correct by calibration standard, (1S)-(+)-Camphor-10-sulfonic acid (CSA) before measuring CD spectrum. A quartz cell length with 1 cm was used for measurement. The CD spectrum was scanned from wavelength of 190 to 240 nm using a bandwidth of 2 nm and a response time of 2 sec with 50 mm/min scanning speed. The CD spectra were converted to molar ellipticity in units of degree*cm^2*$dmol^{-1}$ using the equation

$$[\theta] = \theta/ (10 \times n \times C_p \times l)$$

Where　　　θ is the ellipticity in millidegrees

　　　　　　n is the number of amino acid residues

C_p is the peptide molar concentration (M)

l is the cell path length (cm)

The percentage of helical and β-sheet content of protein was analyzed using K2D3 software (http://www.ogic.ca/projects/k2d3/).

2.9 Crystallization of rcrustin*Pm*1

2.9.1 Determination of suitable protein concentration for crystallization

Precipitate and clear drops are typical crystallization screen results for reagent conditions which do not promote crystallization and are part of every crystallization screen (Figure 2.4). By optimizing protein concentration for screening, the number of clear and precipitate results can often be reduced, which in turn results in more efficient sample utilization while at the same time enhancing the chances for crystallization.

PCT™ or Pre-Crystallization Test Kit (Hampton Research) was used to test and optimize the suitable protein concentration for crystallization screens. Over-concentrated samples can result in amorphous precipitate, while over-diluted samples can lead to in clear drops. First, 0.5 to 1.0 ml PCT reagent A1 (0.1 M TRIS hydrochloride pH 8.5, 2.0 M Ammonium sulfate) was pipetted into reservoir A1 of a VDX Plate with sealant, and then 0.5 to 1.0 ml of PCT reagent A2 (0.1 M TRIS hydrochloride pH 8.5, 0.2 M Magnesium chloride hexahydrate, 30% w/v Polyethylene glycol 4,000) was pipetted into reservoir A2 of a VDX Plate with sealant. After that, 0.05 to 1 µl of protein sample was dropped onto the center of a single glass cover slide of both reservoirs. A volume equal of PCT Reagent A1 from reservoir A1 that used in prior step was pipetted into the protein sample drop on the siliconized cover slide and invert the cover slide with the drop over reservoir A1 and seal. The same steps were repeated for reagent and reservoir A2. After 30 min, both drops were observed by a light microscope and compared to the results show in Figures 2.4. Protein samples with suitable protein concentration should have a microcrystalline or light granular precipitate throughout the drop.

(A) (B)
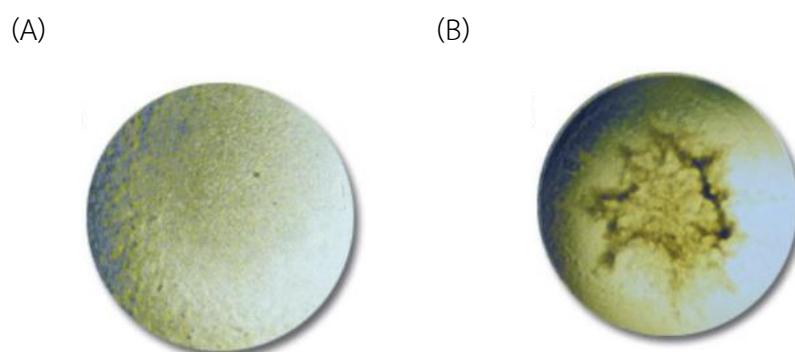
Figure 2.3 Pre-crystallization test results light precipitate (A) and heavy amorphous precipitate (B).

2.9.2 Crystallization screening of rcrustin*Pm*1

The rcrustin*Pm*1 was screened for crystallization conditions using crystal screening kits (Hampton Research and Emerald Biosystems) and based on sitting drop vapor diffusion method (Figure 2.5A). Drops were set up in ratio of the reservoir : purified protein of 1:1 in 96-well crystallization plate and the plate was sealed off before incubating at 18 °C. Crystallization plates were observed every week up to three months.

After preliminary screening, the conditions that gave crystals were optimized in 24-well crystallization method using hanging drop vapor diffusion method (Figure 2.5B). First, 1 μl of reagent from reservoir and 1 of purified protein were pipetted onto a 0.22 mm siliconized glass cover slide. Then, the cover slide was turned over and held on the grease plate and well. Crystallization plates were incubated at 18 °C and observed under a light microscope every week.
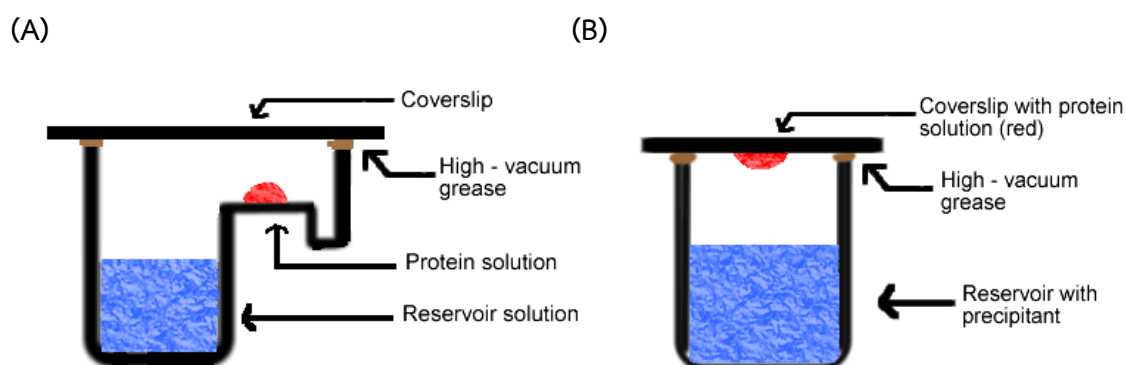
Figure 2.4 Two of the most commonly used methods for protein crystallization (A) Sitting drop vapor diffusion method and (B) Hanging drop vapor diffusion method.

2.9.3 Co-crystallization of rcrustin*Pm*1

Co-crystallization is one of the common methods for obtaining crystals of a protein–ligand complex. The definition of co-crystal is a crystalline structure.

Sometimes, co-crystallization could help improve crystal's quality. The co-crystallization of purified rcrustin*Pm*1 and phosphatidic acid (PA) was prepared by mixing the purified protein with lipid (PA). Briefly, the purified protein in 2.04 mM were mixed with PA in concentration of 10 times higher (20.4 mM PA) and incubated at 18 °C for 2 hr. Then, 20 mM Tris-Cl pH 7.4 was pipetted into the mixed solution and transferred onto a protein concentrator. To remove unbound protein ligands, a protein concentrator was centrifuged at 10,000 xg, 4°C for 5 min. This washing step was performed twice. After that, the solution was concentrated to remain volume of 100 µl. Finally, the protein solution was screened for crystallization condition using crystal screening kits (Hampton Research and Emerald Biosystems). The ratio of the reservoir solution : purified protein was kept at 1:1. Crystallization screening was performed as previously described.

Next, additive screening was carried out in order to improve crystal's quality. After additive screening, crystallization conditions were in ratio of protein : precipitant (1:1 or 2:1) in 24-well crystallization plates.

A single crystal was then cryo-protected flash frozen in liquid nitrogen. And then, they were bombarded with X-rays or synchrotron radiation that showed a

diffraction pattern of the protein. A crystal was then put on X-ray generator machine in order to test its X-ray.

2.10 Pathogen challenged shrimp

2.10.1 Shrimp

The black tiger shrimp, *P. monodon* (weight about 6-10 g) were obtained from the local farm at Suratthani province, Southern Thailand, and accommodated in laboratory aquaria at a temperature (28±4 °C) and a salinity of 20 ppt for at least 5 days before use in the experiments.

2.10.2 Preparation of *V. harveyi* and *S. aureus* for injection

2.10.2.1 *Vibrio harveyi*

In *Vibrio harveyi* challenge experiments, *V. harveyi* was grown overnight on Thiosulfate Citrate Bile Salt Sucrose (TCBS) plate at 30 °C. A single colony was inculated in Tryptic Soy Broth (TSB) containing 2% NaCl and grown at 30°C with 250 rpm shaking for 16-18 h. After that, the diluted culture of 1:100 was inoculated into the TSB and grown until OD_{600} reached 0.6 where bacterial cell densities were 10^8 CFU/ml by plate count method. The cell culture was heat-killed at 60 °C for 2 h and resuspended in 0.85% (w/v) NaCl in ratio of 1:100 to be 10^6 CFU/ml.

2.10.2.2 *Staphylococcus aureus*

In *Staphylococcus aureus* challenge experiments, *S. aureus* was grown overnight on LB agar plate at 37 °C. A single colony was inoculated in LB broth containing 1% NaCl and grown at 37 °C with 250 rpm shaking for 16-18 h. After that, the diluted culture of 1:100 was inoculated in the LB and grown until OD_{600} reached 0.6 where bacterial cell densities were 10^8 CFU/ml by plate count method. The cell culture was heat-killed at 80 °C for 30 min and resuspended in 0.85% (w/v) NaCl in ratio of 1:100 to be 10^6 CFU/ml.

2.10.3 Pathogen challenge

In each experiment, shrimps were divided into 2 groups such as infected and non-infected group. Either 150 mM NaCl (a control group) or 50 µl of 10^6 CFU/ml bacteria (an experimental group) were injected into the shrimps at the fourth abdominal segment. Hemocytes of nine individuals at each time point (3, 6, 12, 24 and 48 h post-injection, hpi) were collected.

2.11 The effect of the cell wall components on gene expression

In this study, the effect of the cell wall components on genes expression of crustin*Pm*1, crustin*Pm*7 and the other genes in shrimp immunity such as Immune deficiency (IMD) pathway : *Pm*Relish, Toll pathway : *Pm*Spätzle, Dorsal and *Pm*MyD88.

2.11.1 Pathogen challenges and sample preparation

2.11.1.1 Hemocyte collections

In this experiment, hemolymph was collected from the ventral sinus of shrimps using 500 µl of MAS solution (27 mM sodium citrate, 336 mM NaCl, 115 mM glucose and 9 mM EDTA, pH 7.0) as an anticoagulant. Hemolymph was centrifuged at 800 xg for 10 min at 4 °C to collect the hemocyte pellet and stored in -80 °C for total RNA extraction.

2.11.1.2 Total RNA extraction

Total RNA from hemocytes was extracted using Tissue Total RNA Purification Mini Kit (FavorPrep™) (Figure 2.3). Firstly, 250 µl of FARB buffer (β-ME added) was added into hemocyte sample, vortexed and incubated at room temperature for 5 min to lyse cell. The solution was transferred into the filter column and centrifuged at 14,000 rpm for 2 min at 4°C. Then, the supernatant was transferred into the new collection tube. One volume of 70% ethanol was added and mixed by pipetting. Sample mixture was pipetted into FARB mini column set, then centrifuged at 14,000 rpm for 1 min at 4°C. RNA bound to the column and the ethanol solution was discarded. At washing step, 250 µl of wash buffer 1 was added, centrifuged at 14,000 rpm for 1 min at 4°C and the supernatant was discarded. Then, 20 µl of RQ1 RNase-

free DNase (Promega) was added into the center of membrane column and left at room temperature for 25 min. After that, 250 µl of wash buffer 1 was added, centrifuged at 14,000 rpm for 1 min at 4°C and the supernatant was discarded. RNA bound membrane column was washed by 700 µl of wash buffer 2, centrifuged at 14,000 rpm for 1 min at 4°C and the supernatant was discarded. Next, the membrane column was dried by centrifuged at 14,000 rpm for 3 min and FARB mini column was placed on new microcentrifuge tube. RNA was eluted from the column by addition of 15 µl RNase-free water and incubated at room temperature for 10 min before centrifugation at 14,000 rpm for 2 min at 4°C. Eluting RNA and kept in -80 °C until use.
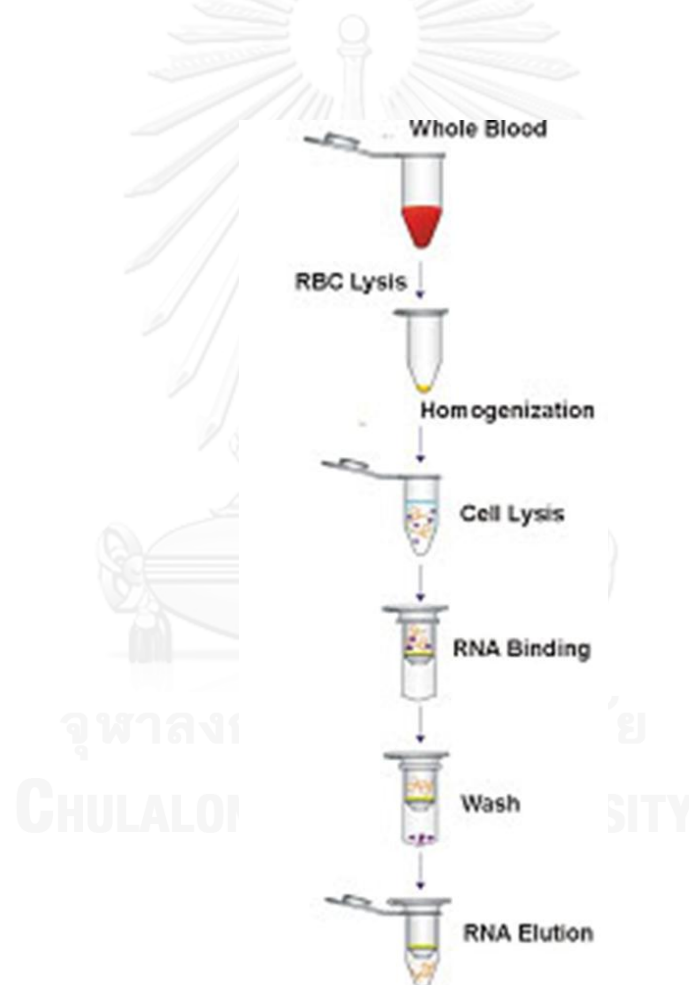
Figure 2.5 The steps for total RNA extraction

2.11.1.3 First-strand cDNA synthesis

After purification, total RNA concentration was determined by measuring the absorbance at 260 nm by UV spectrophotometer and determined in ng/µl using the equation (1) (Sambrook et al.,1989) :

$$[RNA] = A_{260} \times \text{dilution factor} \times 40 \quad \text{...} \quad (1)$$

The first strand cDNA synthesis was performed using ImProm-II™ Reverse Transcription Kit (Promega). Reaction of total volume 10 µl contained 1 µg of total RNA, 0.5 µg of the oligo(dT)$_{18}$ primer and DEPC-treated water. The reaction mixture was incubated at 70 °C for 5 min and placed on ice for 5 min. The reaction mixture was incubated at 42 °C for 60 min and heated at 70 °C for 15 min. The cDNA was kept at -20 °C until used.

2.11.2 Expression analysis of interested genes in response to pathogen infection

2.11.2.1 Cloning of partial PmMyD88 gene

*Pm*MyD88 gene was cloned from cDNA library of the black tiger shrimp *P. monodon*. Degenerate primers, *Pm*MyD88_F and *Pm*MyD88_R, were designed from conserved regions of published MyD88 nucleotide sequences of *Fenneropenaeus chinesis* (GenBank: JX501341.1) and *Litopenaeus vannamei* (GenBank: JX073566.1). A cDNA fragment of *Pm*MyD88 was initially amplified by PCR with specific primers using cDNA from *P. monodon* hemocytes. *Pm*MyD88_F: CTTACTTGGAAGCAATGGATCG and *Pm*MyD88_R: CACACCAAACGCAGAATCAAG. The partial DNA fragment of *Pm*MyD88 gene (approximately 655 bp) was ligated into pGEM-T Easy vector. The ligation mixture was then transformed into *Escherichia coli* TOP10 (Invitrogen). Finally, the recombinant plasmid of *Pm*MyD88 was sequenced (Macrogen).

2.11.2.2 Primer design for RT-PCR and real-time RT-PCR analysis

Gene specific primers were designed from nucleotide sequence of interested genes to amplify a product of 100-200 bp. EF1-α was used as an internal reference control (Table 2.1)

Table 2.1 Nucleotide sequences of the primer pairs and size of PCR products

Gene	Primers	Sequence (5′-3′)	Product size (bp)
EF1- α	EF1α-F	GGTGCTGGACAAGCTGAAGGC	149
	EF1α-R	CGTTCCGGTGATCATGTTCTTGATG	
crustin*Pm*1	PmCrus1-F	CTGCTGCGAGTCAAGGTATG	178
	PmCrus1-R	AGGTACTGGCTGCTCTACTG	
crustin*Pm*7	PmCrus7-F	GGCATGGTGGCGTTGTTCCT	152
	PmCrus7-R	TGTCGGAGCCGAAGCAGTCA	
*Pm*Relish	Relish-F	TCTCCAGGTGAGCACTCAGTTGGC	157
	Relish-R	GCTGTAGCTGTTGCTGTTGTTGAG	
*Pm*Spätzle	Spätzle-F	TAAGCAAGGAGCAGGAAGAG	132
	Spätzle-R	TGGCATACACCACATCTGAG	
Dorsal	Dorsal-F	TCACTGTTGACCCACCTTAC	198
	Dorsal-R	GGAAAGGGTCCACTCTAATC	
*Pm*MyD88	MyD88-F	GTGCACCAGAGTCATTGTAG	170
	MyD88-R	GGGAGTGGCAGAAACTTATC	

2.11.2.3 Quantification of mRNA expression by real-time PCR

Quantitative real-time PCR (qRT-PCR) was performed with iCycler-iQ^{TM} system (BIO-RAD) and SsoFast™ EvaGreen$^®$ Supermix (BIO-RAD) was used as dye. Gene-specific primers used in the experiment are listed in Table 2.1. EF1α was used as an internal control gene to correct RNA loading variation.

The reaction (10 µl total volume) contained 1 µl diluted cDNA template equivalent to 15 ng total RNA and 9 µl of reaction mixture consisting of 5 µl SsoFast™ EvaGreen$^®$ Supermix, 0.5 µl each of 10 µM forward and reverse primers, and 3 µl RNase/DNase free water. The qRT-PCR was run using a standard cycling program as follows: 1 cycle of 95 °C for 30 s, followed by 40 cycles of 95 °C for 15 s and 55 °C for 30 s. The PCR reaction of each sample was carried out in triplicates.

To evaluate the threshold cycle (C_T) by comparative C_T model (Livak and Schmittgen, 2001). Statistical analysis was subjected to a one-way ANOVA followed by post-hoc test was performed using the Duncan's new multiple range test. Expression levels were considered to be significantly different when $P < 0.05$.

In addition, comparative C_T method was used to compare the expression level of two different samples (normal and infected shrimp). The fold change of gene expression was calculated as follows;

$$\text{Fold change} = 2^{-\Delta\Delta C_T}$$

$\Delta\Delta C_T = [(C_T \text{ of target gene } - C_T \text{ internal control}) \text{ normal } - (C_T \text{ of target gene } - C_T \text{ internal control}) \text{ infected}]$

2.12 Silencing of *Pm*Relish and *Pm*MyD88 gene by dsRNA

2.12.1 Preparation of double strand RNA (dsRNA)

The purified DNA fragments of T7-Rel, Rel-T7, T7-MyD, MyD-T7, T7-GFP and GFP-T7 were used as templates for dsRNA synthesis. Briefly, transcription templates are needed with T7 RNA polymerase promoters positioned at 5' terminus to transcribe sense and antisense RNA corresponding to the target RNA.

The dsRNA synthesis reaction contained 8 µl of linear DNA templates of target genes, 10 µl of RiboMAX™ Express T7 2x buffer (Promega) and 2 µl of Enzyme Mix T7 Express in the final volume of 20 µl per reaction. Then, each solution of DNA fragments was incubated at 37 °C for 1 hour. Each DNA fragments of the same gene (For *Pm*Relish: T7-Rel and Rel-T7, *Pm*MyD88: T7-MyD and MyD-T7 and GFP: T7-GFP and GFP-T7) were mixed and heated at 70 °C for 10 min before cooling down to room temperature. DNA template was removed by addition of 2 µl of RQ1 RNase-free DNase (1U/µg of DNA template) and incubation at 37°C for 30 min. Total RNA was precipitated by mixing with 4 µl of 3M sodium acetate and 45 µl of isopropanol. After thoroughly mixed, the solution was frozen at -20°C for 20 min and then centrifuged at 13,500 xg for 15 min at 4°C. The upper phase was discarded and the pellet was washed with 1 ml of 75% ethanol. Then, the sample was centrifuged at 13,500 xg for 15 min at 4°C and the upper phase was discarded. The pellet was air-dried for 5 min. Finally, 40 µl of Nuclease free water was used to dissolve the pellet and stored at -80°C until used. After purification, the quality of dsRNA was determined by measured the concentration at A_{260} and determined the size shift in 1.8% agarose gel electrophoresis and stored at -80 °C.

The green fluorescent protein (GFP), *Pm*Relish, and *Pm*MyD88 primer pairs (Table 2.2) were used for dsRNA synthesis. The reaction was carried out with the annealing temperature of 55 °C.

Table 2.2 Nucleotide sequences of the primer pairs for RNA interference

Name	Sequence (5′-3′)
GFP1-T7-F	TAATACGACTCACTATAGGATGGTGAGCAAGGGCGAGGA
GFP1-R	TTACTTGTACAGCTCGTCCA
GFP2- F	ATGGTGAGCAAGGGCGAGGA
GFP2-T7-R	TAATACGACTCACTATAGGTTACTTGTACAGCTCGTCCA
Rel-T7-F	GGATCCTAATACGACTCACTATAGGCTCGTGGTCAGGAAGACTCAAT
Rel-R	GACTGGAGATGGAGACTGAATG
Rel-F	CTCGTGGTCAGGAAGACTCAAT
Rel-T7-R	GGATCCTAATACGACTCACTATAGGGACTGGAGATGGAGACTGAATG
MyD-T7-F	TAATACGACTCACTATAGGCCTCAGCAAAGGTCTTGAAC
MyD-R	CAGTCCACCAATTAGGTCTC
MyD-F	CCTCAGCAAAGGTCTTGAAC
MyD-T7-R	TAATACGACTCACTATAGGCAGTCCACCAATTAGGTCTC

　　　　2.12.2 Knockdown of *Pm*Relish and *Pm*MyD88 gene by dsRNA-mediated RNA interference

　　　　In knockdown experiments, shrimps (weight about 2-5 g) were injected with either ds*Pm*Relish (5 µg per g shrimp) or ds*Pm*MyD88 (5 or 7.5 µg per g shrimp) or dsGFP (control group) or 150 mM NaCl (control group). A total of 27 healthy shrimp were divided into three treatment groups (9 individuals in each group) including (i) NaCl, (ii) dsGFP, and (iii) ds*Pm*Relish or ds*Pm*MyD88. All hemolymph samples in each group were collected at 24 h post-dsRNA injection (hpi) for RNA extraction and cDNA preparation to determine effects of gene silencing. RT-PCR was conducted specific primers to determine *Pm*Relish, *Pm*MyD88, and elongation factor 1-**α** gene expression. The RT-PCR was carried out as followed: 1 cycle of 94 °C for 3 min, followed by 30 cycles of 94 °C for 30 s, 50 °C for 30 s and 72 °C for 30 s.

2.12.3 Bacterial challenge to shrimp after ds*Pm*Relish and ds*Pm*MyD88 gene knockdown

Shrimps were divided into two groups for *S. aureus* and *V. harveyi* challenge. Each group contains 9 individual shrimps that were injected with 20 µl in saline solution containing either i) 150 mM NaCl, ii) 5 µg per g shrimp dsGFP, or iii) 5 µg per g shrimp ds*Pm*Relish or 7.5 µg per g shrimp ds*Pm*MyD88. After 24 h, inactivated *S. aureus* and *V. harveyi* with density of 10^6 CFU/ml were mixed with either 150 mM NaCl, 5 µg per g shrimp dsGFP, 5 µg per g shrimp ds*Pm*Relish or 7.5 µg per g shrimp of ds*Pm*MyD88 and injected intramuscularly to shrimp. The hemolymph was taken from each individual at 12 and 24 hpi. Total RNA was extracted and used for cDNA synthesis. Transcription levels of crustin*Pm*1 and crustin*Pm*7 in each sample were analyzed by real-time PCR.

2.13 Statistic analysis

Statistic analysis was carried out from triplication experiment using SPSS version 21 software in a One-Way ANOVA and Post Hoc test, with significance accepted at P < 0.05 (*) and P < 0.01 (**).

CHAPTER III

RESULTS

3.1 Construction of recombinant pPIC9K_crustin*Pm*1 and pPIC9K_crustin*Pm*7

Previously, crustin genes have been identified in *P. monodon*. From the *P. monodon* EST database, crustin*Pm*1 and crustin*Pm*7 are two most abundant isoforms in hemocytes. According to the sequence analysis, crustin*Pm*1 (Supungul *et al.* 2008) and crustin*Pm*7 (Amparyup *et al.* 2008) were identified and produced in *E. coli* expression system. Both proteins were purified under denaturing condition which may lead protein misfolding during refolding process. As a result, some batches of recombinant crustin*Pm*1 and crustin*Pm*7 produced in *E. coli* exhibited no antimicrobial activity. From glycosylation sites analysis, potential N-linked glycosylation sites of crustin*Pm*1 and crustin*Pm*7 were predicted as one and three sites, respectively. This work aims to express both crustin*Pm*s in *P. pastoris* expression system and purified the recombinant protein under its native form.

Previously, crustin*Pm*1 was constructed in *P. pastoris* expression vector, pPIC9K by Dr. Premruethai Supungul, and the recombinant protein was produced in soluble forms. Similar to crustin*Pm*1, crustinPm7 gene was constructed in *P. pastoris* expression system to express crustin genes in soluble forms. Crutin*Pm*7 gene was cloned into pPIC9K vector which has histidine tag (His-tag) at N-terminus. The pPIC9K_crutin*Pm*7 was amplified from cDNA of normal shrimp (Figure 3.1) by primer crusF (5' GATGAATTCCATCATCATCATCATCACCAGGATAAAGGCAATGCCGA 3'), which introduced an *Eco*R I site and a 6 x His-tag at N-terminus, and crusR (5' CTGCGGCCGCCTATCCCTGAGAACCTGCCA 3'), which introduced a *Not* I site at C-terminus. The purified PCR product and pPIC9K vector were digested with same restriction enzymes *Eco*R I and *Not* I and were ligated into pPIC9K vector. The size of digested recombinant plasmid was analyzed by agarose gel electrophoresis to ensure the correct fragment was inserted into pPIC9K. Crutin*Pm*7 gene fragment is approximately 426 bp. Figure 3.2 shows that the recombinant plasmid digested with *Eco*R I and *Not* I produced a DNA band of approximately 400 bp fragment. This fragment was then verified by sequencing.
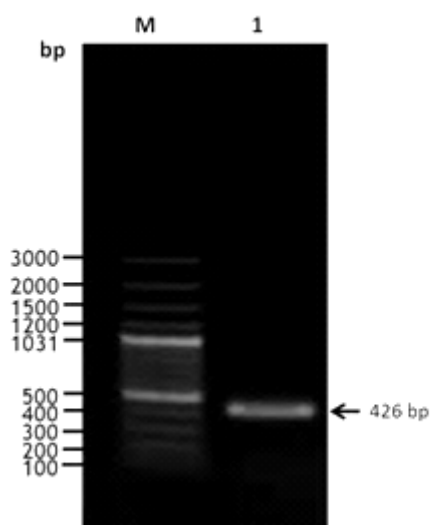
Figure 3.1 Amplification of the crutin*Pm*7 gene from cDNA of normal shrimp. The crusF and crusR primers were used to amplify the mature crutin*Pm*7 gene and analyzed by 1.5% agarose gel electrophoresis.

Lane M : 100 bp DNA ladder marker (GeneRuler^{TM} 100 bp DNA ladder, Fermentas).

Lane 1: PCR product of crutin*Pm*7 gene (426 bp).
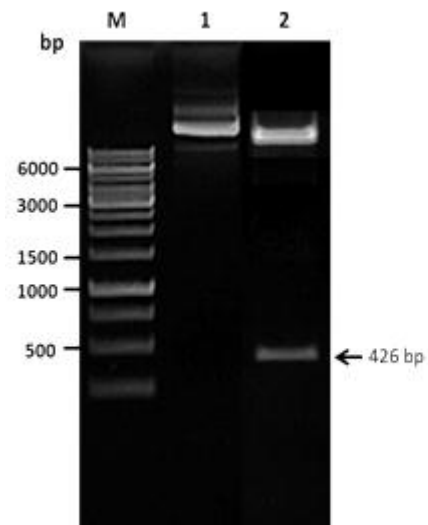
Figure 3.2 The recombinant pPIC9K_crustin*Pm*7 plasmid was digested with *Eco*R I and *Not* I, and then analyzed by 1.5% agarose gel electrophoresis.

Lane M : 1 kb DNA ladder marker (GeneRuler$^{\text{TM}}$ 1 kb DNA ladder, Fermentas)

Lane 1 : Undigested recombinant pPIC9K_crustin*Pm*7

Lane 2 : Recombinant pPIC9K_crustin*Pm*7 digested with *Eco*R I and *Not* I

The recombinant pPIC9K_crustin*Pm*7 was linearized by *Sac* I and precipitated before transforming into *P. pastoris* strain GS115 (Figure 3.3). And then, the His[+] transformants, Mut[+] and Mut[s] phenotype were screened and were confirmed using PCR amplification of the fragment containing the gene of interest (Figure 3.4).
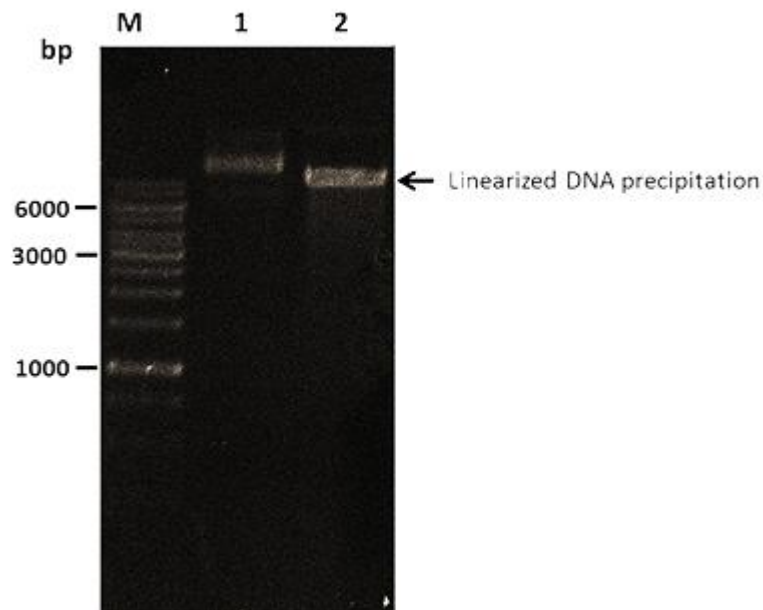
Figure 3.3 The recombinant pPIC9K_crustin*Pm*7 plasmid was linearized with *Sac* I and precipitated. Both undigested and digested pPIC9K_crustin*Pm*7 plasmids were analyzed by 0.8% agarose gel electrophoresis.

Lane M : 1 kb DNA ladder marker (GeneRuler[TM] 1 kb DNA ladder, Fermentas)

Lane 1 : Undigested recombinant pPIC9K_crustin*Pm*7

Lane 2 : Recombinant pPIC9K_crustin*Pm*7 digested with *Sac* I
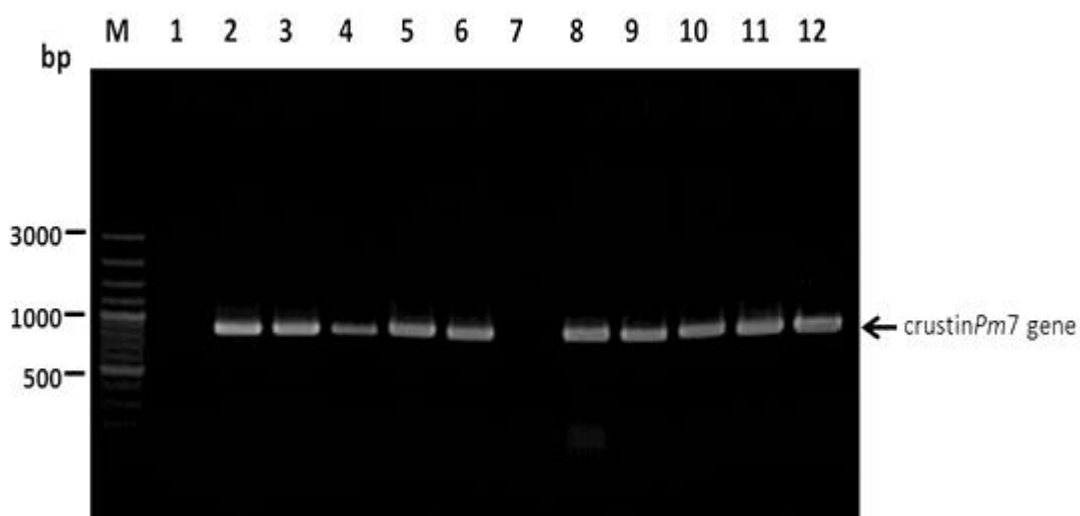
Figure 3.4 Screening of *P. pastoris* containing the recombinant pPIC9K_crustin*Pm*7 plasmid by Geneticin resistance. The 3'AOX1 and 5' AOX1 primers were used to amplify the crustin*Pm*7 gene and analyzed by 1.0% agarose gel electrophoresis. The expected size of crustin*Pm*7 fragment was approximately 800 bp.

Lane M: 100 bp DNA ladder marker (GeneRuler^{TM} 100 bp DNA ladder, Fermentas)

Lane 1: Negative control

Lane 2-12 : PCR product of crustin*Pm*7 gene

3.2 Expression and purification of the recombinant crustin*Pm*1 and crustin*Pm*7 in *Pichia pastoris* expression system

The rcrustin*Pm*1 and rcrustin*Pm*7 were successfully produced in *P. pastoris* strain GS115 in soluble form and the tranformants that produced the highest recombinant protein expression were selected by Geneticin. The rcrustin*Pm*1 and rcrustin*Pm*7 were overproduced upon induction by adding 100% methanol to a final concentration of 0.5% every 24 h for 3 days (Figure 3.5A and 3.5B). Protein was harvested by centrifugation and the supernatant was kept for purification. Soluble rcrustin*Pm*1 and rcrustin*Pm*7 were purified by Ni-NTA column (GE Healthcare). The proteins were eluted by 50 mM Tris-HCl pH 7.4, 150 mM imidazole and 300 mM NaCl (Figure 3.6A and 3.6B). Finally, purified proteins were dialyzed against 10 mM Tris-HCl, pH 7.4. After that, the purified protein was analyzed by 15% SDS-PAGE (Silver staining) and Western blotting using antibody against 6X His. The expected size of the rcrustin*Pm*1 and rcrustin*Pm*7, approximately 14.7 kDa and 12.8 kDa, was observed on the gel (Figure 3.7A and 3.7B). The gel showed a minor protein of band about 30 kDa. This band was presumably a dimer form of crustin*Pm*s which may from through the disulphide cross-link among protein molecules (crustins have 12 cysteine residues). The purified proteins were concentrated by 10 kD cut-off membrane of centricon column (Millipore). Protein concentration was determined by Pierce® BCA Protein Assay Kit (Thermo scientific). Both proteins were used for antimicrobial activity assay, proteinase inhibition assay, and other studies.
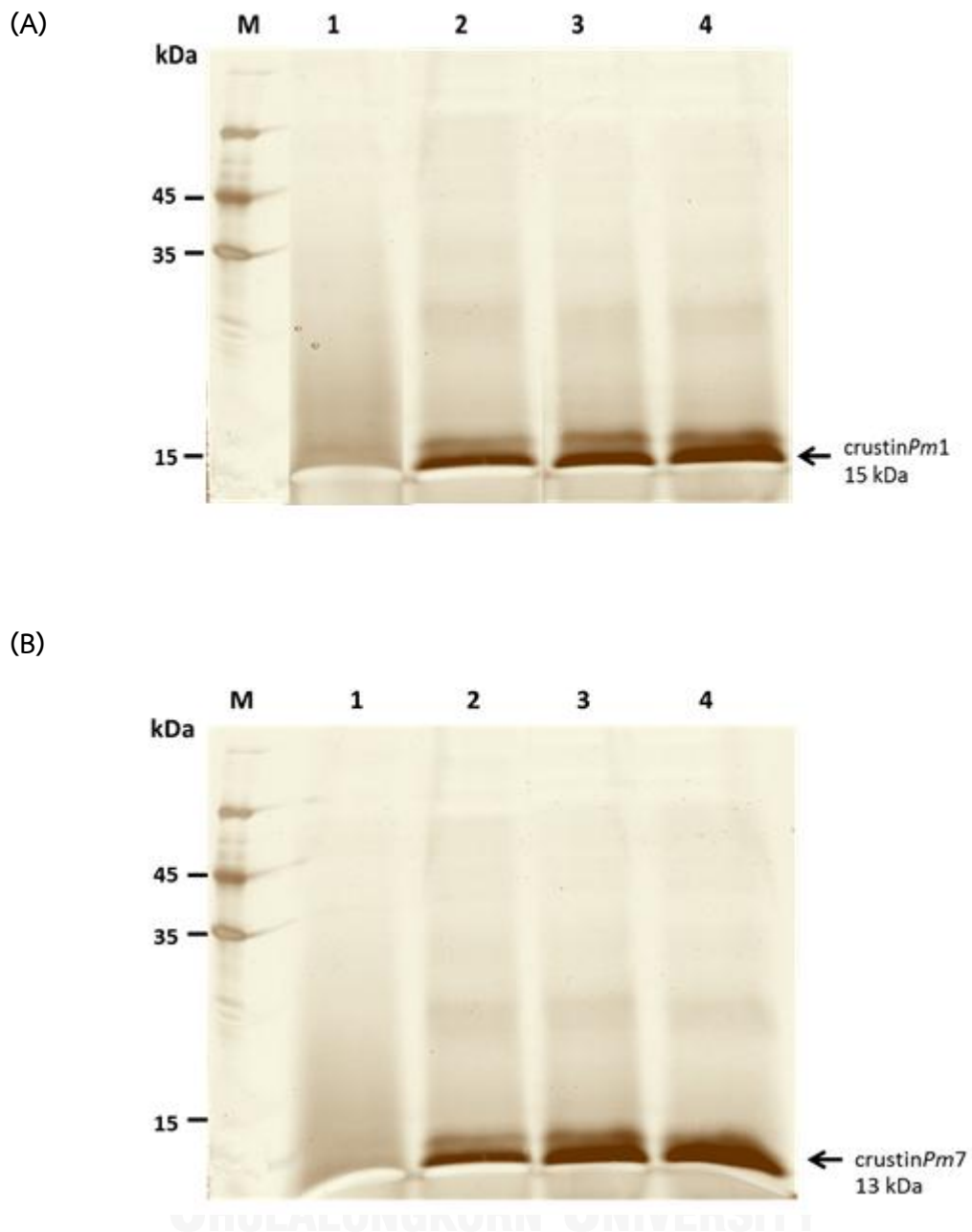
Figure 3.5 Expression of rcrustin*Pm*1 (A) and rcrustin*Pm*7 (B) in *P. pastoris* strain GS115. The recombinant clone was cultured and induced by 100% methanol to a final concentration of 0.5% for 3 days. The supernatant was kept and checked for protein expression by 15% Silver stained SDS-PAGE.

Lane M : Prestained protein marker (PageRuler^{TM} Prestained protein ladder, Fermentas).

Lane 1 : The soluble protein at 0 h with methanol induction

Lane 2 : The soluble protein at 24 h with methanol induction

Lane 3 : The soluble protein at 48 h with methanol induction

Lane 4 : The soluble protein at 72 h with methanol induction
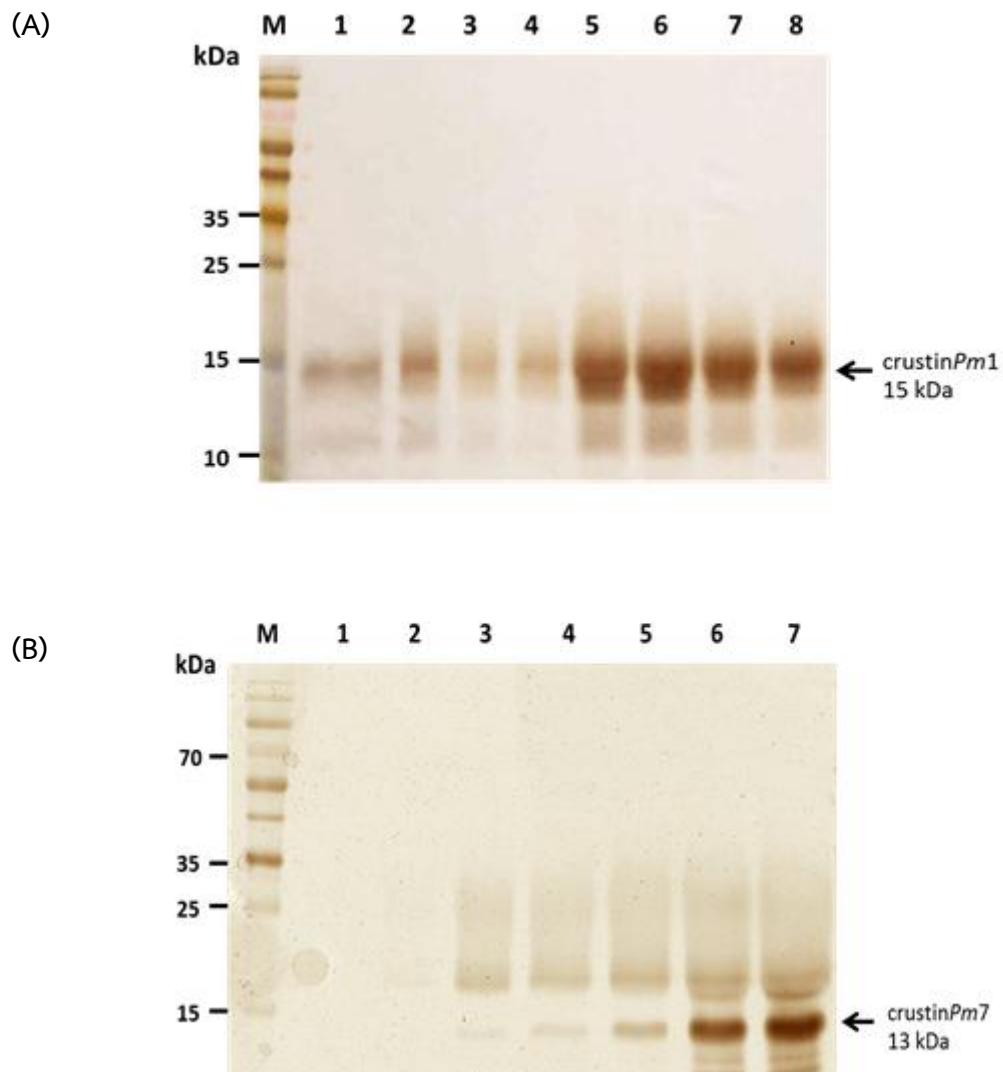
Figure 3.6 SDS-PAGE of purified rcrustin*Pm*1 (A) and rcrustin*Pm*7 (B) by silver staining. The rcrustin*Pm*1 and rcrustin*Pm*7 were purified by Ni-NTA column.

Lane M : Prestained protein marker (PageRuler^{TM} Prestained protein ladder, Fermentas)

Lane 1: Flow through fraction

Lane 2-4: Wash fraction

Lane 5-7: Elution fractions with eluted by 50 mM Tris-HCl pH 7.4, 150 mM imidazole and 300 mM NaCl
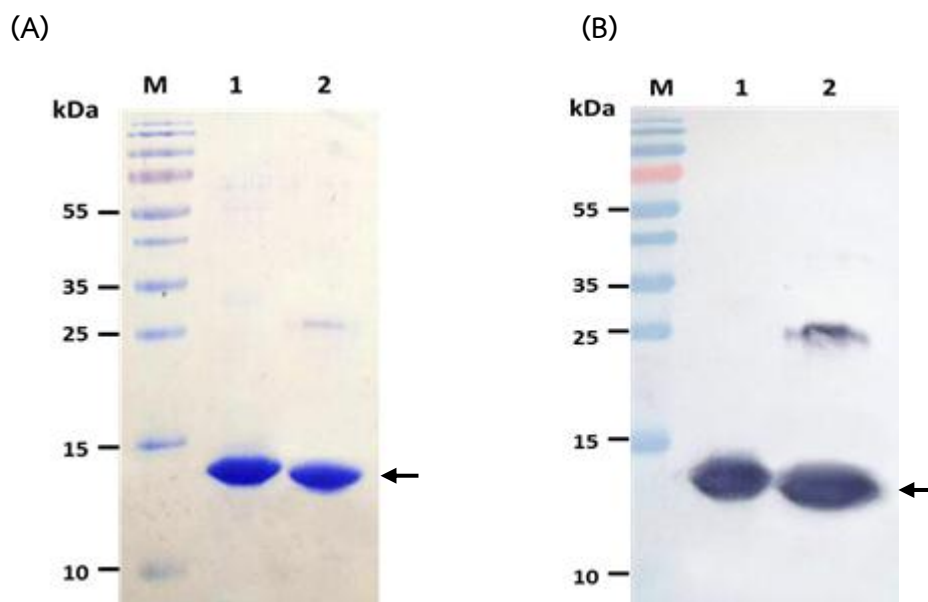
Figure 3.7 Analysis of rcrustin*Pm*1 and rcrustin*Pm*7 expressed in *P. pastoris* and purified by Ni-NTA column. The purified rcrustin*Pm*1 and rcrustin*Pm*7 were detected by coomassie staining SDS-PAGE (A) and Western blot (B) analysis using anti-His6 antibody as primary antibody. The expected band of the rcrustin*Pm*1 and rcrustin*Pm*7 are shown by the arrow.

Lane M : Prestained protein marker (PageRuler$^{\text{TM}}$ Prestained protein ladder, Fermentas)

Lane 1: purified rcrustin*Pm*1

Lane 2: purified rcrustin*Pm*7

3.3 Antimicrobial activity assay

Purified rcrustin*Pm*1 and rcrustin*Pm*7 were assayed for their antimicrobial activities. Antimicrobial activities of the purified rcrustin*Pm*1 and rcrustin*Pm*7 were investigated against Gram-positive and Gram-negative bacteria to confirm the whether they are active. Activities of rcrustin*Pm*1 were tested against Gram-positive bacteria : *Staphylococcus aureus* and *Micrococcus luteus*, and Gram-negative bacteria : *Escherichia coli* 363 and *Vibrio harveyi*. The minimal inhibitory concentration (MIC) value was determined and recorded as the range between the highest concentration of the protein where bacterial growth was observed and the lowest concentration that kills 100% of bacteria. The result showed that purified rcrustin*Pm*1 exhibited strong antibacterial activity against Gram-positive bacteria, *S. aureus* and *M. luteus*. No activity was found against Gram-negative bacteria, *E. coli* 363 and *V. harveyi*. The MIC values were summarized in Table 3.1. Meanwhile, the antibacterial activity of rcrustin*Pm*7 was active against Gram-positive and Gram-negative bacteria. The MIC was determined and the result showed that purified rcrustin*Pm*7 exhibited strong antibacterial activity against *S. aureus*, *M. luteus*, *E. coli* 363 and *V. harveyi* with MIC values ranging from 2 to 10 µM (Table 3.2). The MIC values obtained from rcrustin*Pm*1 and rcrustin*Pm*7 produced in *P. pastoris* were similar to those produced in *E. coli* (Amparyup *et al.* 2008, Supungul *et al.* 2008).

Table 3.1 Antimicrobial activity of the rcrustin*Pm*1 measured by liquid growth inhibition assay

Microorganisms	MIC value (µM)	MIC value (µM) (Supungul *et al.* 2008)
Gram-positive bacteria		
Staphylococcus aureus	3.5–5.0	3.13-6.25
Micrococcus luteus	20–50	25-50
Gram-negative bacteria		
Escherichia coli 363	50–80	50-100
Vibrio harveyi	na	na

** MIC are expressed as the interval a–b, where a is the highest concentration tested at which microorganisms are growing and b is the lowest concentration that causes 100% growth inhibition.

** Data from Supungul *et al.* 2008

Table 3.2 Antimicrobial activity of the rcrustin*Pm*7 measured by liquid growth inhibition assay

Microorganisms	MIC value (µM)	MIC value (µM) (Amparyup *et al.* 2008)
Gram-positive bacteria		
Staphylococcus aureus	5-10	5-10
Micrococcus luteus	2–8	2.5-5
Gram-negative bacteria		
Escherichia coli 363	2.5–8.0	2.5-5
Vibrio harveyi	2.5-10.0	2.5-5

** MIC are expressed as the interval a–b, where a is the highest concentration tested at which microorganisms are growing and b is the lowest concentration that causes 100% growth inhibition.

** Data from Amparyup *et al.* 2008

3.4 Proteinase inhibitory activity assay

3.4.1 Serine proteinase inhibitor assay

To investigate the inhibition of serine proteinase activity of rcrustin*Pm*1 and rcrustin*Pm*7, the purified rcrustin*Pm*1 and rcrustin*Pm*7 were tested against four commercial proteinases : trypsin, subtilisin, **α**-chymotrypsin, and elastase by measuring the change of absorbance at 405 nm. The inhibitor : proteinase mole ratios up to 50 exhibited the inhibitory activity against all commercial proteinases. Considering at the highest mole ratio of inhibitor to tested proteinase about 50, the remaining proteinase activity in the presence of rcrustin*Pm*1 and rcrustin*Pm*7 had no proteinase inhibitory activity against the commercial proteinases (Figure 3.8 and 3.9).

3.4.2 Proteinase inhibition assay by Agar diffusion

The rcrustin*Pm*1 and rcrustin*Pm*7 proteins were tested for proteinase inhibition against the crude proteinase from bacterial cultures of *Bacillus subtilis*. In this study, the crude proteinase was prepared from the overnight culture media of *B. subtilis*. The crude proteinase secreted from *B. subtilis* produced a clear zone on the skim milk plate. Crude crustins were added into the wells of the skim milk plate and incubated overnight at room temperature. The result showed that rcrustin*Pm*1 weakly inhibited proteinase from *B. subtilis* (Figure 3.10), while rcrustin*Pm*7 caused no clear zone, suggesting that rcrustin*Pm*7 may possess proteinase inhibition against crude proteinase from *B. subtilis*. However, the inhibition occurred only when an excess amount rcrustin*Pm*7 (>1.5 mM) was used (Figure 3.11). As a result, it is unlikely that rcrustin*Pm*1 and rcrustin*Pm*7 from *B. subtilis* have the proteinase inhibitory activities against crude proteinase from *B. subtilis*.
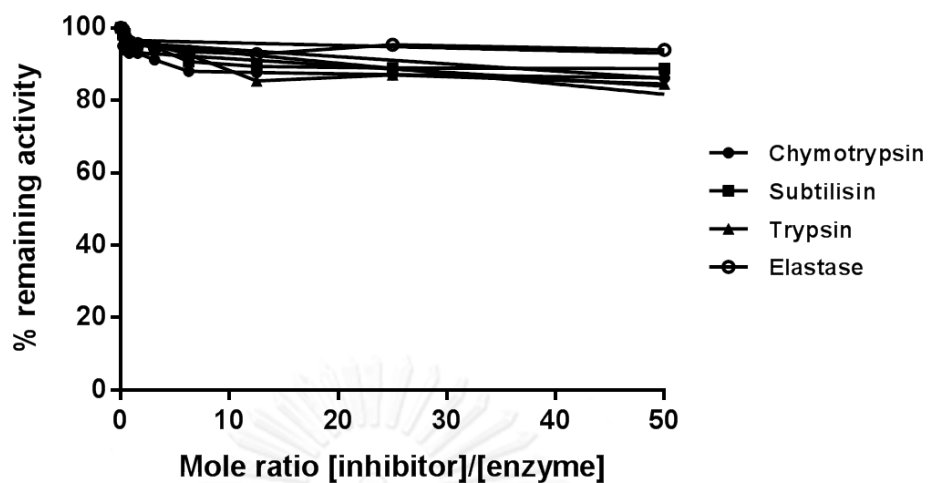
Figure 3.8 Proteinase inhibitory activity of rcrustin*Pm*1 against commercial proteinases. rCrustin*Pm*1 was incubated with each proteinase: trypsin chymotrypsin (●), subtilisin (■), trypsin (▲) or elastase (○), at various mole ratios in the reaction containing appropriate chromogenic substrate. The percentage of remaining activity of proteinase was determined.
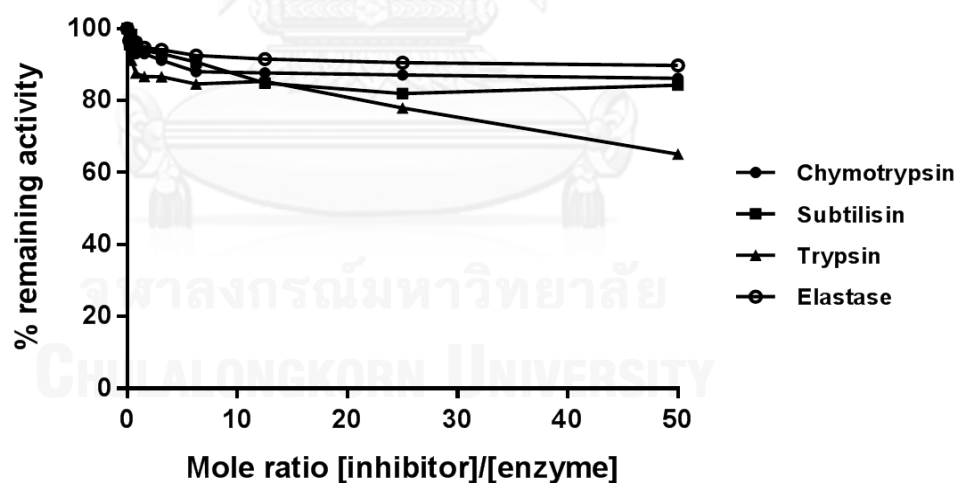
Figure 3.9 Proteinase inhibitory activity of rcrustin*Pm*7 against commercial proteinases. rCrustin*Pm*7 was incubated with each proteinase: trypsin chymotrypsin (●), subtilisin (■), trypsin (▲) or elastase (○), at various mole ratios in the reaction containing appropriate chromogenic substrate. The percentage of remaining activity of proteinase was determined.
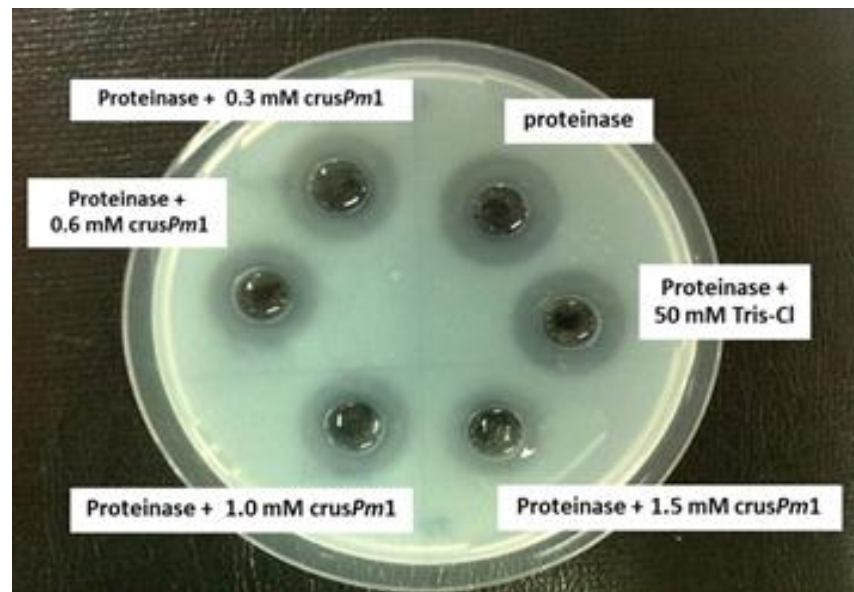
Figure 3.10 Agar diffusion assay of the proteinase inhibition of rcrustin*Pm*1 against the crude proteinase from *B. subtilis*. The crude proteinase was mixed with various concentration of rcrustin*Pm*1 before adding into the wells in a milk agar plate. The transparent zones observed after overnight incubation at room temperature indicate proteinase inhibitory activity.
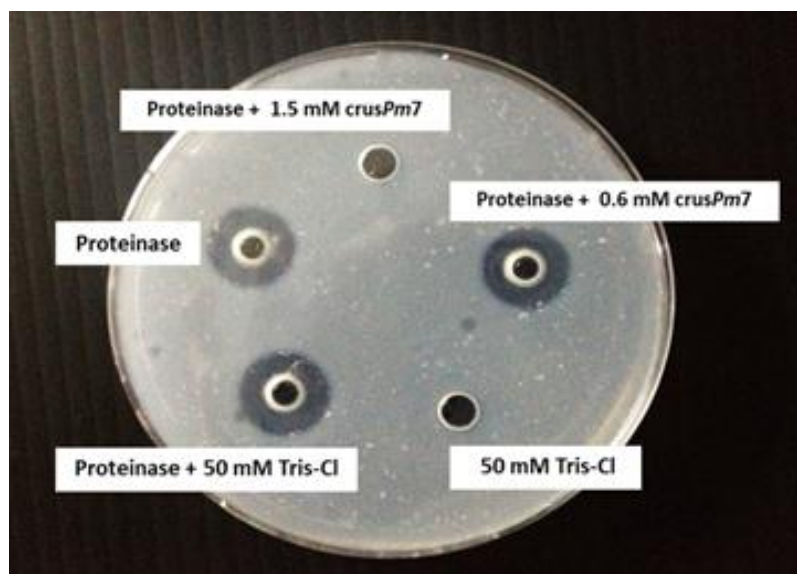
Figure 3.11 Agar diffusion assay of the proteinase inhibition of rcrustin*Pm*7 against the crude proteinase from *B. subtilis*. The crude proteinase was mixed with various concentration of rcrustin*Pm*7 before adding into the wells in a milk agar plate. The transparent zones observed after overnight incubation at room temperature indicate proteinase inhibitory activity.

3.5 Cell wall components and lipid binding assay

3.5.1 Lipid-protein interaction

To investigate the binding ability of rcrustin*Pm*1 and rcrustin*Pm*7 to lipid components, PIP strips™ was used. PIP strips™ hydrophobic membranes have been spotted with 15 different biologically active lipids at 100 pmol per spot. This membrane was used to determine lipid-protein interactions. After incubation rcrustin*Pm*1 and rcrustin*Pm*7 proteins in concentration of 0.5 µl/ml with lipid membranes, and then, incubated with primary and secondary antibodies that specific to both proteins. Color changed of the reaction as purple spot occurred when developed with chemiluminescent ECL solution (Figure 3.12A and 3.12B). The result showed that phosphatidic acid developed a strong purple spot within a few minute, suggesting that rcrustin*Pm*1 and rcrustin*Pm*7 can be bind sharply to phosphatidic acid (PA). Phosphatidic acid is a part of common phospholipids that is major constituents of prokaryote cell membranes.

(A)
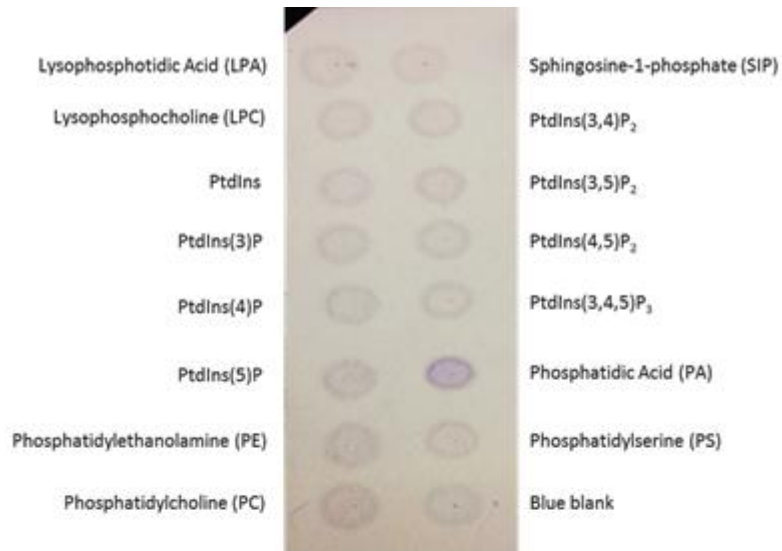
(B)
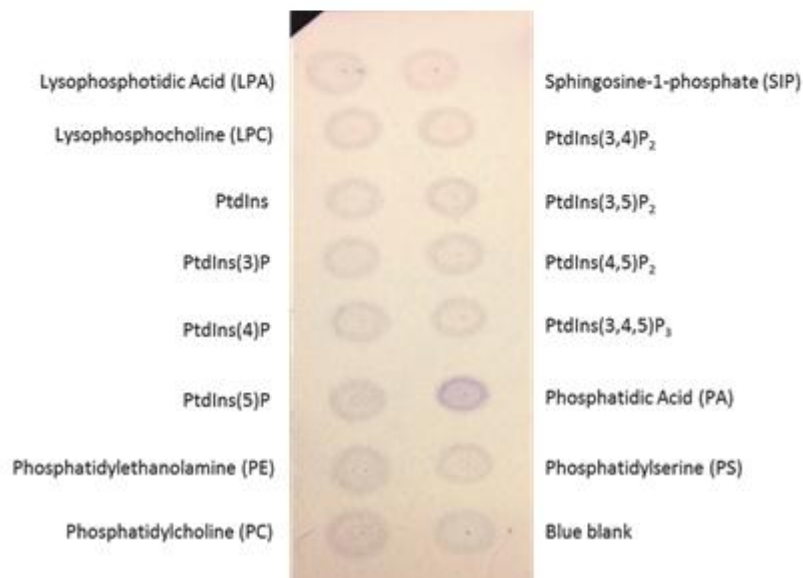
Figure 3.12 The rcrustin*Pm*1 (A) and rcrustin*Pm*7 (B) were incubated on PIP Strips at 0.5 µl/ml in PBS-T 3% BSA, then, developed with chemiluminescent solution ECL.

3.5.2 Binding properties of crustin*Pm*1 and crustin*Pm*7 to the cell wall components and lipid by Enzyme-linked immunosorbent assay (ELISA)

In previous study, the rcrustin*Pm*1 and rcrustin*Pm*7 can bind to the bacterial cell wall components of Gram-negative and Gram-positive bacteria such as lipopolysaccharide (LPS) and lipoteichoic acid (LTA). Binding to cell wall components may be a key action of crustins to kill bacteria. Enzyme-linked immunosorbent assay (ELISA) was used to quantitatively measure of crustins to LPS, LTA and PA. The data showed that the rcrustin*Pm*1 and rcrustin*Pm*7 can bind to LPS, LTA and PA in concentration-dependent and saturated manner. The data was analyzed by Graphpad Prism 6.0 software using nonlinear regression analysis with a One-site : Specific binding with Hill slope model. The result showed that both rcrustin*Pm*1 and rcrustin*Pm*7 bound to LPS, LTA, and PA with dissociation constant (K_d) values or followed: of rcrustin*Pm*1 is 4.131×10^{-6} M (LPS), 1.146×10^{-7} M (LTA), and 8.672×10^{-8} M (PA) with Hill slope (H) = 2.771 (LPS), 2.241 (LTA), and 2.153 (PA) (R^2 = 0.9925, 0.9842, and 0.9905 for LPS, LTA, and PA, respectively) (Figure 3.13A); of rcrustin*Pm*7 is 1.658×10^{-7} M (LPS), 1.499×10^{-7} M (LTA), and 9.719×10^{-8} M (PA) with Hill slope (H) = 2.169 (LPS), 2.141 (LTA), and 2.276 (PA) (R^2 = 0.9818, 0.9850, and 0.9906 for LPS, LTA, and PA, respectively) (Figure 3.13B). Hill slope (H) is value which presents the ligand or receptor binding sites with positive co-operativity.

(A)
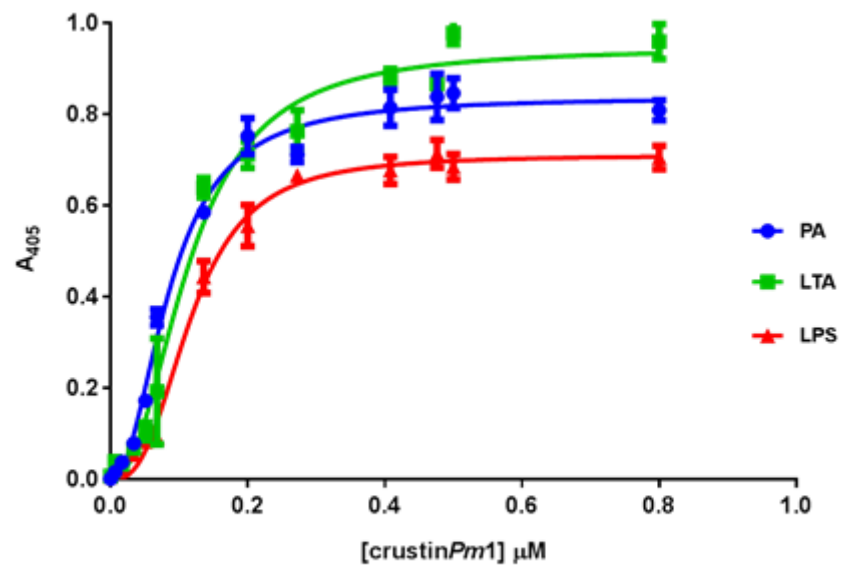
(B)
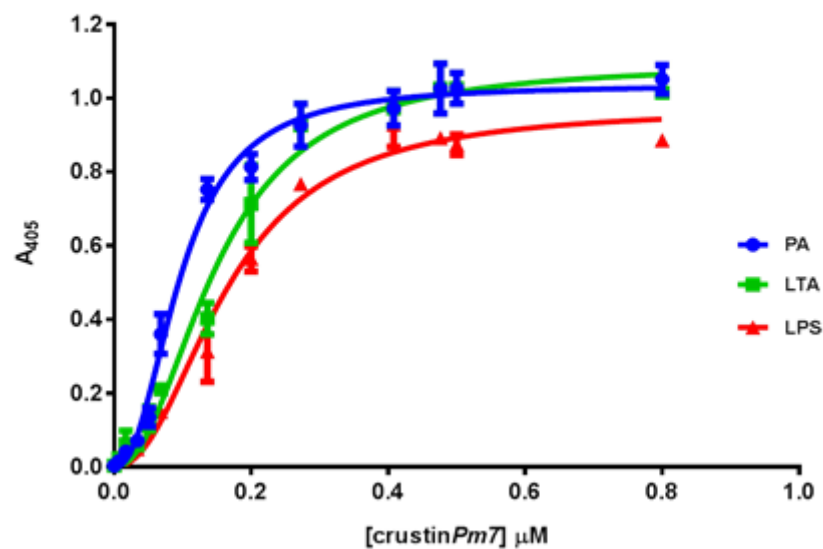
Figure 3.13 Quantitative binding of the rcrustin*Pm*1 (A) and rcrustin*Pm*7 (B) to LPS, LTA, and PA. 3 µg of LPS (red), LTA (green) or PA (blue) were coated in the wells and incubated with various amounts of rcrustin*Pm*1 and rcrustin*Pm*7. For rcrustin*Pm*1, dissociation constant (K_d) values are 4.131×10^{-6} M (LPS), 1.146×10^{-7} M (LTA), and

8.672×10^{-8} M (PA) with Hill slope (H) = 2.771 (LPS), 2.241 (LTA), and 2.153 (PA). For rcrustin*Pm*7, dissociation constant (K_d) values are 1.658×10^{-7} M (LPS), 1.499×10^{-7} M (LTA), and 9.719×10^{-8} M (PA) with Hill slope (H) = 2.169 (LPS), 2.141 (LTA), and 2.276 (PA).

3.6 Determination of the secondary structure by Circular Dichroism (CD) Spectroscopy

Assessment of protein conformation of rcrustin*Pm*1 and rcrustin*Pm*7 was performed by Circular Dichroism (CD) spectroscopy. CD is the technique to study chiral molecules. CD is measured in or near the absorption bands of the molecule of interest. The structural elements are more clearly discriminated because their recorded bands do not overlap widely at particular wavelengths. The far-UV (ultraviolet) CD spectrum of proteins is used to examine the secondary structure. CD spectra can be used to evaluate the molecules that form in the alpha-helix conformation, the beta-sheet conformation, the beta-turn conformation, or random coil conformation.

Circular dichroism (CD) studies were determined using J-715 CD Spectropolarimeter (JASCO). The CD spectra were represented and recorded between the far-UV (190-240 nm) using 0.8 mg/ml of purified protein in 10 mM Tris-HCl beffer, pH 7.4. In this experiment, the obtained CD spectra value at each wavelength that was an average of three consecutive scans using a bandwidth of 2 nm and a response time of 2 sec with 50 mm/min scanning speed. The spectra of blank buffer with 10 mM Tris-HCl buffer, pH 7.4 was subtracted with the protein spectra. The CD spectra was converted to molar ellipticity in units of degree*cm^2*$dmol^{-1}$ using the equation:

$$[\theta] = \theta / (10 \times n \times C_p \times l) \tag{1}$$

where θ is the ellipticity in millidegrees, C_p is the peptide molar concentration (M), l is the path length of the cell in cm, and n is the number of amino acid residues.

The CD spectra showed that rcrustin*Pm*1 and rcrustin*Pm*7 proteins have trend to form helical structure and beta-sheet structure. The negative peaks observed by a typical double absorption minimum at 208 nm and 222 nm represent a helical content (Greenfield 2006), and the beta-sheet structure has the negative peak of CD angle at 218 nm. CD spectra of rcrustin*Pm*1 and rcrustin*Pm*7 proteins presented that the major secondary structure of both proteins were **α** - helix and **β** - sheet, respectively compare to standard protein which known secondary structure (Figure 3.14). The percentages of amount the secondary structures such as **α**-helix and **β**-strand were analyzed and predicted by K2D3 program (Andrade *et al.* 1993). The result showed that the percentages of predicted secondary structure type of

rcrustin*Pm*1 proteins were 40.81% **α**-helix and 22.34% **β**-strand (Figure 3.15A), while rcrustin*Pm*7 proteins were 32.86% **α**-helix and 27.53% **β**-strand (Figure 3.15B). From CD spectra, both rcrustin*Pm*s proteins had a similar secondary structure.

Source : http://www.fbs.leeds.ac.uk/facilities/cd/
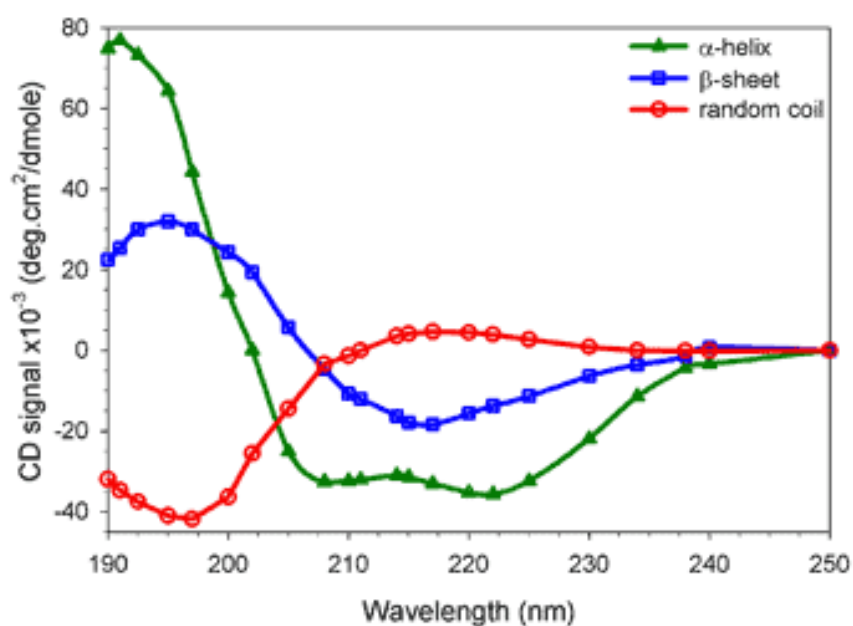
Figure 3.14 Three basic secondary structures of a polypeptide chain (helix, sheet, coil) show a characteristic CD spectrum.

(A)
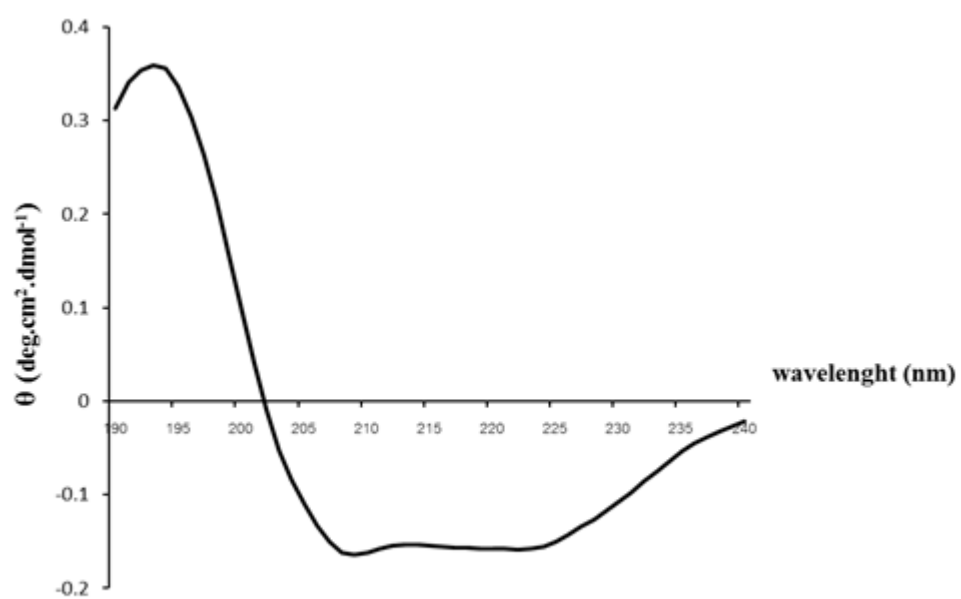
(B)
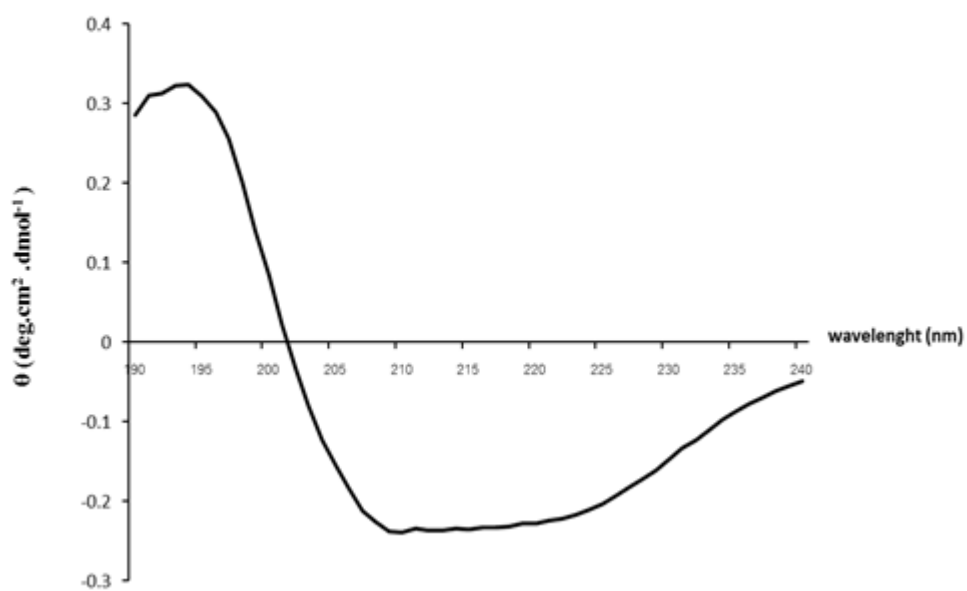
Figure 3.15 CD spectra of rcrustin*Pm*1 (A) and rcrustin*Pm*7 (B).

3.7 Crystallization of rcrustin*Pm*1 protein

3.7.1 Pre-crystallization test by PCT™ (Hampton Research)

The PCT™ was used to determine the appropriate protein concentration for crystallization screening (Aleksandra and Christopher 2005). The precipitate was observed in the drop by a light microscope and compared to those in Figures 2.3. The result showed that PCT reagent A1/A2 was a clear/light granular precipitate and PCT reagent with B1/B2 was a clear/light granular precipitate (data not shown). This indicated that the concentration of rcrustin*Pm*1 that was suitable for crystallization.

3.7.2 Crystallization screening of rcrustin*Pm*1

Crystallization of purified rcrustin*Pm*1 was screened by crystal screening kits (Hampton Research and Emerald Biosystems screening kits), using sitting drop vapor diffusion method. Proteins were mixed with Index reservoir solutions (Hampton Research) in 96-well plate in ratio 1:1. Crystals appeared in different 3 conditions (Figure 3.16).

- 2 M Lithium sulfate

- 2% PEG400

- 100 mM Tris-HCl pH 8.5
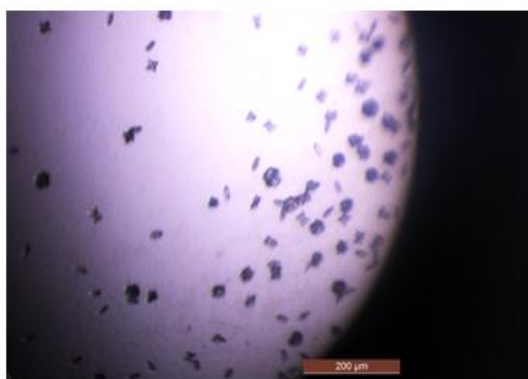
- 1.5M Lithium sulfate

- 1.5% PEG 400

- 100mM Tris-HCl pH 8.4

- 30% xylitol

- 0.5M Lithium sulfate

- 1.7% PEG 400

- 100mM Tris-HCl pH 8.6

Figure 3.16 Crystals appeared in different conditions in 96-well plate.

3.7.3 Co-crystallization of rcrustinPm1 and phosphatidic acid (PA)

Co-crystallization of purified rcrustin*Pm*1 and phosphatidic acid (PA) was prepared by mixing the purified protein with lipid (PA) at 1:1 molar ratio. The protein solution was then used for crystallization screening. Crustin*Pm*1-PA solution was mixed with reservoir solution at 1:1 in 96-well crystallization plate. Crystals appeared in various conditions. Then, crystallization conditions by Additive screen kit (Hampton Research). Each condition was optimized in 24-well plate using different ratio of protein : precipitant (1:1 or 2:1). Figure 3.17 shows crystal produced by mixing crustin*Pm*1-PA solution with the reservoir solution at ratio 2:1.
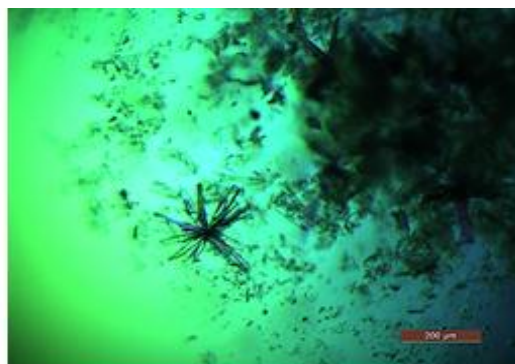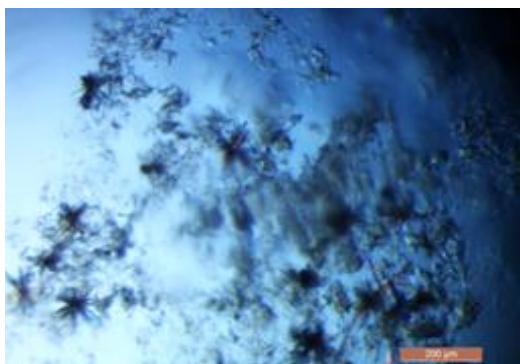
- 0.05 M Zinc acetate dehydrate

- 20% w/v PEG 3350

- 0.05 M Zinc acetate dehydrate

- 20% w/v PEG 3350

- 30% v/v glycerol
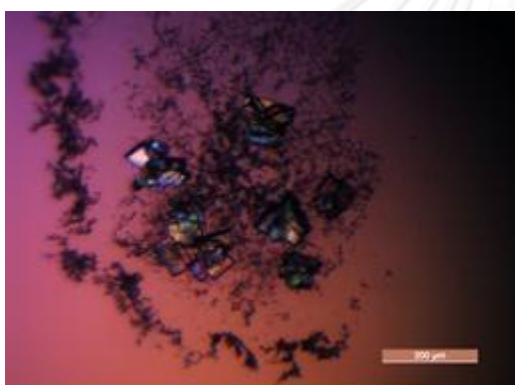
- 0.05 M Zinc acetate dehydrate

- 20% w/v PEG 3350

- 20% w/v TCEP hydrochlorid

- 0.05 M Zinc acetate dehydrate

- 20% w/v PEG 3350

- 20% w/v Benzamidine hydrochlorid

- 0.05 M Zinc acetate dehydrate

- 20% w/v PEG 3350

- 20% w/v Benzamidine hydrochloride

Figure 3.17 Crystals appeared using the additive screen.

3.8 Sequence analysis of *Pm*MyD88 gene

*Pm*MyD88 is a gene in Toll pathway. *Pm*MyD88 was found in *P. monodon* and generated by PCR amplification using primers that were designed from conserved regions of the published MyD88 nucleotide sequences of *F. chinensis* (Wen *et al.* 2013) and *L. vannamei* (Zhang *et al.* 2012) (Figure 3.18). A partial *Pm*MyD88 DNA fragment of 655 bp was amplified (Figure 3.19). After cloning and sequencing, a partial *Pm*MyD88 gene was compared with a full-length nucleotide sequences from *F. chinensis* and *L. vannamei* database using the ClastalX program. Amino acid sequence alignment showed that the *Pm*MyD88, like the *Fc*MyD88 and *Lv*MyD88, which contained conserved amino acid sequences such as a death domain (DD) and interleukin-1 receptor (IL-1R)-related (TIR) domain (Figure 3.20). BlastX search showed that *Pm*MyD88 showed the highest similarity 46% amino acid sequence homology from *F. chinensis* (AFP49302.1), *L. vannamei* (AFU61120.1) and *Scylla Serrata* (AFZ95001.1) with Max ident score of 46%, 45% and 38%, respectively (Table 3.3).

```
FcMyD88    351 TCTGTGGGGCCAGAAGGGTGGACTTATAGGACAACTGTGGACTTACTTGG 400
               |||||||||||||||||||||||||||||||||||.|||||||||||||||
LvMyD88    213 TCTGTGGGGCCAGAAGGGTGGACTTATAGGACAACTTTGGACTTACTTGG 262

FcMyD88    401 AAGCAATGGATCGCTTTGATGTCATTGATGACACACTTCAGATGATATAT 450
               ||||||||||||||||||||||||||||||||.||||||||||||||||||
LvMyD88    263 AAGCAATGGATCGCTTTGATGTCATTGATGATACACTTCAGATGATATAT 312

FcMyD88    451 GTTGATTATGACAAGTGTATGACTCAGAGTGGAGGGGCCTTGACAGCTGT 500
               |.|||||||||||||||||||||||||||||||||||||||..|||||
LvMyD88    313 GCTGATTATGACAAGTGTATGACTCAGAGTGGAGGGGCCTTGATGGCTGT 362

FcMyD88    501 TCCTCCTCCATTTGACCAAAGGGTGCCACAGATAGCAGAACAAGATAGCC 550
               |||.||.|||||||||||.|||||||||||.||||||||||||||||||||
LvMyD88    363 TCCACCGCCATTTGACCAGAGGGTGCCACAGGTAGCAGAACAAGATAGCC 412

FcMyD88    551 AAATCCTTACTGTAGATGATCTGAACAACCTCAGCAAAGGTCTTGAACTA 600
               |||||.|||||||||||||||||||||||||||||||||||||.||||
LvMyD88    413 AAATTCTTACTGTAGATGATCTGAACAACCTCAGCAAAGGTCTTGGACTA 462

FcMyD88    601 CAGCACTATGATGCACTTGTCTTATTTGCTGATGAAGATATTGACTTTGT 650
               |||||||||||||||||||||||||||||||||||||||||||||||||
LvMyD88    463 CAGCACTATGATGCACTTGTCTTATTTGCTGATGAAGATATTGACTTTGT 512

FcMyD88    651 ACAAGAAATGTTAGAAAAATTAGAGGGAGAATATAATCTTAAGCTGTGTC 700
               |||||||||||||||||||||||||||||||||||||||||||||||||
LvMyD88    513 ACAAGAAATGTTAGAAAAATTAGAGGGAGAATATAATCTTAAGCTGTGTC 562

FcMyD88    701 ACAAGAACAGAGACCTAATTGGTGGACTGCAGTTTGAGTCAGAAAGCATT 750
               |||||||||||||||.|||||||.|||||||||||||||.|||||||||
LvMyD88    563 ACAAGAACAGAGACCTTATTGGTGGTCTGCAGTTTGAGTCTGAAAGCATT 612

FcMyD88    751 GTTAAACTCATCATGGAGAGGTGCACCAGAGTCATTGTAGTTTTGTCTCC 800
               |||||||||||||||||.||||||||||||||||||||||||||||||
LvMyD88    613 GTTAAACTCATCATGGAGCGGTGCACCAGAGTCATTGTAGTTTTGTCTCC 662

FcMyD88    801 AGAATTCTTAGAGTCCAGTACAAACACCTTTTTCACTTTATTTGCTCATG 850
               |||||||||||||||.|||||||||||||||||||||||||||||||
LvMyD88    663 AGAATTCTTAGAGTCGAGTACAAACACCTTTTTCACTTTATTTGCTCATG 712

FcMyD88    851 CTCTCAGTATAGATCAGCGTCGTCGCATAGTCATTCCTTGCTTATACAAG 900
               ||||||||.||||||||||||||.|||||||||||||||||||||||||
LvMyD88    713 CTCTCAGTGTAGATCAGCGTCGTCGTATAGTCATTCCTTGCTTATACAAG 762

FcMyD88    901 CCATGTGTAAAACCTGCTGTGATAAGTTTCTGCCACTCCCTTGATTACTA 950
               ||||||||||||||||||||||||||||||||||||||||||.||||||.||
LvMyD88    763 CCATGTGTAAAACCTGCTGTGATAAGTTTCTGCCACTCCCTCGATTATTA 812

FcMyD88    951 TAGGGCAAAGGGCTATTGGAACTATTGGGAAAAGTTACGTGATTCTTTAA 1000
               ||||||||||||||||||||||||||||||||||||||||||||.|||
LvMyD88    813 TAGGGCAAAGGGCTATTGGAACTATTGGGAAAAGTTACGTGATTCTCTAA 862

FcMyD88   1001 TCTGGCAACCACAAAATACTCCCAGCACACCAAACGCAGAATCAAGACAA 1050
               |||||||||||||||||||||||.|||||||||||.|.|||||||||||
LvMyD88    863 TCTGGCAACCACAAAATACTCCAAGCACACCAAATGTAGAATCAAGACAA 912
```

Figure 3.18 Sequence alignment of MyD88 nucleotide sequences of *Fenneropenaeus chinesis* (GenBank: JX501341.1) and *Litopenaeus vannamei* (GenBank: JX073566.1).
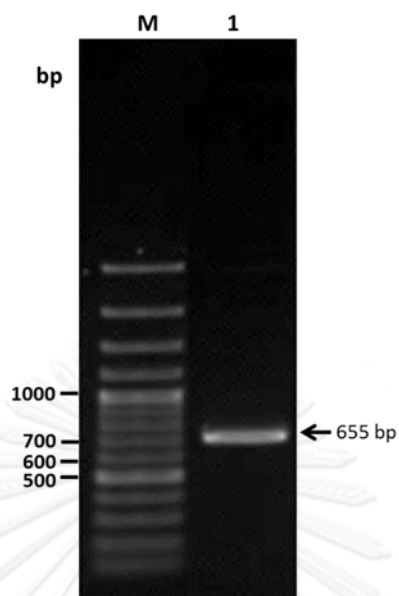
Figure 3.19 Amplification of a partial fragment of *Pm*MyD88 from cDNA of unchallenged *P. monodon* using MyD88F and MyD88R primer (Table 2.1).

Lane M: 100 bp DNA ladder marker (GeneRuler^{TM} 100 bp DNA ladder, Fermentas)

Lane 1: The purified PCR product of *Pm*MyD88 amplification

Table 3.3 Lists of homology search result of *Pm*MyD88 gene blast against NCBI database using blastX program.

Accession	Description	Max ident
AFU61120.1	myeloid differentiation factor 88 [*F. chinensis*]	46%
AFP49302.1	myeloid differentiation factor 88 [*L. vannamei*]	45%
AFP49300.1	myeloid differentiation factor 88 [*L. vannamei*]	45%
AFZ95001.1	myeloid differentiation primary response protein 88 [*Scylla serrata*]	38%
AFP49301.1	myeloid differentiation factor 88-1 [*L. vannamei*]	37%

```
 10  CCTACATGGATGCAAAGGATTATTTGAATGGTCTTTGCTGCAGATGATATACGCTGAAGA  60
      L  H  G  C  K  G  F  F  E  W  S  L  L  Q  M  I  Y  A  E  D

 61  TGAAGAGTGTATGGAGCAGTTAGGAGGGGCCTTGACTTCAAATCCACCGTCATTAGTCCA 120
      E  E  C  M  E  Q  L  G  G  A  L  T  S  N  P  P  S  L  V  Q

121  GAGGGTGCCACAGGATGTTGCTTCAGGTAGCCAAAAATTTACGGTAGAGATGGTAACAAT 180
      R  V  P  Q  D  V  A  S  G  S  Q  K  F  T  V  E  I  V  T  I

181  ATCAGCAAATGTCTCAAACTACAGCACTTTGTTGCACCCAGTCTTATTTGCTGTTTCTAA 240
      S  A  N  V  S  N  Y  S  T  L  L  H  P  V  L  F  A  V  S  K

241  AATTGACTTTGTACAAGAAATGGAGCAACCATTAGAGGGAGAAGATATACAACAGATTTG 330
      I  D  F  V  Q  E  M  E  Q  P  L  E  G  E  D  I  Q  Q  I  C

231  TATATCGTTTACTTATTGGTTATGCAATATGAGTCGGAAAGCCAAGTTAAACTCATCTTA 360
      I  S  F  T  Y  W  L  C  N  M  S  R  K  A  K  L  N  S  S  T

361  GCGGAGTTCCAGAGTCATTGTAGTTTTGTCTCCAGAATTCTTAGAGTCAAGTACAAACTA 420
      R  S  S  R  V  I  V  V  L  S  P  E  F  L  E  S  S  T  N  Y

421  CAGATACACTTTATTTGCTCTTGCTCGGAAAGTGTTGAACAATGTCGTCGCATAGTCATT 480
      R  Y  T  L  F  A  L  A  R  K  V  L  N  N  V  V  A  Y  S  F

481  CCTTGATGAAGCAAGCCTGTGTAAAACTCTATGTGAAAGGTTTTTGCCACTCCCTCGAAT 540
      L  D  E  A  S  L  C  K  T  L  C  E  R  F  L  P  L  P  R  M

541  GATATAAAAAATTACTTCAGAAGTTTATTGGAACTATGTTTTTGTAAGTAAGTTACGTGA 610
      I  Y  K  I  T  S  E  V  Y  W  N  Y  V  L  V  S  K  L  R  D

611  TTCTCTAATCTGGCAACCACGTAAATACTCCAAGCACACCAAATGTAGAATCAAG       660
      S  L  I  W  Q  P  R  K  Y  S  K  H  T  K  C  R  I  K
```

Figure 3.20 The partial amino acid sequence of *Pm*MyD88 in *Penaeus monodon*. The numbers showed the number of nucleotides. The TIR domain is shown in shadow.

3.9 The effect of the cell wall components injection on genes expression

It was clear from previous reports that crustins act against bacterial infection in *P. monodon* (Amparyup *et al.* 2008, Supungul *et al.* 2008). This experiment aims to investigate a pathway that regulates crustin*Pm*1 and crustin*Pm*7 expression. To do so, shrimps were injected with crude cell wall components of bacteria and then expressions of genes in shrimp immune system were measured. These genes are crustin*Pm*1, crustin*Pm*7, *Pm*Relish (belongs to Imd pathway), *Pm*Spätzle, *Pm*MyD88 and Dorsal (all three genes belong to Toll pathway).

The expression profiles of crustin*Pm*1 in shrimp after stimulation by heat-inactivated *V. harveyi* and *S. aureus* were shown in Figure 3.21. The expression of crustin*Pm*1 responded to *S. aureus* injection. At 3 and 6 hpi, the expression levels of crustin*Pm*1 in shrimp stimulated by *V. harveyi* and *S. aureus* were significantly down-regulated, compared with NaCl group at the same sampling point. At 12 and 24 hpi, crustin*Pm*1 expression in *S. aureus* injected group was remarkably up-regulated, but shown no expression change in shrimp stimulated by *V. harveyi*, compared to those in control group. At 48 hpi, the expression level of crustin*Pm*1 in *V. harveyi* group was kept at the same level, but significantly down-regulated in shrimp stimulated by *S. aureus*, compared to that of NaCl group. Clearly, crustin*Pm*1 was highly response to *S. aureus* injection, but not to *V. harveyi*.

The expression profiles of crustin*Pm*7 in shrimp after stimulation by heat-inactivated *V. harveyi* and *S. aureus* were analyzed in Figure 3.22. Expression of crustin*Pm*7 was responsive to *V. harveyi* and *S. aureus* injection. At 3 hpi, the transcription level of crustin*Pm*7 after stimulation by *V. harveyi* and *S. aureus* were down-regulated, compared with that of NaCl group. At 6 hpi, the transcription level was unchanged in shrimp stimulated by both *V. harveyi* and *S. aureus*. At 12-24 hpi, the transcription level of crustin*Pm*7 in *V. harveyi* and *S. aureus* group were significantly up-regulated and kept a highest level at 12 hpi for *S. aureus* group, but kept a highest level at 24 hpi for *V. harveyi* group. At 48 hpi, the transcription level was gradually down-regulated in shrimp stimulated by *S. aureus*, but significantly up-regulated in shrimp stimulated by *V. harveyi*, compared to those in its group. Unlike crustin*Pm*1, crustin*Pm*7 was highly response to both *S. aureus* and *V. harveyi* injection.

Figure 3.21 The expression profiles of crustin*Pm*1 in shrimp hemocyte after bacterial challenge in different time points. The relative expression of crustin*Pm*1 in treated groups, NaCl : experiment group with NaCl; SA: experiment group with *S. aureus* injection; VH: experiment group with *V. harveyi* injection. Each sample had three replicates. The mRNA expression levels of crustin*Pm*1 were analyzed by Quantitative Real-time RT-PCR. The data was normalized to EF1α gene, which served as an internal control and shown as the mean ± SD. * indicates significant difference ($P < 0.05$) and ** indicates significant difference ($P < 0.01$) compared with control group.
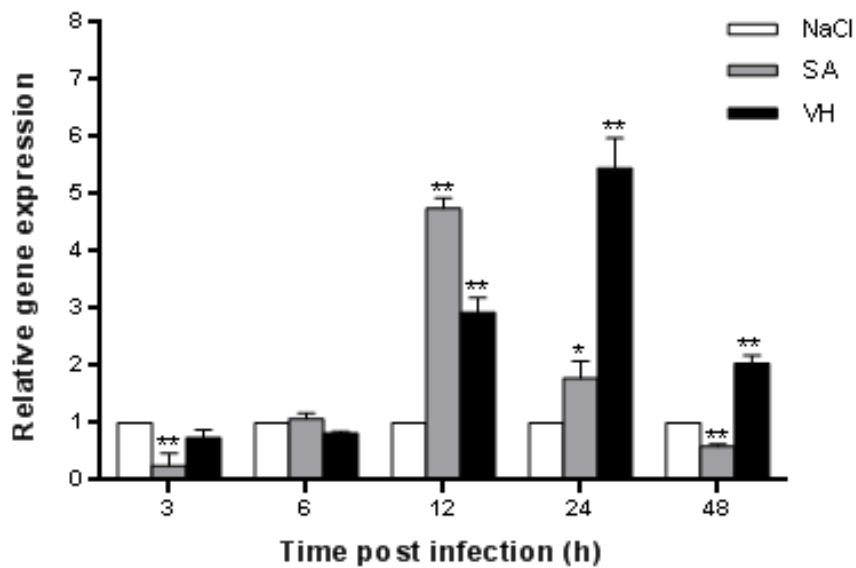
Figure 3.22 The expression profiles of crustin*Pm*7 in shrimp hemocyte after bacterial challenge in different time points. The relative expression of crustin*Pm*7 in treated groups, NaCl : experiment group with NaCl; SA: experiment group with *S. aureus* injection; VH: experiment group with *V. harveyi* injection. Each sample had three replicates. The mRNA expression levels of crustin*Pm*7 were analyzed by Quantitative Real-time RT-PCR. The data was normalized to EF1α gene, which served as an internal control and shown as the mean ± SD. * indicates significant difference ($P < 0.05$) and ** indicates significant difference ($P < 0.01$) compared with control group.

The expression of *Pm*Relish, a gene of Imd pathway, after stimulation by *V. harveyi* and *S. aureus* was shown in Figure 3.23. The transcription level of *Pm*Relish was responsive to *V. harveyi* and *S. aureus* injection. At 3 and 6 hpi, the transcription level of *Pm*Relish of *S. aureus* group was significantly down-regulated, but remarkably up-regulated in shrimp stimulated by *V. harveyi*. At 12 and 24 hpi, the transcription level was gradually up-regulated in shrimp stimulated by both *V. harveyi* and *S. aureus*, compared with that of NaCl group. At 48 hpi, the transcription level was up-regulated after *V. harveyi* injected group, but kept in a same level after *S. aureus* injected group, compared to those in its group. *V. harveyi* injection seemed to trigger larger scale changes in *Pm*Relish expression (up to 7.3 fold at 6 h post injection), while *S. aureus* injection caused small changes in *Pm*Relish expression (1.87 fold at 24 h post injection).
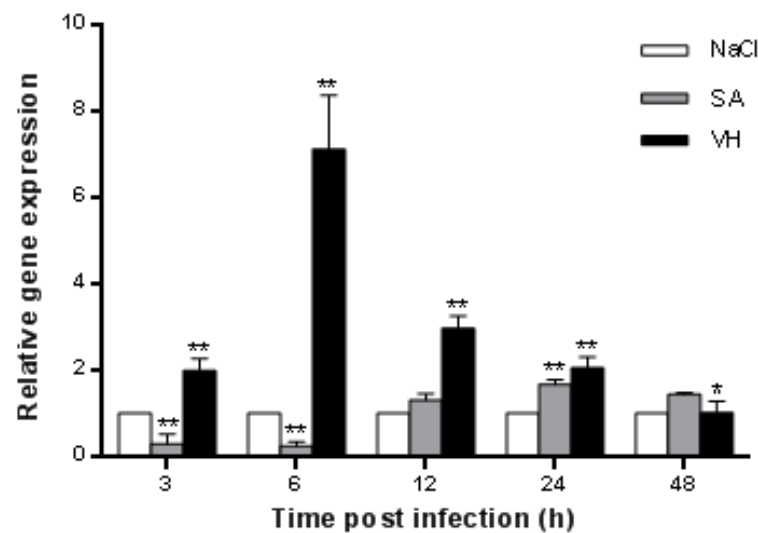
Figure 3.23 The expression profiles of *Pm*Relish in shrimp hemocyte after bacterial challenge in different time points. The relative expression of *Pm*Relish in treated groups, SA: experiment group with *S. aureus* injection; VH: experiment group with *V. harveyi* injection. Each sample had three replicates. The mRNA expression levels of *Pm*Relish were analyzed by Quantitative Real-time RT-PCR. The data was normalized to EF1α gene, which served as an internal control and shown as the mean ± SD. * indicates significant difference ($P < 0.05$) and ** indicates significant difference ($P < 0.01$) compared with control group.

Figure 3.24 shows the expression of *Pm*Spätzle, a gene in Toll pathway, after stimulation by *V. harveyi* and *S. aureus*. The *Pm*Spätzle expression level was responded to both *V. harveyi* and *S. aureus* injection. At 3-24 hpi, the expression level of *Pm*Spätzle after stimulation by both *S. aureus* and *V. harveyi* group were continuously up-regulated, but reached their peak at 24 hpi. *Pm*Spätzle was highestly up-regulated to 14.2 and 7.3 fold after *S. aureus* and *V. harveyi* injection, respectively. It is likely that expression of *Pm*Spätzle could be turned on by both *S. aureus* and *V. harveyi* injection.
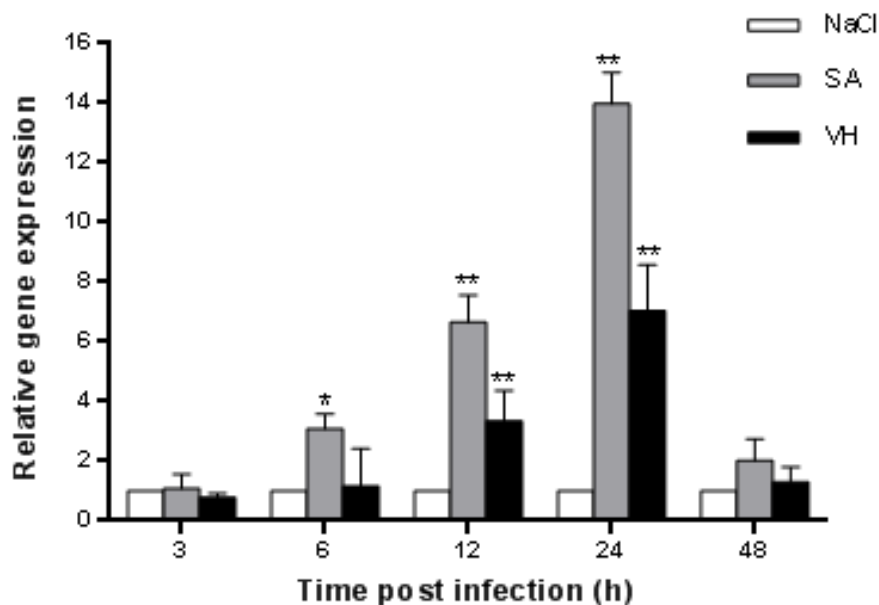
Figure 3.24 The expression profiles of *Pm*Spätzle in shrimp hemocyte after bacterial challenge in different time points. The relative expression of *Pm*Spätzle in treated groups, NaCl : experiment group with NaCl; SA: experiment group with *S. aureus* injection; VH: experiment group with *V. harveyi* injection. Each sample had three replicates. The mRNA expression levels of *Pm*Spätzle were analyzed by Quantitative Real-time RT-PCR. The data was normalized to EF1α gene, which served as an internal control and shown as the mean ± SD. * indicates significant difference ($P < 0.05$) and ** indicates significant difference ($P < 0.01$) compared with control group.

Expression of Dorsal, a gene in Toll pathway, after *V. harveyi* and *S. aureus* were illustrated in Figure 3.25. The Dorsal expression level was responsive to both *V. harveyi* and *S. aureus* injection. The result showed that the Dorsal expression level started to increase at 3 hpi for *S. aureus* and *V. harveyi* injected group. Interestingly, Dorsal was significantly up-regulated at 24 (>15 fold) and 48 hpi (>25 fold) with both *V. harveyi* and *S. aureus* injection when compared with the control group. Similar to *Pm*Spätzle expression, dorsal gene was dramatically up-regulated at late phase of *S. aureus* and *V. harveyi* injection.
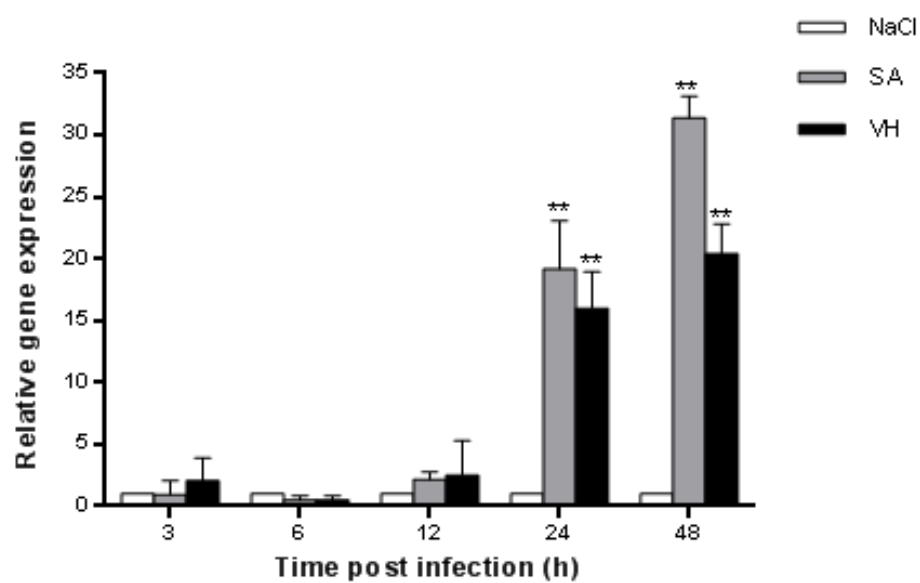
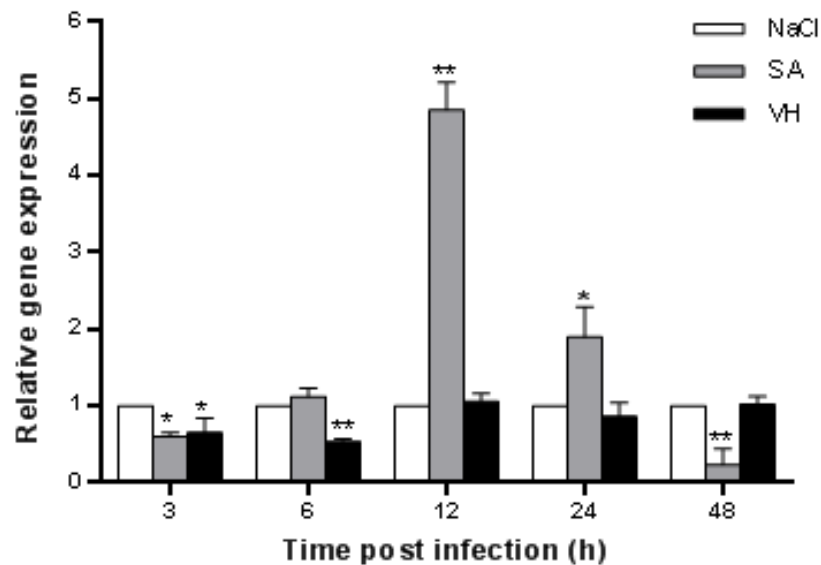**Figure 3.25** The expression profiles of Dorsal in shrimp hemocyte after bacterial challenge in different time points. The relative expression of Dorsal in treated groups, NaCl : experiment group with NaCl; SA: experiment group with *S. aureus* injection; VH: experiment group with *V. harveyi* injection. Each sample had three replicates. The mRNA expression levels of Dorsal were analyzed by Quantitative Real-time RT-PCR. The data was normalized to EF1α gene, which served as an internal control and shown as the mean ± SD. * indicates significant difference ($P < 0.05$) and ** indicates significant difference ($P < 0.01$) compared with control group.

Expression of *Pm*MyD88, a gene in Toll pathway, after stimulation by *V. harveyi* and *S. aureus* was presented in Figure 3.26. The expression level of *Pm*MyD88 after *S. aureus* infection was apparently up-regulated compared with that in NaCl group at 3-48 hpi and reached its peak at 24 hpi. A similar trend of *Pm*MyD88 expression was also obtained by *V. harveyi* injection. At 24 hpi, *Pm*MyD88 was up-regulated by 11.8 and 5.9 fold upon *S. aureus* and *V. harveyi* injection, respectively.
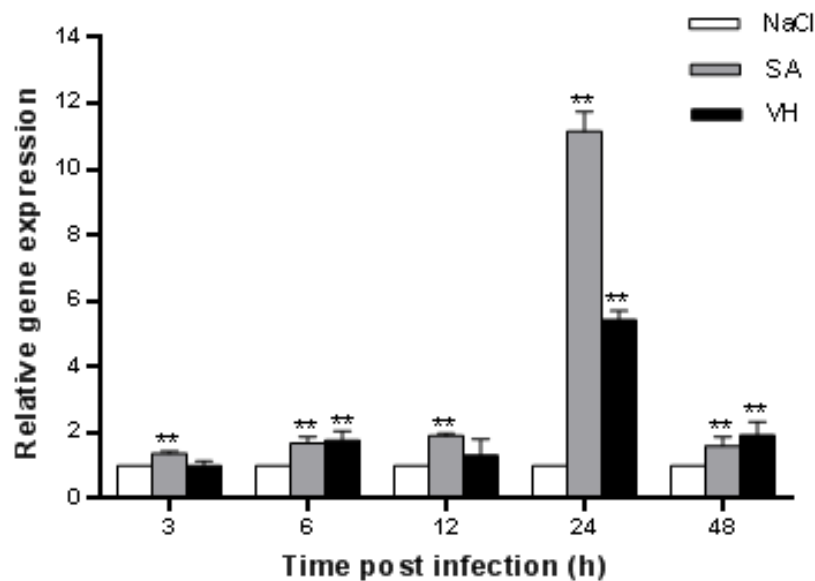
Figure 3.26 The expression profiles of *Pm*MyD88 in shrimp hemocyte after bacterial challenge in different time points. The relative expression of Dorsal in treated groups, NaCl : experiment group with NaCl; SA: experiment group with *S. aureus* injection; VH: experiment group with *V. harveyi* injection. Each sample had three replicates. The mRNA expression levels of Dorsal were analyzed by Quantitative Real-time RT-PCR. The data was normalized to EF1α gene, which served as an internal control and shown as the mean ± SD. * indicates significant difference ($P < 0.05$) and ** indicates significant difference ($P < 0.01$) compared with control group.

3.10 Knockdown of *Pm*Relish and *Pm*MyD88 gene in the black tiger shrimp

The Imd and Toll pathway are two distinct signal transduction pathways for the gene expression of antimicrobial peptides. The Rel/NF-kB transcription factors, Relish are activated in the signaling cascade of Imd pathway for antibacterial responses, while Spätzle, Dorsal and MyD88 are required for Toll pathway to activate the gene expression of AMPs.

Study of genes expression of crustin*Pm*1, crustin*Pm*7, *Pm*Relish, *Pm*Spätzle, Dorsal and *Pm*MyD88 after bacterial infection, pointed out that genes in Imd and Toll pathways may regulate crustin expression upon bacterial infection. To confirm this, *Pm*Relish and *Pm*MyD88, candidate genes of Imd and Toll pathways, respectively, were knockdowned, and expressions of crustin*Pm*1 and crustin*Pm*7 were measured.

3.10.1 Silencing efficiency of dsRelish

To tested ds*Pm*Relish-mediated silencing of expression of *Pm*Relish gene, NaCl, dsRelish or dsGFP of 5 µg /g shrimp were injected into individual shrimp. At 24 hpi, shrimp hemocytes were collected for total RNA extraction. The cDNA was synthesized and used for RT-PCR analysis. EF1α was used as an internal control. The result revealed that *Pm*Relish transcript level was significantly decreased in the *Pm*Relish dsRNA knockdown shrimps, whereas injection of GFP dsRNA had no effect on the *Pm*Relish mRNA transcript level when compared to the injection of NaCl in control shrimps (Figure 3.27). This indicated that dsRNA of *Pm*Relish significantly suppress the expression of *Pm*Relish at 24 hpi.
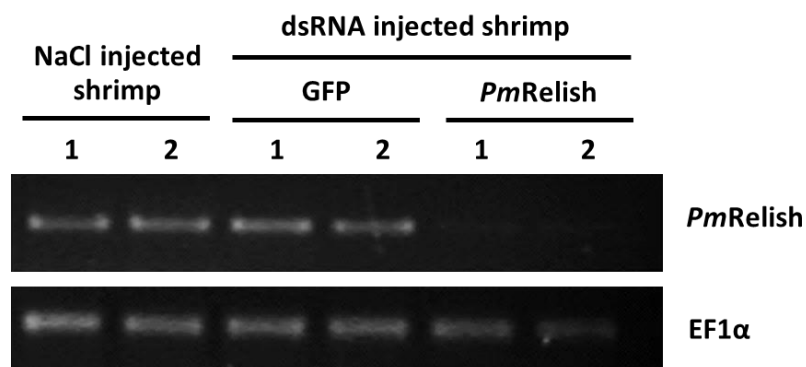
Figure 3.27 Effective gene silencing of the *Pm*Relish transcription in the hemocytes of *P. monodon*. The efficiency of dsRNA-mediated gene knockdown of *Pm*Relish gene was examined by RT-PCR analysis using the gene-specific primers (Table 2.1). GFP dsRNA or NaCl injected shrimps were served as controls. EF1α was used as the internal control gene to normalize the amount of cDNA template. Lane 1 and 2 represent the cDNA from each of two individual shrimps.

3.10.2 Effect of dsRelish on the transcription of crustin*Pm*1 and crustin*Pm*7

To investigate the effects of dsRelish-silencing upon Gram-positive (*S. aureus*) and Gram-negative (*V. harveyi*) infection, dsRelish was injected into shrimp and crustin*Pm*1 and crustin*Pm*7 transcripts were monitored by qRT-PCR.

After challengeing dsRelish-silenced shrimp with *S. aureus* and *V. harveyi*, crustin*Pm*7 expression level significantly decreased at 12 and 24 hpi (Figure 3.28A and 3.28B). However, *Pm*Relish silencing showed no effect on crustin*Pm*1 expression upon *S. aureus* and *V. harveyi* injection. It is likely that crustin*Pm*7 was regulated by Imd pathway but crustin*Pm*1 did not.

(A)

(B)
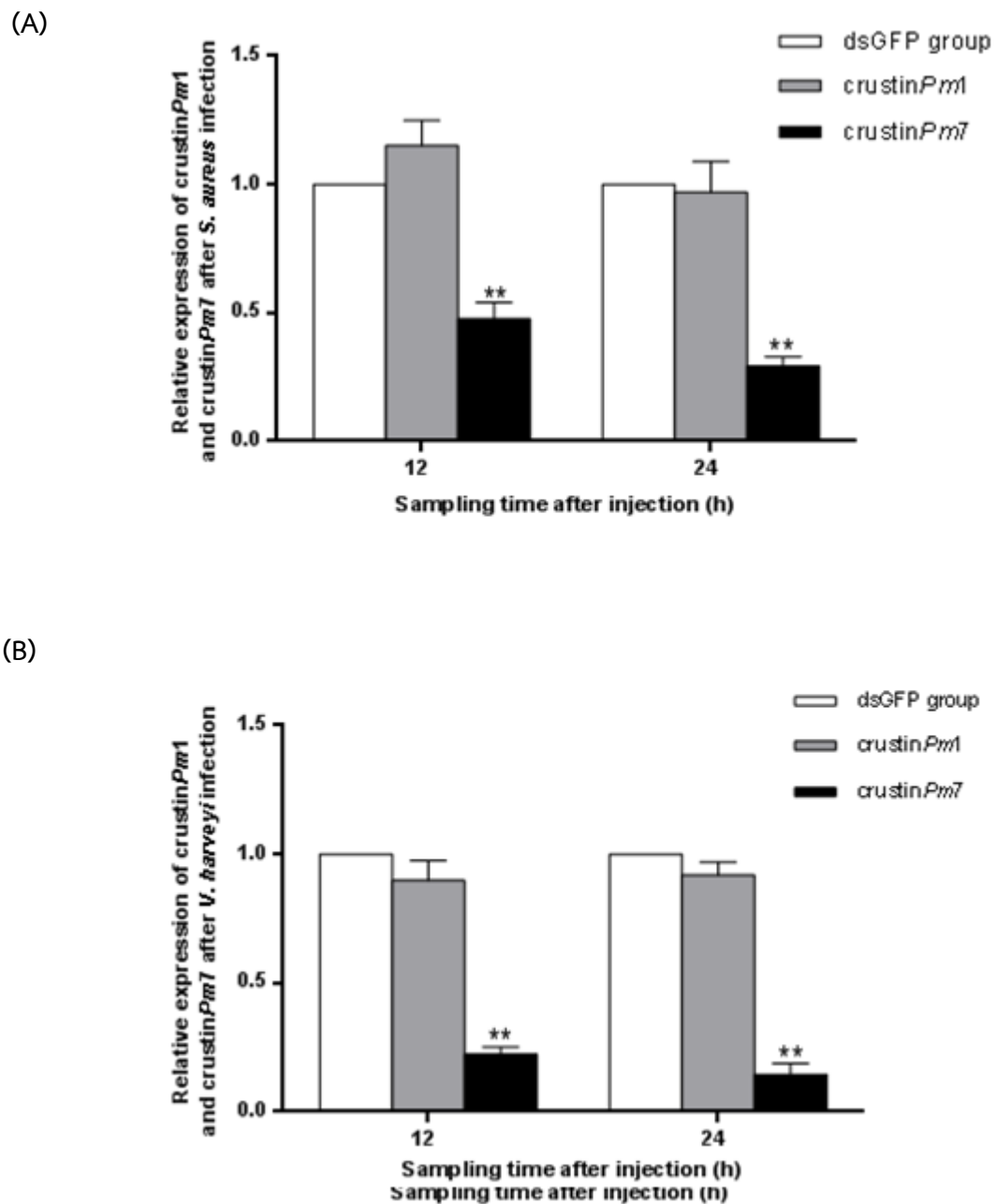
Figure 3.28 Expression profiles of crustinPm1 and crustinPm7 gene of dsPmRelish-silenced shrimp after *S. aureus* and *V. harveyi* challenge. dsGFP group represents shrimps injected with GFP dsRNA. 12 h indicates shrimp at 12 hpi of *S. aureus* or *V. harveyi* treatment group; 24 h indicates shrimp at 24 hpi of *S. aureus* or *V. harveyi* treatment group. The genes expression level of infected group was normalized to that of the control group. * indicates significant difference ($P < 0.05$) and ** indicates significant difference ($P < 0.01$) compared with control group.

3.10.3 Silencing efficiency of dsMyD88

To determine the amount of dsRNA MyD88 that could knockdown MyD88 gene in shrimp hemocytes, dsMyD88 of 5.0 and 7.5 µg/ g shrimp were injected into shrimps. The hemocytes were collected after 24 hours for total RNA extraction. The cDNA was synthesized and used for RT-PCR analysis. The 7.5 µg/g shrimp of dsRNA MyD88 was completely knockdown *Pm*MyD88, so this amount of dsRNA MyD88 was used for knocking down MyD88 gene in the next experiment (Figure 3.29).
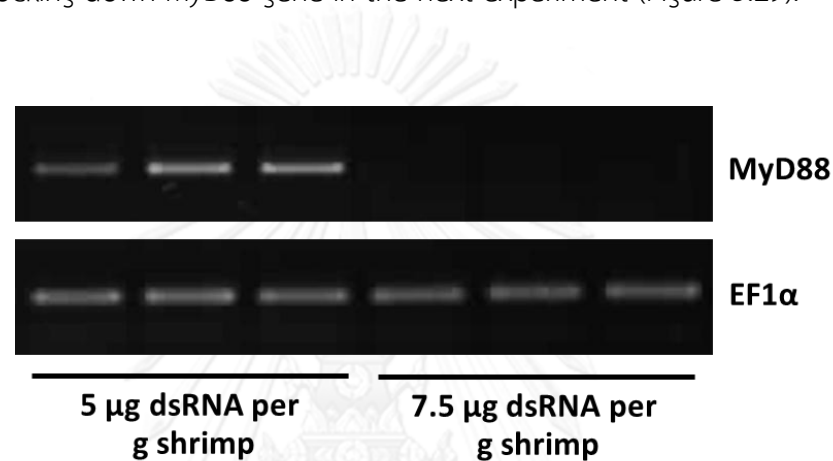
Figure 3.29 The expression of *Pm*MyD88 after different amounts of dsRNA MyD88 infection.

Next, 150 mM NaCl, 7.5 µg of dsMyD88 and 7.5 µg of dsGFP were injected into shrimp separately. At 24 hpi, shrimp hemocytes were collected for total RNA extraction. The cDNA was synthesized and used for RT-PCR analysis. EF1α was used as an internal control. The result showed that dsGFP and NaCl did not affect to the expression level of MyD88. In contrast, after dsMyD88 injection, the expression level of *Pm*MyD88 at 24 hpi was completely decreased (Figure 3.30).
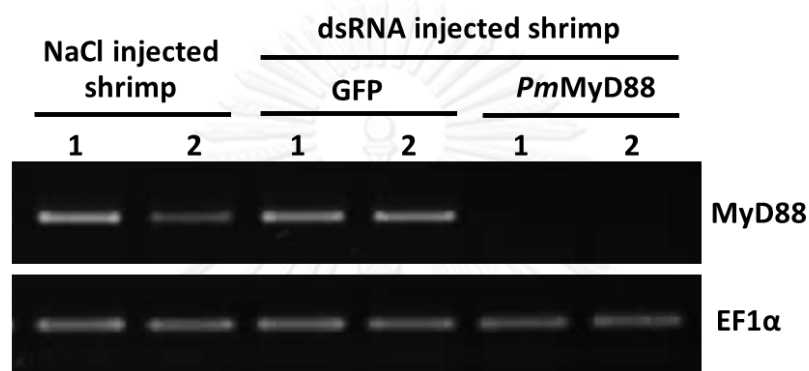
Figure 3.30 Effective gene silencing of the *Pm*MyD88 transcription in the hemocytes of *P. monodon*. The efficiency of dsRNA-mediated gene knockdown of *Pm*MyD88 gene was examined by RT-PCR analysis using the gene-specific (Table 2.1). dsRNA GFP or NaCl injected shrimps were served as controls. EF1α was used as the internal control gene to normalize the amount of cDNA template. Lane 1 and 2 represent the cDNA from each of two individual shrimps.

3.10.4 Effect of dsMyD88 on the transcription of crustin*Pm*1 and crustin*Pm*7

Shrimps were separated into 3 groups and injected with 150 mM NaCl, 7.5 µg of dsRNA GFP/g shrimp, and 7.5 µg of dsRNA MyD88/g shrimp. After 24 hours, all shrimps were injected with the mixture of Gram-positive (*S. aureus*) or Gram-negative bacteria (*V. harveyi*), containing dsRNA to ensure gene knockdown. After 12 and 24 hpi, shrimp hemocytes were collected and used for total RNA extraction. The cDNA synthesis and qRT-PCR were performed.

Crustin*Pm*1 and crustin*Pm*7 expression level were measured in *Pm*MyD88 dsRNA knockdown shrimps. In ds*Pm*MyD88-silenced shrimp injected with *S. aureus* transcription level of crustin*Pm*1 was decreased by 2 and 7 fold at 12 and 24 hpi, respectively, when compared with control group (Figure 3.31A and 3.31B). Similar effects were found in *V. harveyi* infected shrimp whose crustin*Pm*1 transcripts were dropped by 2 and 5 fold at 12 and 24 hpi. Meanwhile, expression level of crustin*Pm*7 in *Pm*MyD88 silenced shrimp was decreased by 2 and 5 times at 12 and 24 hpi after *S. aureus* infection. Crustin*Pm*7 transcripts in *Pm*MyD88-depleted shrimp were also down by 2.5 and 5 times at 12 and 24 hpi by *V. harveyi* infection. Clearly, knockdown of *Pm*MyD88, a gene in Toll pathways, caused a reduction of crustin*Pm*1 and crustin*Pm*7 transcripts.

(A)
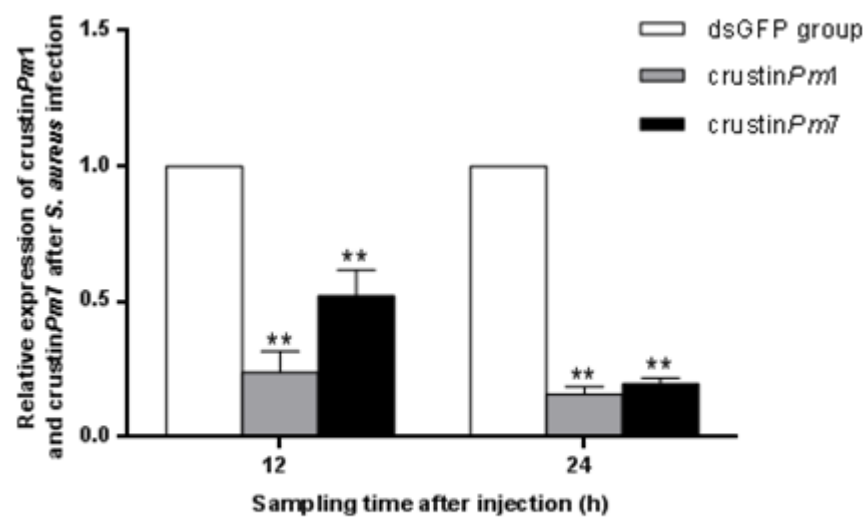
(B)
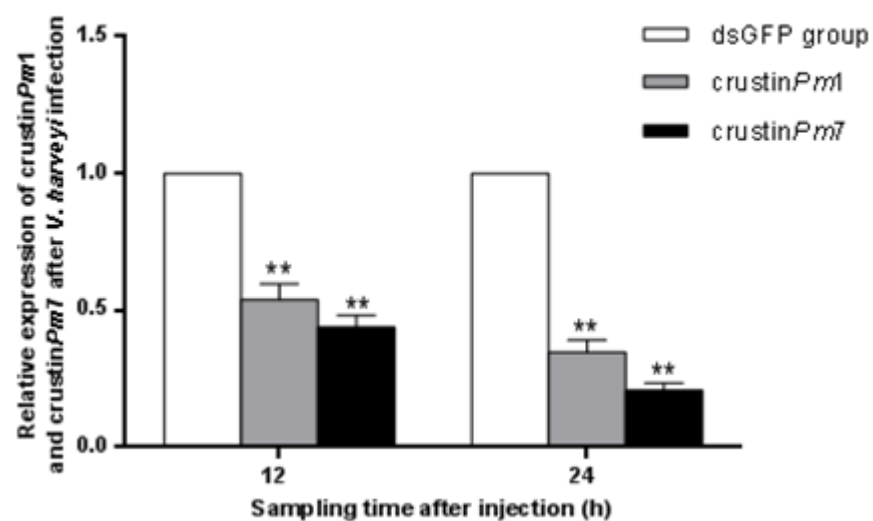
Figure 3.31 Expression profiles of crustin*Pm*1 and crustin*Pm*7 gene of *Pm*MyD88-silenced shrimp upon *S. aureus* and *V. harveyi* challenge. dsGFP group represents shrimps injected with GFP dsRNA. 12 h indicates shrimp at 12 hpi of *S. aureus* or *V. harveyi* treatment group; 24 h indicates shrimp at 24 hpi of *S. aureus* or *V. harveyi* treatment group. The genes expression level of infected group was normalized to that of the control group. * indicates significant difference (P < 0.05) and ** indicates significant difference (P < 0.01) compared with control group.

CHAPTER IV

DISCUSSION

Antimicrobial peptides (AMPs) are small molecules and have amphipathic structure that play an important role in shrimp innate immune responses and act against invading microorganisms; bacteria, fungi, virus, parasite, and yeast (Hancock *et al.* 2006). The mechanisms of AMPs may occur through electrostatic bonding between AMPs and negatively charged surface of bacteria or viruses, leading to interruption of the cell function (Skarnes and Watson 1957).

WAP domains contribute to various biological functions such as protease inhibitors or antimicrobial properties. Previously, in mammalian, the SLPI contains two WAP domains which one WAP domain at N-terminus is related to antimicrobial activity but WAP domain at C-terminus acts as a proteinase inhibitory activity (Fitch *et al.* 2006, Moreau *et al.* 2008).

Crustins contain a single WAP domain. They are antimicrobial peptides. Some antimicrobial peptides have anti-proteinase activities. In previous study, crustin type III exhibit antimicrobial and anti-proteinase activities (Amparyup *et al.* 2008, Jiang *et al.* 2008) but the crustin type II such as the crus*Fc* (Zhang *et al.* 2007) can exhibit only antimicrobial acitivity. In this study crustin*Pm*1 and crustin*Pm*7 do not show proteinase inhibitory acitivity when they were tested against the commercial proteinases (Amparyup *et al.* 2008, Suthianthong *et al.* 2012) and proteinase from *B. subtilis*. Each crustin has WAP domain that acts in different functions; antimicrobial or anti-proteinase activities. The different functions may be caused by the P_1 that codes Leu residue in the active site and other amino acid residues in the WAP domain the WAP domain. P_1' Met residue might has proteinase inhibitory activity or antibacterial activity or both (Vargas-Albores *et al.* 2004). The glycine-rich and cysteine-rich regions are important for antimicrobial activity and probably crustin*Pm*1 is inactive in proteinase inhibitory activities (Suthianthong *et al.* 2012). The proteinase inhibitory activities may depend on several factors not only the P_1' Met residue. For example, the amino acid spacing between conserved Cys2 and Cys3 give to different geometry of the loop which affects the P_1 amino acid side chain into the active site of proteinase (Bingle and Vyakarnam 2008).

The rcrustin*Pm*1 and rcrustin*Pm*7 proteins were further investigated for its ability to bind to their cell wall components and lipid in order to better understand

the properties of bacterial and lipid binding. The assay showed that the both rcrustin*Pm*1 and rcrustin*Pm*7 could bind to LPS (lipopolysaccharide from Gram-negative bacteria), LTA (lipoteichoic acid from Gram-positive bacteria), and PA (phosphatidic acid). Both crustins bind more tightly to PA than LPS and LTA. rCrustin*Pm*1 can bind to immobilized LPS, LTA, and PA with dissociation constant (K_d) as 4.131×10^{-6}, 1.146×10^{-7}, and 8.672×10^{-8} M, respectively. rCrustin*Pm*7 can bind to immobilized LPS, LTA, and PA with dissociation constant (K_d) as 1.658×10^{-7}, 1.499×10^{-7} M and 9.719×10^{-8} M, respectively. Binding properties of rcrustin*Pm*1 and rcrustin*Pm*7 to LPS and LTA is similar to the previous report (Krusong *et al.* 2012). Other antimicrobial peptides also bind to bacterial cells before performing its function in killing the cells. For example, Anti-lipopolysaccharide factor (ALF*Pm*3) from *P. monodon* showed the binding properties against Gram-negative and Gram-positive bacterial cells and their major cell wall components as LPS and LTA (Somboonwiwat et al., 2008). rCrustin*Pm*1 and rcrustin*Pm*7 can strongly bind to PA and the quantitative binding of rcrustin*Pm*1 and rcrustin*Pm*7 to LPS, LTA, and PA demonstrated the increasing of signal in S-shape with Hill slope. Hill slope value is greater than 1.0, indicating that the ligand has multiple binding sites with positive co-operativity. PA is the acid forms of phosphatidates, a part of common phospholipids, and major constituents of cell membranes. It is possible that PA is one of the target molecules for the rcrustin*Pm*1 and rcrustin*Pm*7 binding and both rcrustin*Pm*s bind to bacterial cells by attracting to anionic phospholipids and phosphate groups on Phosphatidic acid (PA). The ability of cecropin–bee melittin hybrid (CEME)-related peptides bind to LTA does not relate with their ability to kill bacteria, indicating that peptides might use this mechanism to contact other targets, such as the cytoplasmic membrane. The affinity of these peptides to LTA is related to the ability to block LTA-induced inflammation but not to kill bacteria (Scott *et al.* 1999). These peptides have gained access to the cytoplasmic membrane they can interact with lipid bilayers. In *in vitro* studies, antimicrobial peptides incubated with single or mixed lipids in membranes or vesicles showed that peptides bind in two physically distinct states such as S state, neutron scattering showed no pores present in the membrane and I state, neutron scattering showed the presence of pores (He *et al.* 1996, Yang *et al.* 2001, Huang 2006)

Furthermore, Circular Dichroism (CD), a technique for determining the secondary structure of proteins in solution, was used in this study. Circular dichroism studies were carried out with a JASCO J-715 CD spectropolarimeter and spectra were recorded between 190-260 nm, using 0.8 mg/ml of purified rcrustin*Pm*1 and

rcrustin*Pm*7 proteins in 10 mM Tris-HCl buffer pH 7.4. The secondary structure was performed using K2D3 software (Louis-Jeune *et al.* 2011). CD spectra of rcrustin*Pm*1 and rcrustin*Pm*7 presented that the major secondary structure type was alpha-helix compare to standard protein which known secondary structure. The predicted secondary structure (**α**-helix and **β**-strand) percentages of rcrustin*Pm*1 and rcrustin*Pm*7, rcrustin*Pm*1 proteins were 40.81% **α**-helix and 22.34% **β**-strand, while rcrustin*Pm*7 proteins were 32.86% **α**-helix and 27.53% **β**-strand.

In previous reports, structure of the antimicrobial peptides from insect is similar to antimicrobial substances from the plant and animal kingdoms. For example, in insect, *Phormia* defensin (Bonmatin *et al.* 1992) and *Sarcophaga* sapecin (Hanzawa *et al.* 1990) contain a central **α**-helix at N-terminal loop and a double stranded **β**-sheet at C-terminal (Hetru *et al.* 1998). Thanatin from a bug, *Podisus maculiventris* is antiparallel double stranded **β**-sheet structure shown in Figure 4.1 (Mandard *et al.* 1998). Three-dimensional structural model for the two-domain WAP proteins of the mature porcine WAP protein (pWAP) is two-strand antiparallel **β**-sheet of human mucous proteinase inhibitor (hSLPI) shown in Figure 4.2 (Ranganathan *et al.* 1999).
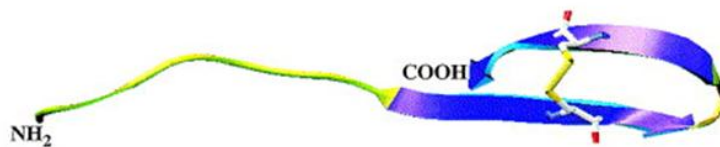
Figure 4.1 3-D structure of thanatin from the Brookhaven Protein Data Bank and draw with Swiss PDBviewer program (Mandard *et al.* 1998) .
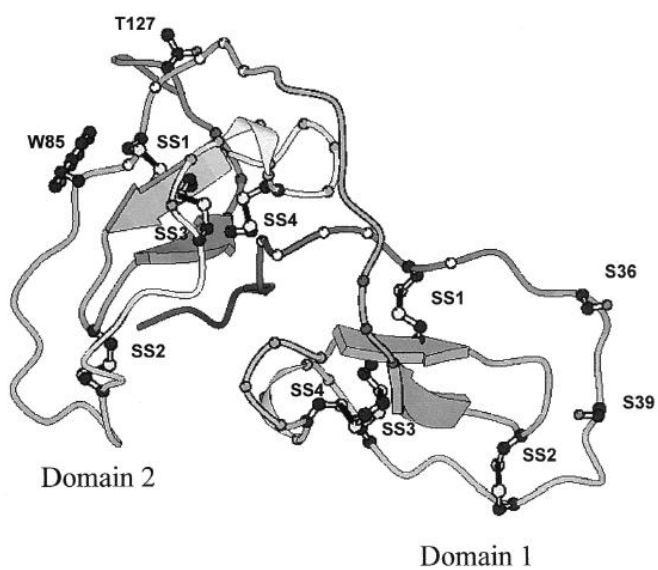
Figure 4.2 Structural model for two domian of pWAP by MOLSCRIPT[31] diagram.

(Ranganathan *et al.* 1999)

X-ray crystallography is a technique used to obtain the three-dimensional structure of protein. Crustin*Pm*1 and crustin*Pm*7 have different functions to inhibit Gram-positive and Gram-negative bacteria. They do not have three dimensional structure of crustins have not been determined yet. In this work, we are focusing to crystallize rcrustin*Pm*1. The purified rcrustin*Pm*1 was used for crystallization screening and co-crystallization with PA in order to obtain a crystal for structure determination by X-ray crystallography. In this study, rcrustin*Pm*1 was crystallized by itself and co-crystallize with PA in ratio of reservoir : purified protein of 2:1. Some crystals were tested on BL13B1 beamline at NSRRC, Taiwan but they did not diffract. This may due to small size of crystal. Further optimization is in need.

The main finding of the present study is that the inactivated Gram-positive and Gram-negative bacteria injection caused a change in transcription levels of crustin*Pm*1, crustin*Pm*7, *Pm*Relish, *Pm*Spätzle, *Pm*MyD88 and Dorsal, suggesting their roles in shrimp immune system. It has been reported that mechanism of AMP gene induction in the model insect *Drosophila melanogaster* has two separated intracellular signal transduction pathways which are the Toll and immune deficiency (Imd) pathways for controlling the antibacterial and antifungal responses (Lemaitre et al., 1995, 1996). The 5'-upstream region of Crus-like*Pm* or crustin*Pm*7 gene have TATA box-like consensus sequence and several putative transcription factor binding motifs such as GATA binding factor, signal transducer and activator of transcription 5 (STAT5), a CAAT enhancer-binding protein β (C/EBPβ), nuclear factor (NF)-kappaB and an activator protein 1 (AP1) cis-acting element (Amparyup et al. 2008). NF-kB is important transcription factors in immune response genes that play an important role in the Toll signaling pathway (Anderson 2000). Crustins gene contains the STAT binding site that was reported to be involved in the regulation of antimicrobial peptide genes in arthropods (Eggleston et al. 2000). The GATA factor binding sites were known to be involved in interactions with NF-kB transcription factor. Crustin*Pm*1 and crustin*Pm*7 transcription is likely to be regulated Rel/NF-kB-like mediated immune antimicrobial response in insects (Winick et al. 1993).The responses of crustin*Pm*1 and crustin*Pm*7 expressions to infection with the inactivated Gram-positive (*S. aureus*) and Gram-negative (*V. harveyi*) bacteria was investigated. For crustin*Pm*1, at 12 and 24 hpi, its expression in heat-killed *S. aureus* injected group was remarkably up-regulated, but shown no change in expression in shrimp

stimulated by heat-killed *V. harveyi*. Meanwhile, crustin*Pm*7 was significantly up-regulated at the highest level of 12 hpi by heat-killed *S. aureus* and at 24 hpi by heat-killed *V. harveyi*. Previous study showed that crustin*Pm*7 mRNA was up-regulated at 24 h after injection with *V. harveyi* (Amparyup et al. 2008). In contrast, in *L. vannamei*, crustin transcription levels decreased at 4 post-injection after LPS challenge (Okumura 2007). The differences in crustin transcription levels could be due to variations between the response to live and dead pathogen cells and also cell wall components. Response of crustin*Pm*1 and crustin*Pm*7 expression level to heat-killed *V. harveyi* and *S. aureus* is in agreement with the fact that crustin*Pm*1 acts against Gram-positive bacteria only while crustin*Pm*7 inhibits both Gram-positive and Gram-negative bacteria.

It was reported that three major signal pathways involved in the activation of antimicrobial peptides in insects in response to infection, including Toll, Imd, and JNK pathways. Spätzle, MyD88 and Dorsal involved in Toll pathway, while Relish involved in Imd pathway (H and Y 2007). The transcription of *Pm*Relish in hemocytes was responsive to *V. harveyi* and *S. aureus* injection, indicating that *Pm*Relish participates in immune response against Gram-negative (*V. harveyi*) and Gram-positive (*S. aureus*) bacterial infection. *Pm*Relish was highly responsive to *V. harveyi* with the highest up-regulated transcription level of 7 fold at 6 hpi (Figure 3.23). In contrast, *Pm*Relish responded to *S. aureus* injection at low level. This suggested that Imd pathway is major responsible pathway to Gram-negative bacteria. This finding was also reported in *Drosophila* (KS *et al.* 2001, E *et al.* 2002). In *A. aegypti*, the Relish transcript was induced by Gram-positive and Gram-negative bacteria injection (SW. *et al.* 2002). In *F. chinesis*, *Fc*Relish transcript was up-regulated rapidly at 1 hpi after Gram-negative bacterial infection by 4 fold and after Gram-positive bacterial infection by 1.5 fold at 6 hpi (Li *et al.* 2009).

In order to know whether *Pm*Relish can affect the transcription of AMPs, RNAi approach was used to silence the expression of *Pm*Relish in shrimp and the *Pm*Relish-depleted shrimp was then stimulated with different heat-killed bacteria. The data showed that transcription level of crustin*Pm*1 in *Pm*Relish-silenced shrimp did not change much after *S. aureus* and *V. harveyi* injection (Figure 3.28). In contrast, transcription level of crustin*Pm*7 in *Pm*Relish-silenced shrimp was greatly suppressed after bacterial infection. We can assume that the proteins which contain similar RHD domain regulate the transcription of crustin*Pm*7. The result showed that *Pm*Relish

was responded to bacteria injection especially to Gram-negative bacteria, and it can regulate the transcription level of crustin*Pm*7. Therefore, we conclude that crustin*Pm*7 related with Imd pathway while crustin*Pm*1 does not.

Genes in Toll pathway, *Pm*Spätzle, *Pm*MyD88 and Dorsal are also involved in the shrimp immunity to bacterial infection. As shown in Figure 3.24, the expression level of *Pm*Spätzle after stimulation by both *S. aureus* and *V. harveyi* group were continuously up-regulated, and reached its peak at 24 hpi. Dorsal was significantly up-regulated at 24 and 48 hpi with both *V. harveyi* and *S. aureus* injection (Figure 3.25). Similar to *Pm*Spätzle and Dorsal, the expression level of *Pm*MyD88 after *S. aureus* and *V. harveyi* infection was apparently up-regulated and reached its peak at 24 hpi (Figure 3.26). These results showed that the transcription of *Pm*Spätzle, *Pm*MyD88 and Dorsal were responsive to both Gram-positive and Gram-negative bacteria challenge. When compared the transcription levels of genes in Toll pathway: *Pm*Spätzle, *Pm*MyD88, Dorsal with *Pm*Relish in Imd pathway in response to Gram-positive and Gram-negative bacteria challenge, it is likely that Imd pathway responded in early bacterial infection, while Toll patway was triggered at the late phase of bacterial infection. It was reported in the oyster, *C. gigas,* that *Cg*-Rel was constitutively expressed in the tissues which were not affected by *Vibrio* injection at transcription level, but it can modulate the transcription of some antibacterial peptides (C *et al.* 2004). In the abalone, *Haliotis diversicolor supertexta*, *Ab*-Rel transcripts were not modified remarkably by the stimulation with LPS, but its NF-kB activity of *Ab*-Rel was induced in the hemocytes of the abalone by stimulation with LPS (Jiang and Wu 2007). Different from *Cg*-Rel and *Ab*-Rel, the transcripts of *Fc*Relish and *Fc*Dorsal were modulated by bacteria injection (C *et al.* 2004). In order to investigate effects of *Pm*MyD88 silencing on the transcription of crustin*Pm*1 and crustin*Pm*7, dsRNA MyD88 was injected into shrimp and the shrimp was then challenge with heat-killed *S. aureus* and *V. harveyi*. MyD88 was chosen because it is an important adapter protein which links members of the toll-like receptor to the downstream components to activate related Toll signaling pathways. After bacterial infection, both crustin*Pm*1 and crustin*Pm*7 in *Pm*MyD88-silenced shrimp significantly lower than those in control group. This indicated that crustin*Pm*1 and crustin*Pm*7 related with Toll pathway. In addition, Toll pathway seems to be responsible for both Gram-positive and Gram-negative bacterial infection in shrimp.

It was already proved that many types of AMPs are regulated by different signal pathways. Most AMPs in *Drosophila* were regulated by Imd pathway as illustrated for the Diptericin (Dpt) gene, some AMPs are regulated by Toll pathway

such as the Drosomycin (Drs) gene while some other AMPs are regulated by Toll and Imd pathways such as the Cecropin A1 (CecA1), Metchnikowin (Mtk), Attacin (AttA) and Defensin genes (H and Y 2007).

In previous report, the expression of some antimicrobial peptide genes such as Penaeidin3 and crustin*Pm*7 were significantly decreased in proPO gene-silenced shrimp. Therefore, proPOs not only contributes to control the expression of genes in proPO cascade but also AMPs in shrimp (Amparyup *et al.* 2012). Base on this information, expressions of crustin*Pm*s were regulated by several pathways including Imd pathway, Toll pathway and proPO.

CHAPTER V

CONCLUSIONS

1. Crustin*Pm*1 and crustin*Pm*7 were successfully cloned, expressed, and purified in *P. pastoris* expression system. Recombinant proteins were produced in soluble form.

2. Recombinant crustin*Pm*1 and crustin*Pm*7 produced in *P. pastoris* showed antibacterial activity. rCrustin*Pm*1 was active against Gram-positive bacteria only while rcrustin*Pm*7 showed antibacterial activity against both Gram-positive and Gram-negative bacteria.

3. rCrustin*Pm*1 and rcrustin*Pm*7 had no proteinase inhibitory activity against the commercial proteinases and the crude proteinase from *B. subtilis*.

4. The binding abilities of rcrustin*Pm*1 and rcrustin*Pm*7 to lipid and cell wall components suggested that rcrustin*Pm*1 and rcrustin*Pm*7 can be bind specifically to phosphatidic acid (PA) which is a part of common phospholipids of cell membranes. ELISA analysis showed that the rcrustin*Pm*1 and rcrustin*Pm*7 can bind to LPS, LTA and PA in concentration-dependent and saturated manner with Hill slope that presents the ligand or receptor binding sites with positive co-operativity.

5. In responses to inactivated Gram-positive and Gram-negative bacteria challenges,

- Expression profile of crustin*Pm*1 that challenged by *S. aureus* was remarkably up-regulated at 12 hpi by 4.9 times, but shown no change in shrimp stimulated by *V. harveyi*, compared to that in a control group.

- The transcription level of crustin*Pm*7 were significantly up-regulated and kept a highest level at 12 hpi (4.8 fold) for *S. aureus* group, but kept a highest level at 24 hpi (5.2 fold) for *V. harveyi* group.

- The transcription level of *Pm*Relish of *S. aureus* group was significantly up-regulated at 24 hpi by 1.7 fold, but in shrimp stimulated by *V. harveyi* was remarkably up-regulated at 6 hpi by 7.6 times

- The expression level of *Pm*Spätzle after stimulation by both *S. aureus* and *V. harveyi* group were up-regulated at 24 hpi by 14 and 7 fold, respectively, compared to that of control group.

- The Dorsal expression level was significantly up-regulated and kept a highest level at 48 hpi by 30 and 20 fold in shrimp stimulated by *S. aureus* and *V. harveyi* injection, respectively.

- The expression level of *Pm*MyD88 after *S. aureus* and *V. harveyi* infection was highest up-regulated at 24 hpi by 11 and 5 fold, respectively when compared with the control group.

6. From *Pm*Relish and *Pm*MyD88 silencing experiments, it is likely that crustin*Pm*1 transcript was related via Toll pathway while crustin*Pm*7 transcript was controlled via Imd and Toll pathway.

REFERENCES

Aggarwal, K. and N. Silverman (2008). "Positive and negative regulation of the *Drosophila* immune response." BMB Rep **41**(4): 267-277.

Amparyup, P., W. Charoensapsri and A. Tassanakajon (2009). "Two prophenoloxidases are important for the survival of *Vibrio harveyi* challenged shrimp *Penaeus monodon*." Dev Comp Immunol **33**(2): 247-256.

Amparyup, P., S. Donpudsa and A. Tassanakajon (2008). "Shrimp single WAP domain (SWD)-containing protein exhibits proteinase inhibitory and antimicrobial activities." Dev Comp Immunol **32**(12): 1497-1509.

Amparyup, P., H. Kondo, I. Hirono, T. Aoki and A. Tassanakajon (2008). "Molecular cloning, genomic organization and recombinant expression of a crustin-like antimicrobial peptide from black tiger shrimp *Penaeus monodon*." Mol Immunol **45**(4): 1085-1093.

Amparyup, P., J. Sutthangkul, W. Charoensapsri and A. Tassanakajon (2012). "Pattern recognition protein binds to lipopolysaccharide and beta-1,3-glucan and activates shrimp prophenoloxidase system." J Biol Chem **287**(13): 10060-10069.

Anderson, K. V. (2000). "Toll signaling pathways in the innate immune response." Curr Opin Immunol **12**(1): 13-19.

Andrade, M. A., P. Chacon, J. J. Merelo and F. Moran (1993). "Evaluation of secondary structure of proteins from UV circular dichroism spectra using an unsupervised learning neural network." Protein Eng **6**(4): 383-390.

Aspan, A., T. S. Huang, L. Cerenius and K. Soderhall (1995). "cDNA cloning of prophenoloxidase from the freshwater crayfish *Pacifastacus leniusculus* and its activation." Proc Natl Acad Sci U S A **92**(4): 939-943.

Balachandran, S., E. Thomas and G. N. Barber (2004). "A FADD-dependent innate immune mechanism in mammalian cells." Nature **432**(7015): 401-405.

Bartlett, T. C., et al. (2002). "Crustins, homologues of an 11.5-kDa antibacterial peptide, from two species of penaeid shrimp, *Litopenaeus vannamei* and *Litopenaeus setiferus*." Mar Biotechnol (NY) **4**(3): 278-293.

Bingle, C. D. and A. Vyakarnam (2008). "Novel innate immune functions of the whey acidic protein family." Trends Immunol **29**(9): 444-453.

Bischoff, V., et al. (2004). "Function of the drosophila pattern-recognition receptor PGRP-SD in the detection of Gram-positive bacteria." Nat Immunol **5**(11): 1175-1180.

Boman, H. G. (2003). "Antimicrobial peptides: basic facts and emerging concepts." J Intern Med **254(3)**: 197-215.

Bonmatin, J. M., et al. (1992). "Two-dimensional 1H NMR study of recombinant insect defensin A in water: resonance assignments, secondary structure and global folding." J Biomol NMR **2**(3): 235-256.

Boutros, M., H. Agaisse and N. Perrimon (2002). "Sequential activation of signaling pathways during innate immune responses in *Drosophila*." Dev Cell **3**(5): 711-722.

Brock, J. A. and D. V. Lightner (1990). "Chapter 3: Diseases of Crustacea. In Kinne, O. (ed.)." Diseases of Marine Animals **3**: 245-424.

Brockton, V., J. A. Hammond and V. J. Smith (2007). "Gene characterisation, isoforms and recombinant expression of carcinin, an antibacterial protein from the shore crab, *Carcinus maenas*." Mol Immunol **44**(5): 943-949.

Brockton, V. and V. J. Smith (2008). "Crustin expression following bacterial injection and temperature change in the shore crab, *Carcinus maenas*." Dev Comp Immunol **32**(9): 1027-1033.

Brogden, K. A. (2005). "Antimicrobial peptides: pore formers or metabolic inhibitors in bacteria." Nat Rev Microbiol **3**(3): 238-250.

Bulet, P., R. Stocklin and L. Menin (2004). "Anti-microbial peptides: from invertebrates to vertebrates." Immunol Rev **198**: 169-184.

C, M., K. C, R. J.M. and E. J.M. (2004). "Cg-Rel, the first Rel/NF-kB homolog characterized in a mollusk, the Pacific oyster *Crassostrea gigas*." FEBS Lett **561**: 75-82.

Cerenius, L., B. L. Lee and K. Soderhall (2008). "The proPO-system: pros and cons for its role in invertebrate immunity." Trends Immunol **29**(6): 263-271.

Chaikeeratisak, V., K. Somboonwiwat and A. Tassanakajon (2012). "Shrimp alpha-2-macroglobulin prevents the bacterial escape by inhibiting fibrinolysis of blood clots." PLoS One **7**(10): e47384.

Chantanachookin, C., et al. (1993). "Histology and ultrastructure reveal a new granulosis-like virus in *Penaeus monodon* affect by yellow-head disease. ." Diseases of Aquatic Organisms. **17(2)**: 145-157.

Charoensapsri, W., P. Amparyup, I. Hirono, T. Aoki and A. Tassanakajon (2009). "Gene silencing of a prophenoloxidase activating enzyme in the shrimp, *Penaeus monodon*, increases susceptibility to *Vibrio harveyi* infection." Dev Comp Immunol **33**(7): 811-820.

Charoensapsri, W., P. Amparyup, I. Hirono, T. Aoki and A. Tassanakajon (2011). "*Pm*PPAE2, a new class of crustacean prophenoloxidase (proPO)-activating enzyme and its role in PO activation." <u>Dev Comp Immunol</u> **35**(1): 115-124.

Choe, K. M., T. Werner, S. Stoven, D. Hultmark and K. V. Anderson (2002). "Requirement for a peptidoglycan recognition protein (PGRP) in Relish activation and antibacterial immune responses in *Drosophila*." <u>Science</u> **296**(5566): 359-362.

Chou, H. Y., C. Y. Huang, C. H. Wang, H. C. Chiang and C. F. Lo (1995). "Pathologenicity of a baculovirus infection causing white spot syndrome in cultured shrimp in Taiwan." <u>Aquaculture</u> **23**: 161-173.

Christie, A. E., et al. (2007). "Identification and characterization of a cDNA encoding a crustin-like, putative antibacterial protein from the American lobster *Homarus americanus*." <u>Mol Immunol</u> **44**(13): 3333-3337.

Cowland, J. B., A. H. Johnsen and N. Borregaard (1995). "hCAP-18, a cathelin/pro-bactenecin-like protein of human neutrophil specific granules." <u>FEBS Lett</u> **368**(1): 173-176.

Cuthbertson, B. J., E. E. Bullesbach, J. Fievet, E. Bachere and P. S. Gross (2004). "A new class (penaeidin class 4) of antimicrobial peptides from the Atlantic white shrimp (*Litopenaeus setiferus*) exhibits target specificity and an independent proline-rich-domain function." <u>Biochem J</u> **381**(Pt 1): 79-86.

D., S. (2002). "Activation of prophenoloxidase and removal of *Bacillus subtilis* from the hemolymph of *Acheta domesticus L. Orthoptera*: Gryllidae." <u>Neotropical Entomology</u> **31**: 487-491.

Demchick, P. and A. L. Koch (1996). "The permeability of the wall fabric of Escherichia coli and Bacillus subtilis." <u>J Bacteriol</u> **178**(3): 768-773.

Destoumieux, D., et al. (1997). "Penaeidins, a new family of antimicrobial peptides isolated from the shrimp *Penaeus vannamei* (Decapoda)." <u>J Biol Chem</u> **272**(45): 28398-28406.

Diamond, G., et al. (1991). "Tracheal antimicrobial peptide, a cysteine-rich peptide from mammalian tracheal mucosa: peptide isolation and cloning of a cDNA." <u>Proc Natl Acad Sci U S A</u> **88**(9): 3952-3956.

E, D. G., S. PT, T. P, R. GM and L. B (2002). "The Toll and Imd pathway are the major regulators of the immune response in *Drosophila*." <u>Dev Cell</u> **3**: 711-722.

Eggleston, P., W. Lu and Y. Zhao (2000). "Genomic organization and immune regulation of the defensin gene from the mosquito, *Anopheles gambiae*." <u>Insect Mol Biol</u> **9**(5): 481-490.

Fabricius, J. C. (1798). "Supplementum entomologiae systematicae." Hafniae. (Proft & Storch): 1-572.

Fitch, P. M., A. Roghanian, S. E. Howie and J. M. Sallenave (2006). "Human neutrophil elastase inhibitors in innate and adaptive immunity." Biochem Soc Trans 34(Pt 2): 279-282.

Foley, E. and P. H. O'Farrell (2004). "Functional dissection of an innate immune response by a genome-wide RNAi screen." PLoS Biol 2(8): E203.

Ganz, T., M. P. Sherman, M. E. Selsted and R. I. Lehrer (1985). "Newborn rabbit alveolar macrophages are deficient in two microbicidal cationic peptides, MCP-1 and MCP-2." Am Rev Respir Dis 132(4): 901-904.

Georgel, P., et al. (2001). "Drosophila immune deficiency (IMD) is a death domain protein that activates antibacterial defense and can promote apoptosis." Dev Cell 1(4): 503-514.

Gillespie, J. P., M. R. Kanost and T. Trenczek (1997). "Biological mediators of insect immunity." Annu Rev Entomol 42: 611-643.

Gobert, V., et al. (2003). "Dual activation of the Drosophila toll pathway by two pattern recognition receptors." Science 302(5653): 2126-2130.

Gottar, M., et al. (2002). "The Drosophila immune response against Gram-negative bacteria is mediated by a peptidoglycan recognition protein." Nature 416(6881): 640-644.

Greenfield, N. J. (2006). "Using circular dichroism spectra to estimate protein secondary structure." Nat Protoc 1(6): 2876-2890.

Gross, P. S., T. C. Bartlett, C. L. Browdy, R. W. Chapman and G. W. Warr (2001). "Immune gene discovery by expressed sequence tag analysis of hemocytes and hepatopancreas in the Pacific White Shrimp, Litopenaeus vannamei, and the Atlantic White Shrimp, L. setiferus." Dev Comp Immunol 25(7): 565-577.

H, U. and E. Y (2007). "A multilayered defense against infection: combinatorial control of insect immune genes." Trends Genet 23: 342-349.

Hall, M., R. Wang, R. van Antwerpen, L. Sottrup-Jensen and K. Soderhall (1999). "The crayfish plasma clotting protein: a vitellogenin-related protein responsible for clot formation in crustacean blood." Proc Natl Acad Sci U S A 96(5): 1965-1970.

Hancock, R. E., K. L. Brown and N. Mookherjee (2006). "Host defence peptides from invertebrates--emerging antimicrobial strategies." Immunobiology 211(4): 315-322.

Hanzawa, H., et al. (1990). "1H nuclear magnetic resonance study of the solution conformation of an antibacterial protein, sapecin." FEBS Lett 269(2): 413-420.

Hauton, C., V. Brockton and V. J. Smith (2006). "Cloning of a crustin-like, single whey-acidic-domain, antibacterial peptide from the haemocytes of the European lobster, *Homarus gammarus*, and its response to infection with bacteria." <u>Mol Immunol</u> **43**(9): 1490-1496.

He, K., S. J. Ludtke, D. L. Worcester and H. W. Huang (1996). "Neutron scattering in the plane of membranes: structure of alamethicin pores." <u>Biophys J</u> **70**(6): 2659-2666.

Hetru, C., D. Hoffmann and P. Bulet (1998). "Antimicrobial peptides from insects." <u>P.T. Brey, D. Hultmark (Eds.), Molecular mechanisms of immune responses in insects, Chapman & Hall</u>: 40-66.

Hetru, C. and J. A. Hoffmann (2009). "NF-kappaB in the immune response of *Drosophila*." <u>Cold Spring Harb Perspect Biol</u> **1**(6): a000232.

Hoffmann, A. A. and L. G. Harshman (1999). "Desiccation and starvation resistance in *Drosophila*: patterns of variation at the species, population and intrapopulation levels." <u>Heredity (Edinb)</u> **83 (Pt 6)**: 637-643.

Holmbald, T. and K. Söderhäll (1999). "Cell adhesion molecules and antioxidative enzymes in a crustacean, posible role in immunity." <u>Aquaculture</u> **172**: 111-123.

Homvises, T., A. Tassanakajon and K. Somboonwiwat (2010). "*Penaeus monodon* SERPIN, *Pm*SERPIN6, is implicated in the shrimp innate immunity." <u>Fish Shellfish Immunol</u> **29**(5): 890-898.

Horng, T. and R. Medzhitov (2001). "Drosophila MyD88 is an adapter in the Toll signaling pathway." <u>Proc Natl Acad Sci U S A</u> **98**(22): 12654-12658.

Hu, X., Y. Yagi, T. Tanji, S. Zhou and Y. T. Ip (2004). "Multimerization and interaction of Toll and Spätzle in *Drosophila*." <u>Proc Natl Acad Sci U S A</u> **101**(25): 9369-9374.

Huang, H. W. (2006). "Molecular mechanism of antimicrobial peptides: the origin of cooperativity." <u>Biochim Biophys Acta</u> **1758**(9): 1292-1302.

Hultmark, D. (2003). "*Drosophila* immunity: paths and patterns." <u>Curr Opin Immunol</u> **15**(1): 12-19.

Jiang, H. and M. R. Kanost (1997). "Characterization and functional analysis of 12 naturally occurring reactive site variants of serpin-1 from *Manduca sexta*." <u>J Biol Chem</u> **272**(2): 1082-1087.

Jiang, Y. and X. Wu (2007). "Characterization of a Rel\NF-kappaB homologue in a gastropod abalone, *Haliotis diversicolor supertexta*." <u>Dev Comp Immunol</u> **31**(2): 121-131.

Jiang, Z., et al. (2008). "Effects of hydrophobicity on the antifungal activity of alpha-helical antimicrobial peptides." <u>Chem Biol Drug Des</u> **72**(6): 483-495.

Jiravanichpaisal, P., B. L. Lee and K. Soderhall (2006). "Cell-mediated immunity in arthropods: hematopoiesis, coagulation, melanization and opsonization." Immunobiology **211**(4): 213-236.

Jiravanichpaisal, P., S. Y. Lee, Y. A. Kim, T. Andren and I. Soderhall (2007). "Antibacterial peptides in hemocytes and hematopoietic tissue from freshwater crayfish *Pacifastacus leniusculus*: characterization and expression pattern." Dev Comp Immunol **31**(5): 441-455.

Jones, D. E. and C. L. Bevins (1992). "Paneth cells of the human small intestine express an antimicrobial peptide gene." J Biol Chem **267**(32): 23216-23225.

Kang, C. J., et al. (2004). "Molecular cloning and expression analysis of Ch-penaeidin, an antimicrobial peptide from Chinese shrimp, *Fenneropenaeus chinensis*." Fish Shellfish Immunol **16**(4): 513-525.

Kanost, M. R. (1999). "Serine proteinase inhibitors in arthropod immunity." Dev Comp Immunol **23**(4-5): 291-301.

Khoo, L., D. W. Robinette and E. J. Noga (1999). "Callinectin, an antibacterial peptide from blue crab, *Callinectes sapidus*, Hemocytes." Mar Biotechnol (NY) **1**(1): 44-51.

Krusong, K., P. Poolpipat, P. Supungul and A. Tassanakajon (2012). "A comparative study of antimicrobial properties of crustinPm1 and crustin*Pm*7 from the black tiger shrimp *Penaeus monodon*." Dev Comp Immunol **36**(1): 208-215.

KS, K., L. F and L. B (2001). "*Drosophila* immunity: two paths to NF-kB." Trends Immunol **22**: 260-264.

Lemaitre, B., et al. (1995). "A recessive mutation, immune deficiency (imd), defines two distinct control pathways in the *Drosophila* host defense." Proc Natl Acad Sci U S A **92**(21): 9465-9469.

Lemaitre, B., E. Nicolas, L. Michaut, J. M. Reichhart and J. A. Hoffmann (1996). "The dorsoventral regulatory gene cassette Spätzle/Toll/cactus controls the potent antifungal response in *Drosophila* adults." Cell **86**(6): 973-983.

Leulier, F., A. Rodriguez, R. S. Khush, J. M. Abrams and B. Lemaitre (2000). "The *Drosophila* caspase Dredd is required to resist gram-negative bacterial infection." EMBO Rep **1**(4): 353-358.

Levashina, E. A., et al. (1999). "Constitutive activation of toll-mediated antifungal defense in serpin-deficient *Drosophila*." Science **285**(5435): 1917-1919.

Lewis, D. H. (1973). "Response of brown shrimp to ihfection with *Vibrio* sp.1." Proceedings of the annual workshop - World Mariculture Society **4(1-4)**: 333-338.

Li, F., et al. (2009). "Identification of a novel relish homolog in Chinese shrimp *Fenneropenaeus chinensis* and its function in regulating the transcription of antimicrobial peptides." Dev Comp Immunol **33**(10): 1093-1101.

Lightner, D. V., R. M. Redman, C. R. Pantoja, B. I. Noble and L. Tran (2012). "Early mortality syndrome affects shrimp in Asia." Aquaculture Advocate, January/February **40**.

Ligoxygakis, P., N. Pelte, J. A. Hoffmann and J. M. Reichhart (2002). "Activation of Drosophila Toll during fungal infection by a blood serine protease." Science **297**(5578): 114-116.

Linnaeus, C. (1758). "Systema naturae per regna tria naturae :secundum classes, ordines, genera, species, cum characteribus, differentiis, synonymis, locis (10th ed)." Stockholm: Laurentius Salvius.

Liu, F., Y. Liu, F. Li, B. Dong and J. Xiang (2005). "Molecular cloning and expression profile of putative antilipopolysaccharide factor in Chinese shrimp(*Fenneropenaeus chinensis*)." Mar Biotechnol (NY) **7**(6): 600-608.

Lo, C. F. (1996). "Detection of baculavirus associated with white spot syndrome (WSBV) in penaeid shrimp using polymerase chain reaction." Dis Aquat Organ **25**: 131-141.

Louis-Jeune, C., M. A. Andrade-Navarro and C. P.-I. Proteins. (2011). "Prediction of protein secondary structure from circular dichroism using theoretically derived spectra." Proteins.

Ma, H., B. Wang, J. Zhang, F. Li and J. Xiang (2010). "Multiple forms of alpha-2 macroglobulin in shrimp *Fenneropenaeus chinesis* and their transcriptional response to WSSV or *Vibrio* pathogen infection." Dev Comp Immunol **34**(6): 677-684.

Mandard, N., et al. (1998). "Solution structure of thanatin, a potent bactericidal and fungicidal insect peptide, determined from proton two-dimensional nuclear magnetic resonance data." Eur J Biochem **256**(2): 404-410.

Marshall, C. J. (1993). "Evolutionary relationships among the serpins." Philos Trans R Soc Lond B Biol Sci **342**(1300): 101-119.

Martin, G. G., J. E. H. S. Omori, C. Chong, T. Hoodbhoya and N. McKrella (1991). "Localization and roles of coagulogen and transglutaminase in hemolymph coagulation in decapod crustaceans." Comp. Biochem. Physiol **100(3)**: 517-522.

Michel, T., J. M. Reichhart, J. A. Hoffmann and J. Royet (2001). "*Drosophila* Toll is activated by Gram-positive bacteria through a circulating peptidoglycan recognition protein." Nature **414**(6865): 756-759.

Moreau, T., et al. (2008). "Multifaceted roles of human elafin and secretory leukocyte proteinase inhibitor (SLPI), two serine protease inhibitors of the chelonianin family." Biochimie **90**(2): 284-295.

Morita, T., et al. (1985). "Isolation and biological activities of limulus anticoagulant (anti-LPS factor) which interacts with lipopolysaccharide (LPS)." J Biochem **97**(6): 1611-1620.

Motoh, H. (1981). "Studies on the fisheries biology of the giant tigen prawn, *Penaeus monodon* in the Philippines. Tigbauan, Philippines." Aquaculture Dept., Southeast Asian Fisheries Development Center.

Muta, T., T. Oda and S. Iwanaga (1993). "Horseshoe crab coagulation factor B. A unique serine protease zymogen activated by cleavage of an Ile-Ile bond." J Biol Chem **268**(28): 21384-21388.

O'Brien, D. and J. McVey (1993). "Blood coagulation, inflammation, and defence." The natural immune system, humoral factors **I. E. Sim. New York: IRL press**: 257-280.

Okumura, T. (2007). "Effects of lipopolysaccharide on gene expression of antimicrobial peptides (penaeidins and crustin), serine proteinase and prophenoloxidase in haemocytes of the Pacific white shrimp, *Litopenaeus vannamei*." Fish Shellfish Immunol **22**(1-2): 68-76.

Otvos, L., Jr. (2002). "The short proline-rich antibacterial peptide family." Cell Mol Life Sci **59**(7): 1138-1150.

Ouellette, A. J. and M. E. Selsted (1996). "Paneth cell defensins: endogenous peptide components of intestinal host defense." FASEB J **10**(11): 1280-1289.

Park, J. M., et al. (2004). "Targeting of TAK1 by the NF-kappa B protein Relish regulates the JNK-mediated immune response in *Drosophila*." Genes Dev **18**(5): 584-594.

Perazzolo, L. M., et al. (2011). "Alpha2-macroglobulin from an Atlantic shrimp: biochemical characterization, sub-cellular localization and gene expression upon fungal challenge." Fish Shellfish Immunol **31**(6): 938-943.

Rafinesque (1815). "Analyse de la Nature ou Tableau de l'Univers et des Corps organises, &c. Rafinesque-Schmaltz." Constantine Samuel: 1783-1840.

Ranganathan, A., et al. (1999). "Knowledge-based design of bimodular and trimodular polyketide synthases based on domain and module swaps: a route to simple statin analogues." Chem Biol **6**(10): 731-741.

Ranganathan, S., K. J. Simpson, D. C. Shaw and K. R. Nicholas (1999). "The whey acidic protein family: a new signature motif and three-dimensional structure by comparative modeling." J Mol Graph Model **17**(2): 106-113, 134-106.

Rattanachai, A., I. Hirono, T. Ohira, Y. Takahashi and T. Aoki (2004). "Molecular cloning and expression analysis of alpha 2-macroglobulin in the kuruma shrimp, *Marsupenaeus japonicus*." Fish Shellfish Immunol **16**(5): 599-611.

Reichhart, J. M., et al. (1993). "Expression and nuclear translocation of the rel/NF-kappa B-related morphogen dorsal during the immune response of *Drosophila*." C R Acad Sci III **316**(10): 1218-1224.

Relf, J. M., J. R. Chisholm, G. D. Kemp and V. J. Smith (1999). "Purification and characterization of a cysteine-rich 11.5-kDa antibacterial protein from the granular haemocytes of the shore crab, *Carcinus maenas*." Eur J Biochem **264**(2): 350-357.

Rimphanitchayakit, V. and A. Tassanakajon (2010). "Structure and function of invertebrate Kazal-type serine proteinase inhibitors." Dev Comp Immunol **34**(4): 377-386.

Rolland, J. L., et al. (2010). "Stylicins, a new family of antimicrobial peptides from the Pacific blue shrimp *Litopenaeus stylirostris*." Mol Immunol **47**(6): 1269-1277.

Sallenave, J. M. (2000). "The role of secretory leukocyte proteinase inhibitor and elafin (elastase-specific inhibitor/skin-derived antileukoprotease) as alarm antiproteinases in inflammatory lung disease." Respir Res **1**(2): 87-92.

Scott, M. G., M. R. Gold and R. E. Hancock (1999). "Interaction of cationic peptides with lipoteichoic acid and gram-positive bacteria." Infect Immun **67**(12): 6445-6453.

Selsted, M. E., D. Szklarek and R. I. Lehrer (1984). "Purification and antibacterial activity of antimicrobial peptides of rabbit granulocytes." Infect Immun **45**(1): 150-154.

Shiao, S. H., et al. (2001). "Effect of prophenoloxidase expression knockout on the melanization of microfilariae in the mosquito *Armigeres subalbatus*." Insect Mol Biol **10**(4): 315-321.

Shugars, D. C. (1999). "Endogenous mucosal antiviral factors of the oral cavity." J Infect Dis **179 Suppl 3**: S431-435.

Sinderman, C. J. (1977). "In: Sinderman CJ (ed) Disease Dianosis and Control in North America Marine Aquaculture." Developments in Aquaculture and Fisheries Sciences. **6**: 292-293.

Skarnes, R. C. and D. W. Watson (1957). "Antimicrobial factors of normal tissues and fluids." Bacteriol Rev **21**(4): 273-294.

Söderhäll, K. and R. Ajaxon (1982). "Effect of quinones and melanin on mycelial growth of aphanomyces spp. and extracellular protease of *Aphanomyces astact*, a parasite on crayfish." <u>J Invertebr Pathol</u> **39(1)**: 105-109.

Söderhäll, K. and L. Cerenius (1998). "Role of the prophenoloxidase-activating system in invertebrate immunity." <u>Curr Opin Immunol</u> **10**(1): 23-28.

Söderhäll, K., V. J. Smith and M. W. Johansson (1986). "Exocytosis and uptake of bacteria by isolated haemocyte populations of two crustacean: evidance for cellular co-operatition in the defence reaction of arthropods." <u>Cell Tissue Res</u> **245**: 43-49.

Söderhäll, K., A. Vey and M. Ramstedt (1984). "Hemocyte lysate enhancement of fungal spore encapsulation by crayfish hemocytes." <u>Dev Comp Immunol</u> **8**(1): 23-29.

Somboonwiwat, K., et al. (2005). "Recombinant expression and anti-microbial activity of anti-lipopolysaccharide factor (ALF) from the black tiger shrimp *Penaeus monodon*." <u>Dev Comp Immunol</u> **29**(10): 841-851.

Somboonwiwat, K., et al. (2006). "Differentially expressed genes in hemocytes of *Vibrio harveyi*-challenged shrimp *Penaeus monodon*." <u>J Biochem Mol Biol</u> **39**(1): 26-36.

Somnuk, S., A. Tassanakajon and V. Rimphanitchayakit (2012). "Gene expression and characterization of a serine proteinase inhibitor *Pm*SERPIN8 from the black tiger shrimp *Penaeus monodon*." <u>Fish Shellfish Immunol</u> **33**(2): 332-341.

Sottrup-Jensen, L. (1989). "Alpha-macroglobulins: structure, shape, and mechanism of proteinase complex formation." <u>J Biol Chem</u> **264**(20): 11539-11542.

Stoss, T. D., M. D. Nickell, D. Hardin, C. D. Derby and T. S. McClintock (2004). "Inducible transcript expressed by reactive epithelial cells at sites of olfactory sensory neuron proliferation." <u>J Neurobiol</u> **58**(3): 355-368.

Sun, H., P. Towb, D. N. Chiem, B. A. Foster and S. A. Wasserman (2004). "Regulated assembly of the Toll signaling complex drives Drosophila dorsoventral patterning." <u>EMBO J</u> **23**(1): 100-110.

Supungul, P., et al. (2004). "Antimicrobial peptides discovered in the black tiger shrimp *Penaeus monodon* using the EST approach." <u>Dis Aquat Organ</u> **61**(1-2): 123-135.

Supungul, P., et al. (2008). "Cloning, expression and antimicrobial activity of crustin*Pm*1, a major isoform of crustin, from the black tiger shrimp *Penaeus monodon*." <u>Dev Comp Immunol</u> **32**(1): 61-70.

Suthianthong, P., S. Donpudsa, P. Supungul, A. Tassanakajon and V. Rimphanitchayakit (2012). "The N-terminal glycine-rich and cysteine-rich regions are essential for antimicrobial activity of crustin*Pm*1 from the black tiger shrimp *Penaeus monodon*." Fish Shellfish Immunol **33**(4): 977-983.

SW., S., K. V., A. A. and R. AS. (2002). "Characterization of three alternatively spliced isoforms of the Rel/NF-kB transcription factor Relish from the mosquito *Aedes aegypti*." PNAS **99**: 9978-9983.

Tanaka, S., T. Nakamura, T. Morita and S. Iwanaga (1982). "*Limulus* anti-LPS factor: an anticoagulant which inhibits the endotoxin mediated activation of *Limulus* coagulation system." Biochem Biophys Res Commun **105**(2): 717-723.

Tanji, T. and Y. T. Ip (2005). "Regulators of the Toll and Imd pathways in the Drosophila innate immune response." Trends Immunol **26**(4): 193-198.

Tassanakajon, A., P. Amparyup, K. Somboonwiwat and P. Supungul (2011). "Cationic antimicrobial peptides in penaeid shrimp." Mar Biotechnol (NY) **13**(4): 639-657.

Tassanakajon, A., et al. (2008). "Biotechnology of marine invertebrates---Recent Advances in Shrimp and Shellfish." In: Memorial book of the 5th World Fisheries Congress 2008, Tsukamoto, K., Kawamura, T., Takeuchi, T., Beard, Jr. TD., Kaiser, MJ. TERRAPUB Tokyo: 221-239.

Tauszig-Delamasure, S., H. Bilak, M. Capovilla, J. A. Hoffmann and J. L. Imler (2002). "Drosophila MyD88 is required for the response to fungal and Gram-positive bacterial infections." Nat Immunol **3**(1): 91-97.

Tossi, A., L. Sandri and A. Giangaspero (2000). "Amphipathic, alpha-helical antimicrobial peptides." Biopolymers **55**(1): 4-30.

Vargas-Albores, F., G. Yepiz-Plascencia, F. Jimenez-Vega and A. Avila-Villa (2004). "Structural and functional differences of *Litopenaeus vannamei* crustins." Comp Biochem Physiol B Biochem Mol Biol **138**(4): 415-422.

Wang, Y. and H. Jiang (2004). "Purification and characterization of *Manduca sexta* serpin-6: a serine proteinase inhibitor that selectively inhibits prophenoloxidase-activating proteinase-3." Insect Biochem Mol Biol **34**(4): 387-395.

Wang, Y., et al. (2006). "Association of beta-arrestin and TRAF6 negatively regulates Toll-like receptor-interleukin 1 receptor signaling." Nat Immunol **7**(2): 139-147.

Weber, A. N., et al. (2003). "Binding of the *Drosophila* cytokine Spätzle to Toll is direct and establishes signaling." Nat Immunol **4**(8): 794-800.

Wen, R., F. Li, Z. Sun, S. Li and J. Xiang (2013). "Shrimp MyD88 responsive to bacteria and white spot syndrome virus." Fish Shellfish Immunol **34**(2): 574-581.

Whaley, K. and C. Lemercier (1993). "The complement system." <u>The natural immune system, humoral factors</u> **I. E. New York: ILR Press**: 121-150.

Wiedow, O., J. Harder, J. Bartels, V. Streit and E. Christophers (1998). "Antileukoprotease in human skin: an antibiotic peptide constitutively produced by keratinocytes." <u>Biochem Biophys Res Commun</u> **248**(3): 904-909.

Winick, J., et al. (1993). "A GATA family transcription factor is expressed along the embryonic dorsoventral axis in *Drosophila melanogaster*." <u>Development</u> **119**(4): 1055-1065.

Woese, C. R. (1987). "Bacterial evolution." <u>Microbiol Rev</u> **51**(2): 221-271.

Yang, L., T. A. Harroun, T. M. Weiss, L. Ding and H. W. Huang (2001). "Barrel-stave model or toroidal model; A case study on melittin pores." <u>Biophys J</u> **81**(3): 1475-1485.

Zasloff, M. (1987). "Magainins, a class of antimicrobial peptides from Xenopus skin: isolation, characterization of two active forms, and partial cDNA sequence of a precursor." <u>Proc Natl Acad Sci U S A</u> **84**(15): 5449-5453.

Zhang, J., F. Li, Z. Wang and J. Xiang (2007). "Cloning and recombinant expression of a crustin-like gene from Chinese shrimp, *Fenneropenaeus chinensis*." <u>J Biotechnol</u> **127**(4): 605-614.

Zhang, S., et al. (2012). "Identification and function of myeloid differentiation factor 88 (MyD88) in *Litopenaeus vannamei*." <u>PLoS One</u> **7**(10): e47038.

Zou, Z., Z. Picheng, H. Weng, K. Mita and H. Jiang (2009). "A comparative analysis of serpin genes in the silkworm genome." <u>Genomics</u> **93**(4): 367-375.

APPENDICES

APPENDIX A

1. *Pichia* media recipes

Stock Solutions

- 10X YNB (13.4% Yeast Nitrogen Base with Ammonium Sulfate without amino acids)

Dissolve 134 g of yeast nitrogen base (YNB) with ammonium sulfate and without amino acids in 1000 ml of water and filter sterilize. Heat the solution to dissolve YNB completely in water. Store at 4°C.

- 500X B (0.02% Biotin)

Dissolve 20 mg biotin in 100 ml of water and filter sterilize. Store at 4°C.

- 10X D (20% Dextrose)

Dissolve 200 g of D-glucose in 1000 ml of water. Autoclave for 15 minutes or sterilized filter

- 10X M (5% Methanol)

Mix 5 ml of methanol with 95 ml of water. Sterilized filter and store at 4°C.

- 10X GY (10% Glycerol)

Mix 100 ml of glycerol with 900 ml of water. Sterilize either by filtering or autoclaving. Store at room temperature.

- 1 M potassium phosphate buffer, pH 6.0

Combine 132 ml of 1 M K_2HPO_4, 868 ml of 1 M KH_2PO_4 and adjusted the pH by KOH. Sterilize by autoclaving and store at room temperature.

2. Preparation media for Pichia expression system

- YPD (Yeast Extract Peptone Dextrose Medium (1 liter)

   1% yeast extract

   2% peptone

   2% dextrose (glucose)

1. Dissolve 10 g yeast extract and 20 g of peptone in 900 ml of water.

2. Autoclave for 20 minutes on liquid cycle.

3. Add 100 ml of 10X D.

4. Store YPD plates at 4℃.

- BMGY (Buffered Glycerol-complex Medium) and BMMY (Buffered Methanol-complex Medium) (1 liter)

1. Dissolve 10 g of yeast extract, 20 g peptone in 700 ml water.

2. Autoclave 20 minutes on liquid cycle.

3. Cool to room temperature, then add the following and mix well:

    100 ml 1 M potassium phosphate buffer, pH 6.0

    100 ml 10X YNB

    2 ml 500X B

    100 ml 10X GY

4. For BMMY, add 100 ml 10X M instead of glycerol.

5. Store media at 4℃.

3. Preparation for SDS-PAGE electrophoresis

Stock reagents

- 30% Acrylamide, 0.8% bis-acrylamide (100 ml)

    Acrylamide 29.2 g

    N,N′-methylene-bis-acrylamide 0.80 g

    Adjust final volume to 100 ml with distilled water.

- 1.5 M Tris-HCl pH 8.8

    Tris (hydroxymethyl)-aminomethane 18.17 g

Adjust pH to 8.8 with 1 M HCl and adjust volume to 100 ml with distilled water.

- 1.0 M Tris-HCl pH 6.8

Tris (hydroxymethyl)-aminomethane 12.1 g

Adjust pH to 6.8 with 1 M HCl and adjust volume to 100 ml with distilled water.

SDS-PAGE

- 15% Seperating gel

1.5 M Tris-HCl pH 8.8 2.53 ml

30% Acrylamide solution 5 ml

Distilled water 2.26 ml

10% SDS 100 µl

10% APS 100 µl

TEMED 4 µl

- 5.0% Stacking gel

1.0 M Tris-HCl pH 6.8 0.50 ml

30% Acrylamideml solution 0.67 ml

Distilled water 2.75 ml

10% SDS 40 µl

10% APS 40 µl

TEMED 4 µl

- 5X Sample buffer

      1 M Tris-HCl (pH 6.8) 0.6 ml

      10% SDS 2.0 ml

      50% Glycerol 5.0 ml

      1% Bromophenol blue 1.0 ml

      2-Mercaptoethanol 0.5 ml

      Distilled water 0.9 ml

One part of sample buffer was added to four parts of sample. The mixture was heated 5 min. in boiling water before loading to the gel.

- Electrophoresis buffer, 1 litre (25 mM Tris, 192 mM glycine)

      Tris (hydroxymethyl)-aminomethane 3.03 g

      Glycine 14.40 g

      SDS 1.0 g

      Dissolve in distilled water to 1 litre and final pH should be 8.3.

Silver staining

- Fixing solution: 50% Methanol, 10% Acetic acid (100 ml)

      50 ml Methanol (99.8%)

      10 ml Glacial acetic acid (100%)

      Distilled water 40 ml

- Staining solution

Solution A

      Silver nitrate 0.4 g

      Dissolve in distilled water to 1 ml

Solution B

25% Ammonium sulfate 1.4 ml

3.6% Sodium hydroxide 2.1 ml

Mixing solution A and solution B and adjust volume to 50 ml with distilled water

- Developing solution

1% citric acid 0.5 ml

37% formaldehyde 50 μl

adjust volume to 50 ml with distilled water.

- Stopping solution

1% glacial acetic acid

adjust volume to 50 ml with distilled water.

APPENDIX B

NetNGlyc 1.0 Server - prediction results

Technical University of Denmark

Asn-Xaa-Ser/Thr sequons in the sequence output below are highlighted in blue.

Asparagines predicted to be N-glycosylated are highlighted in red.

Name: crusPm1   Length: 145

```
MKGLGVILFCVLAMASAQSWHGGRPGGFPGGGRPGGFPGGGRPGGRPGGFPSVTAPPASCRRWCETPENAFYCCESRYEP   80

EAPVGTKILDCPKVRDTCPPVRFLAVEQPVPCSSDYKCGGLDKCCFDRCLGQHVCKPPSFYEFFA                  160

...............................................................N............       80

........................................................              160
```

(Threshold=0.5)

SeqName   Position Potential Jury   N-Glyc

                                       agreement result

----

crusPm1   69 NAFY 0.5407   (6/9)   +
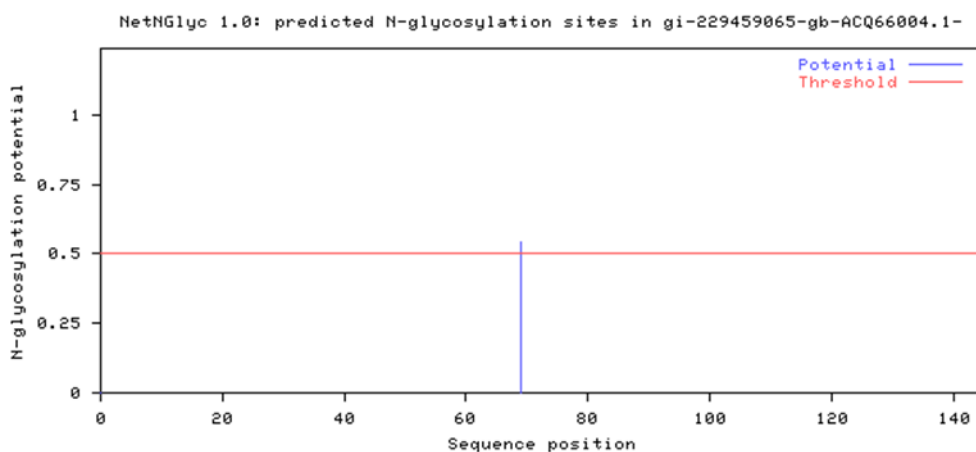
NetNGlyc 1.0: predicted N-glycosylation sites in gi-229459065-gb-ACQ66004.1-

NetNGlyc 1.0 Server - prediction results

Technical University of Denmark

Asn-Xaa-Ser/Thr sequons in the sequence output below are highlighted in blue.

Asparagines predicted to be N-glycosylated are highlighted in red.

Name: crusPm7   Length: 141

```
MLKFVVLSVVAVAVVHAQDKGNADTRFLGGVGVPGGGVPGVGVPGVGGGFLPGVPGHGGVVPGGGGLLPGGQFECNYCRT      80

RYGYVCCKPGRCPQIRDTCPGLRKGVPICRQDTDCFGSDKCCFDTCLNDTVCKPIVAGSQG                        160

.....................N.................................................N....       80

..........................................N............                            160
```

(Threshold=0.5)

SeqName   Position Potential Jury   N-Glyc

                                            agreement result

----

crusPm7   22 NADT 0.5767   (6/9)   +

crusPm7   76 NYCR 0.7768   (9/9)   +++

crusPm7   128 NDTV 0.5270   (4/9)   +
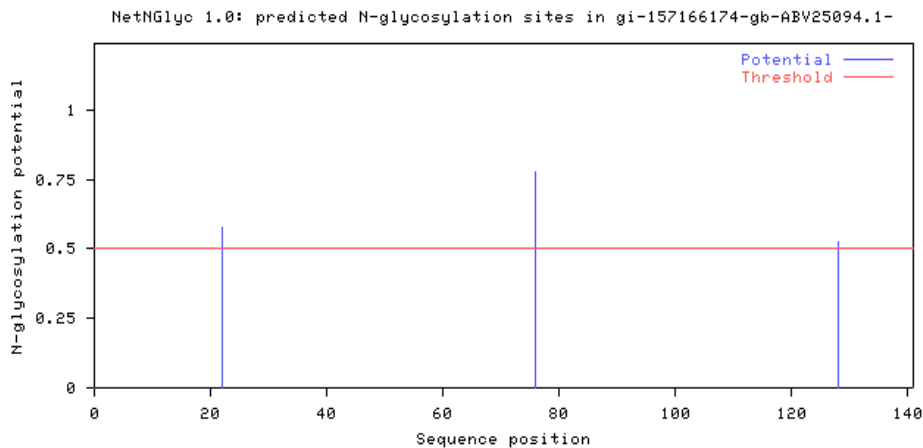
NetNGlyc 1.0: predicted N-glycosylation sites in gi-157166174-gb-ABV25094.1-

APPENDIX C

Circular Dichroism (CD) spectroscopy

- The data of mean residue elliplicity [θ] of crustin*Pm*1

Wavelength (nm)	CD (θ)	HT	[θ] MRE, λ
190	34.048435	856.504333	0.312820133
191	37.059868	854.805664	0.340487685
192	38.479698	848.430298	0.353532379
193	39.117424	836.965027	0.359391489
194	38.724327	819.412659	0.355779909
195	36.606815	796.171021	0.336325259
196	33.000137	769.029968	0.303188891
197	28.674301	739.459351	0.263445255
198	23.399681	708.944641	0.214984663
199	17.179991	678.752319	0.157841236
200	10.506042	649.404663	0.096524303
201	4.41263	621.896362	0.040541056
202	-1.04586	596.512329	-0.009608843
203	-5.692618	573.407349	-0.052300951
204	-9.158092	552.707703	-0.084140007
205	-12.098794	533.962646	-0.111157718
206	-14.542992	517.00238	-0.133613797
207	-16.355606	501.710999	-0.150267196
208	-17.601328	488.032684	-0.161712271
209	-17.931459	475.883331	-0.164745351
210	-17.628462	464.843323	-0.161961565
211	-17.223772	454.799347	-0.158243474
212	-16.80274	445.560333	-0.154375241
213	-16.672113	437.113007	-0.153175105
214	-1.146641	429.445007	-0.153839205
215	-0.203794	422.285004	-0.15460107
216	0.713752	415.527313	-0.15597688
217	1.669074	409.151672	-0.156826559
218	2.510192	403.014679	-0.157277463
219	3.225466	396.999329	-0.157704636

Wavelength (nm)	CD (θ)	HT	[θ] MRE, λ
220	3.771848	391.081665	-0.157645754
221	4.070619	385.409332	-0.157896012
222	4.156118	380.075989	-0.158579314
223	4.037849	374.96167	-0.158000474
224	3.871544	370.004669	-0.155443784
225	3.737459	365.169342	-0.150272138
226	3.687419	360.358337	-0.14264222
227	3.621084	355.556335	-0.134542727
228	3.479864	350.79068	-0.126293699
229	3.207802	346.042999	-0.116815723
230	2.748821	341.383667	-0.107433453
231	2.254185	336.893311	-0.097465122
232	1.860521	332.513	-0.086004491
233	1.534982	328.237671	-0.074999488
234	1.323074	324.141327	-0.064240599
235	1.197855	320.255981	-0.053696836
236	0.968571	316.646667	-0.045291629
237	0.689617	313.309662	-0.03847554
238	0.464426	310.250336	-0.032531215
239	-2.980301	307.514343	-0.027381527
240	-2.398249	305.082336	-0.022033922

- The data of mean residue elliplicity [θ] of crustin*Pm*7

Wavelength (nm)	CD (θ)	HT	[θ] MRE, λ
190	34.528866	760.681641	0.285141585
191	37.489166	759.146667	0.309587932
192	37.822399	753.979675	0.312339792
193	38.983433	744.919983	0.321927685
194	39.169197	731.256348	0.323461736
195	37.461231	713.532654	0.309357243
196	35.005932	693.04834	0.289081227
197	30.918533	670.552673	0.255327224
198	24.247566	647.017334	0.200237952
199	16.885567	623.331665	0.139442093
200	10.160627	599.857666	0.083907108
201	2.776447	577.300964	0.022928077
202	-3.993777	555.966675	-0.032980866
203	-9.73701	536.275696	-0.080408852
204	-14.857266	518.444336	-0.122692253
205	-18.737434	502.152313	-0.154734929
206	-22.175568	487.337677	-0.18312726
207	-25.627266	473.996002	-0.211631603
208	-27.283667	462.005005	-0.225310268
209	-28.804766	451.346344	-0.237871601
210	-29.0123	441.748993	-0.23958543
211	-28.3927	433.047668	-0.234468734
212	-28.602068	425.143677	-0.236197708
213	-28.6679	418.002014	-0.236741353
214	-28.405666	411.541321	-0.234575808
215	-28.427933	405.461334	-0.23475969
216	-28.170534	399.767334	-0.232634073

Wavelength (nm)	CD (θ)	HT	[θ] MRE, λ
217	-28.166668	394.456665	-0.232602147
218	-28.046867	389.339661	-0.231612823
219	-27.661165	384.287659	-0.228427671
220	-27.576	379.335327	-0.227724373
221	-27.224834	374.580017	-0.224824422
222	-26.795033	370.081329	-0.221275097
223	-26.253067	365.859009	-0.216799507
224	-25.543867	361.761017	-0.210942888
225	-24.586899	357.645996	-0.203040186
226	-23.430666	353.576324	-0.193491939
227	-22.145567	349.574005	-0.18287951
228	-20.827566	345.621002	-0.171995373
229	-19.571966	341.667664	-0.161626548
230	-17.872766	337.833984	-0.147594445
231	-16.16	334.140656	-0.133450314
232	-14.892866	330.48999	-0.122986241
233	-13.3897	326.845337	-0.110573
234	-11.748434	323.279999	-0.09701932
235	-10.497367	319.861328	-0.086687929
236	-9.433197	316.632996	-0.077899945
237	-8.457414	313.585327	-0.069841866
238	-7.45842	310.738007	-0.06159211
239	-6.649243	308.158661	-0.054909874
240	-5.999903	305.837982	-0.049547583

Conference experiences

- The 21st Science Forum 2013. Faculty of Science, Chulalongkorn University, Bangkok, Thailand. Poster presentation on title of "Secondary structure analysis of crustin*Pm*7 from black tiger shrimp, *Penaeus monodon*"

- The 18th Biological Sciences Graduate Congress. Faculty of Science, University of Malaya, Kuala Lumpur, Malaysia. Poster presentation on title of "Structure and function analysis of crustin*Pm*1 and crustin*Pm*7 from black tiger shrimp *Penaeus monodon*"

VITA

Miss Sopacha Arayamethakorn was born on June 16, 1988 in Yala. She graduated with the degree of Bachelor of Science from the Department of Biochemistry, Faculty of Science, Chulalongkorn University in 2010. She has studied for the degree of Master of Science at the Program in Biotechnology, Faculty of Science, Chulalongkorn University since 2011. In the third years of research work, she participated in presenting research results in part of poster presentation on the topic of "Cloning, Expression and Characterization of Recombinant CrustinPm7 from Black Tiger Shrimp Penaeus monodon" at the 1st International Graduate Research Congress (iGRC 2013) organized by The Graduates School, Chiang Mai University on December 20, 2013.